

# Клиническая инфектология и паразитология

МЕЖДУНАРОДНЫЙ  
НАУЧНО-ПРАКТИЧЕСКИЙ  
ЖУРНАЛ

2025, том 14, № 1. Электронное приложение

Clinical Infectology and Parasitology  
International Scientific Journal

2025 Volume 14 Number 1. Electronic Supplement



## Special Issue "Water Sources Pollution and Insecticides Chemistry"

ISSN 2306-8787 (print)  
ISSN 2414-360X (online)



International Scientific Journal  
**Clinical infectology and parasitology**  
KLINICHESKAJA INFETOLOGIJA I PARAZITOLOGIJA

**infecto.recipe.by**  
**infecto.recipe-russia.ru**

**2025 Volume 14 Number 1**  
**Electronic Supplement**

---

Founded in 2012

## Belarus

**The journal is registered** by the Ministry of information of the Republic of Belarus April 19, 2013  
Registration certificate № 1619

**Founder:**  
UE "Professional Editions"

**Editorial office:**  
**Director** Evtushenko L.  
**Commissioning editor** Drozdov Yu.  
**Head of advertising and marketing** Koval M.  
**Technical editor** Kaulkin S.

**Address:**  
67 Timiryazev st., office 1103, Minsk,  
220035, Republic of Belarus, P.O. box 5  
Phones: +375 17 322-16-59, 322-16-76  
e-mail: [infecto@recipe.by](mailto:infecto@recipe.by)

## Russia

**The journal is registered** by the Federal Service for Supervision of Communications, Information Technology, and Mass Media (Roskomnadzor)  
April 27, 2024  
Registry entry ПИ № ФС77-87322

**Founder and Publisher**  
LLC "Vilin – Professional Editions"

**Editorial office:**  
**Director** A. Sakmarov  
**Editor-in-Chief** V. Chulanov

**Editorial and publisher address:**  
214522, Smolensk region, Smolensk district,  
rural settlement Katynskoye, Avtoremzavod village, 1A, office 413  
phone: +7 4812 51-59-23  
e-mail: [infecto@recipe.by](mailto:infecto@recipe.by)

---

### Subscription

In the catalogue of the Republican Unitary Enterprise "Belposhta":  
individual index – 00084; departmental index – 000842.  
In the electronic catalogs on web-sites of agencies: LLC "Pressinform",  
LLC "Kriektiv Servis Bend", LLC "Ekaterinburg-OPT", LLC "Globalpress"

Published: 27.03.2025

The electronic version of the journal is available on [infecto.recipe.by](http://infecto.recipe.by),  
on the Scientific electronic library [elibrary.ru](http://elibrary.ru), in the East View  
database, in the electronic library system IPRbooks

Concerning acquisition of the journal address to the editorial office  
The frequency of the journal is 1 time in 3 months

### © "Clinical infectology and parasitology"

Copyright is protected. Any reproduction of materials of the edition is possible only with an obligatory reference to the source.

© UE «Professional Editions», 2025

© Design and decor of UE «Professional Editions», 2025

© LLC "Vilin – Professional Editions", 2025

## Belarus

### Editor-In-Chief

**Igor A. Karpov**, Corresponding Member of the National Academy of Sciences of Belarus, Doctor of Medical Sciences, Professor, Belarusian State Medical University (Minsk)

### Editorial Board:

Yuriy L. Gorbich, Candidate of Medical Sciences, Associate Professor, Ministry of Health of the Republic of Belarus (Minsk)

Anna A. Klyuchareva, Doctor of Medical Sciences, Professor, Institute for Advanced Training and Retraining of Healthcare Personnel of Belarusian State Medical University (Minsk)

Sholpan A. Kulzhanova, Doctor of Medical Sciences, Professor, Medical University of Astana (Astana, Kazakhstan)

Svetlana P. Lukashik, Doctor of Medical Sciences, Associate Professor, Belarusian State Medical University (Minsk)

Oksana N. Romanova, Dr. of Med. Sci., Prof., Belarusian State Medical University (Minsk, Belarus)

Vladimir M. Semenov, Doctor of Medical Sciences, Professor, Vitebsk State Order of Peoples' Friendship Medical University (Vitebsk)

Dmitry V. Tapalsky, Doctor of Medical Sciences, Professor, Institute of Physiology of the National Academy of Sciences of Belarus (Minsk)

Sergei V. Zhavoronok, Doctor of Medical Sciences, Professor, Belarusian State Medical University (Minsk)

### Editorial Council:

Dmitry Y. Danilov, Doctor of Medical Sciences, Professor, Belarusian State Medical University (Minsk)

Natalia V. Matsiyevskaya, Doctor of Medical Sciences, Professor, Grodno State Medical University (Grodno)

Alexandr V. Nersesov, Doctor of Medical Sciences, Professor, Asfendiyarov Kazakh National Medical University (Almaty, Kazakhstan)

Igor O. Stoma, Doctor of Medical Sciences, Professor, Gomel State Medical University (Gomel)

Vladimir M. Tsyrukunov, Doctor of Medical Sciences, Professor, Grodno State Medical University (Grodno)

Gulmira A. Utepbergenova, Doctor of Medical Sciences, Professor, Kazakhstan Medical Academy (Shymkent, Kazakhstan)

## Russia

### Editor-In-Chief

**Vladimir P. Chulanov**, Chief Specialist in Infectious Diseases of the Russian Ministry of Health, Professor of the Department of Infectious Diseases of the I.M. Sechenov First Moscow State Medical University of the Russian Ministry of Health, Deputy Director for Research and Innovative Development of the National Medical Research Center for Phthiisopulmonology and Infectious Diseases of the Russian Ministry of Health, Doctor of Medical Sciences (Moscow)

### Editorial Council:

Viktor V. Maleev, Academician of the Russian Academy of Sciences, Doctor of Medical Sciences, Professor, Central Research Institute of Epidemiology of Rospotrebnadzor (Moscow)

Elena V. Volchkova, Doctor of Medical Sciences, Professor, I.M. Sechenov First Moscow State Medical University of the Ministry of Health of the Russian Federation (Moscow)

Amangul K. Duisenova, Doctor of Medical Sciences, Professor, Kazakh National Medical University named after S.D. Asfendiyarov (Almaty, Kazakhstan)

Narina C. Sargsyants, Candidate of Medical Sciences, National Institute of Health, Ministry of Health of the Republic of Armenia (Yerevan, Armenia)

Igor A. Karpov, Corresponding Member of the National Academy of Sciences of Belarus, Doctor of Medical Sciences, Professor, Belarusian State Medical University (Minsk, Belarus)

Igor O. Stoma, Doctor of Medical Sciences, Professor, Gomel State Medical University (Gomel, Belarus)

Vladimir V. Nikiforov, Doctor of Medical Sciences, Professor, Pirogov Russian National Research Medical University (Moscow)

Olga I. Sagalova, Doctor of Medical Sciences, Professor, South Ural State Medical University of the Ministry of Health of the Russian Federation (Chelyabinsk)

Goran Stevanovic, Director, Clinic for Infectious and Tropical Diseases, University Clinical Centre of Serbia (Belgrade, Republic of Serbia)

Alexander N. Lukashev, Doctor of Medical Sciences, Professor, Corresponding Member of the Russian Academy of Sciences, E.I. Martsinovsky Institute of Medical Parasitology, Tropical and Transmissible Diseases, Sechenov University, Ministry of Health of the Russian Federation (Moscow)

---

### Peer-reviewed publication

The journal is included in the databases Scopus, RSCI, Ulrich's Periodicals Directory, EBSCO, CNKI.

The journal is included into a List of scientific publications of the Republic of Belarus for the publication of the results of the dissertation research. HCC board decision of 06/27/2013 (protocol № 15/3).

Authors are responsible for the accuracy of the facts, quotes, names and other information, and for disclosure of the indicated information.

Editors can publish articles in order of discussion without sharing the author's opinion.

Responsibility for the content of advertising materials and publications with the mark "On the Rights of Advertising" are advertisers.

## **Water Sources Pollution**

*Abdulsalam F. Shtaiwi, Sasan Saghayan*  
Design and Implementation of  
Monitoring and Control System  
for Drinking Water Management  
System Based on Internet of Things  
Structure ..... 4

*Layth Yousif Jebur, Mohsen Kadhim  
Muttaleb, Shaymaa Awad Kadhim,  
Ahmed Alshewered*  
Dangers of Elevated Radon Gas  
Concentration in Surface  
and Ground Waters in Al-Haydaria  
Agricultural Areas, Al-Najaf, Iraq ..... 14

*Alyaa Hussein Talib, Ihsan Flayyih  
Hasan AL-Jawhari*  
Biological Decolorization of Congo  
Red from Textile Effluent and  
Wastewater by *Aspergillus Terreus*,  
and *Penicillium Funiculosum* ..... 26

*Narjes Fadhil Abbas, Salih Hassan  
Jazza, Neran Adnan Abbas Al-Naqeeb*  
Assessment of Water Quality  
in Al-Musharh River  
in Maysan Province ..... 39

*Alyaa A. Hafed, Muslim Abdulrahman  
Mohammed, Adnan Issa Al-Badran*  
Pulmonary Infection  
with *Acanthamoeba Polyphaga*:  
Case Report ..... 46

## **Infectious and Parasitic Diseases**

*Mohamad J. Makki, Waleed K.  
Ghanim, Muhsin S.G. Al-Moziel*  
Evaluate the Lung-Protective Effects  
of Hidrosmin and/or Vitamin C  
in Reducing Lung Fibrosis Caused  
by Bleomycin in Rats ..... 50

*Rasha Jawad Kadhim,  
Basim Hashim Abdullah*  
First Record of Four Species  
of Trematodes Parasitizing Stray  
Cat *Felis Catus* L. .... 61

*Shadia Alhamd*  
Evaluation of GAPDH  
and EF1a Genes as Reference  
Genes in Molly Fish ..... 70

*Mohammed Younus Naji Al Atbee,  
Hala Sami Tuama, Jawad Ibrahim  
Rasheed, Ali Jasim Al Saedi*  
Prevalence of Peritonitis  
in Continuous Ambulatory  
Peritoneal Dialysis Patients:  
Bacteriology Analysis ..... 78

*Naseer Malaky Abbood,  
Ihsan Hameed Khudhair*  
The Adulticidal and Repellent Effect  
of Some Doped Nanoparticles  
in Southern Cowpea Beetle  
(*Coleoptera: Bruchidae*)  
*Callosobruchus Maculatus* F) ..... 89

*Adian A. Dakl, Ikram A. Al-Samrraee*  
Histopathological Alterations  
Caused by *Klebsiella Pneumoniae*  
Infection in Rabbits and the  
Preventive Effects of Whole  
Sonicated Killed Antigen  
and *Albizia Lebbeck* Extract ..... 96

*Zainab Akram, Eman M. Jarallah*  
Antibiotic Resistance Profile  
of *Staphylococcus Aureus* Isolated  
from Milk and Dairy Products ..... 105

<https://doi.org/10.34883/PI.2025.14.1.052>

Abdulsalam F. Shtaiwi , Sasan Saghayan  
Engineering Technical College, University of Shatt AL-Arab, Iraq

# Design and Implementation of Monitoring and Control System for Drinking Water Management System Based on Internet of Things Structure

**Conflict of interest:** nothing to declare.

**Authors' contribution:** Abdulsalam F. Shtaiwi – data curation, investigation, methodology, project administration, resources, software, validation, visualization, writing – original draft and writing – review & editing; Sasan Saghayan – data curation, investigation, methodology, project administration, supervision, validation, visualization, writing – original draft and writing – review & editing.

The article is published in author's edition.

Submitted: 20.01.2025

Accepted: 17.03.2025

Contacts: [abdulsalam.faisal@sa-uc.edu.iq](mailto:abdulsalam.faisal@sa-uc.edu.iq)

## Abstract

**Introduction.** The drinking water quality control program is an important and necessary program that due to the lack of water suitable for human consumption, it is necessary to create an artificial intelligence system to connect drinking water treatment plants.

**Purpose.** The aim of the current study was monitoring turbidity, pH in water treatment plants in Basrah by using Internet of things (IoT) in addition to its related sensors.

**Materials and methods.** In this research, five raw water treatment plants of the Shatt al-Arab river were investigated and the data was analyzed by sensors connected to the system and the data was automatically performed through the online water quality monitoring system Half-liter samples were taken at different times from the aforementioned stations and analyzed.

**Results.** The pH was practically 6.96 to 7.24 H+ within the required standard, 6.5 to 8.5 H+. Practically turbidity 1.65 to 1.84 ntu (Nephelometric turbidity unit) was beyond the measurements standard, 0 to 0.5 ntu is required.

**Conclusion.** Using IOT in monitoring drinking water turbidity and pH proved that it is an effective method and can help in control the quality of water.

**Keywords:** IOT, turbidity sensor, PH sensor, WiFi module, drinking water

## ■ INTRODUCTION

Pollution of water crisis is considered the number one global threat [1]. Low water quality spreads disease and causes deaths and disrupts socio-economic development, with more than 485,000 deaths a year, the majority of which are children in developing countries. Predictive models estimate that global water consumption will double in the next 20 years [2]. Shatt al-Arab water suffers from severe salinity, which has led to the deterioration of the environmental situation in Basra, which has doubled as a result of the high concentration of total soluble solids (TDS) and salinity. Water shortages have led to the depletion of drinking water supplied by desalination plants and the increase in

salt in some liquefaction projects, which are the responsibility of the relevant authorities to address the problem with its dimensions, risks and challenges. In order to protect the environment, the focus has been on salinity, because this is the main problem of the Shatt al-Arab River. The suitable pH for drinking water is 6.5–8.5. When water contaminated with high concentrations of particles, it becomes turbid which increases the possibility of infected with diseases [3]. The "IoT" means that data is transported through the internet from an object or device with the need of specific devices including sensors for controlling the process. These devices include "Intel Galileo", "Raspberry Pi", "Arduino-dependent processor" [4]. It is very important issue to use "IoT" to make every part of life easy and perfect including controlling the water quality. Controlling the pH and turbidity becomes possible in the presence of "IoT". As a routine work, laboratories Provide specific tests to check water quality but these tests need time and a lot of equipment and materials [5]. In the opposite way "IoT" provides monitoring water quality by a different principle, sensors and microcontroller provide all the work needed for detection and monitoring pH and turbidity through the use of technology of WiFi and wireless technology [6].

Between December 2017 and March 2018, researchers examined several physical and chemical indicators at the Al-bradiah water treatment plants in Basra, comparing them to World Health Organization (WHO) and Iraqi standard levels. Except for the pH value, which was 6.9 and within allowed limits, the treatment water characteristics such as turbidity and total suspended solids (TSS) were found to be greater than the WHO and Iraqi standard standards. Other than drinking and cooking, the community began to use the water provided by the plants. Drinking water is typically purchased in containers from private vendors (reverse osmosis water) or supplied in bulk by tank truckers [7].

Many problems regarding to water quality can be avoided by using "IoT" in addition to its related sensors. In that case this provides a chance for monitoring turbidity, pH, temperature and other factors regarding to water quality .IoT allows for new smart systems that are capable of real time water quality monitoring and are smart enough to inter that data. This is a cheap and reliable way to allow environmental management and minimise human health issues [8].

The rapid population growth necessitates the provision of safe, inexpensive water that meets human demands. Because of global climate change, water will be a concern in the future. To maintain water quality and availability, effective water management and treatment is required. The Internet of things (IoT) and information and communication technologies (ICT) are integrated to improve water management and provide efficient operation of water resources. Distribution system that incorporate the IOT and cloud computing technologies with ICT. This architecture is designed for intermittent water supply while the previous works supposed a continuous water supply.no practical step is taken towards any phase, it contains all the theoretical requirements necessary to implement such system especially in third-world countries where the water supply is intermittent. A review of ICT-based water distribution management is provided and an over view of the most promising technologies related to them are thus explained [9].

Olatinwo and Joubert in 2019 demonstrated new wireless technologies in order to see how they could be employed in wireless sensor network systems for water quality monitoring. New communication technologies that are suitable for WSN solution in WQM applications due to the inefficiency such as short communication range and high power

consumption of the legacy communication networks often combined with the WSN systems in WQM applications to achieve this, long range and low power communication networks are desired in WQM applications [10].

Over the time, the user's water can use a smart water-monitoring-system which be predict and propose. This gets advantages of the Internet of Things (IoT). The water flow-sensor input within a NodeMCU 8266 micro-controller. Then mounted a micro-processor device within sensors in the drain. When the information are collected and saved in the cloud storage. This device help user's in maintaining their water utilize in good real-time. By this, we can view the portal of the water used online. Any procedures for water usage are transported to a cloud storage. After that, dictionaries calculate the water monitoring amount information gathered. All water use operations are embedded upon the group of greater or fewer water utilized. In addition, the behavior can be predicted depend on the water volume ingested [11].

With regard to the above research, our research depends on sending data continuously to the control center for the purpose of displaying the data obtained from the filtration stations and presenting the results in real time, unlike the current practice of laboratory testing of water quality in varying periods, which affects water quality, as well as the loss of laboratory materials, human effort, time and the proposal The future is to link the filtration stations from the control center with the R-Zero station, which pumps fresh water to the desalination plants in Basra for the purpose of mixing it with the raw water coming from the Shatt al-Arab. Thus, we have controlled the waste in the fresh water of the filtration stations in which he is currently working through our system, the Internet of Things.

## ■ MATERIALS AND METHODS

In the current research, the idea was how to control and test the drinking water using Internet of things. First step was connecting the network (card, sensors, power supply). The circuit included the Arduino Uno card and the PH sensor and Turbidity sensor that connected through amplification card to Arduino Uno pins. The power used here from the port of USB of laptop (5Volt) supply Arduino Uno card and Arduino Uno card supply the PH and Turbidity sensors by (5Volt). Installation of testing of water quality sampling illustrated in (Fig. 5, 6). The ESP8266NodeMCU was connected with the same circuit, connected the serial pins between Arduino Uno and ESP8266NodeMCU to transfer the data of sampling through the internet. The power of ESP8288NodeMCU was used from Arduino card supply. After installation of network we download Arduino IDE for programming the Arduino Uno card& ESP8266NodeMCU testing samples of drinking water from water treatment station in Basrah city in real time. Different samples were collected from different water treatment stations in Basrah. Sampling was from North Basrah station and South; (Qurna water station) North of Basrah, (Thagir water station) North of Basrah, (Jubiala station) in city center and (Um quasar station) West South of Basrah, (Sebaa station) South of Basrah. Sampling and test in our network and recording test results was done. The designed network included internet of things connected through all water treatment stations in Basrah city to collect the data testing through monitoring data of water quality in real time. Data collected from the sensors was send to Arduino card. Then data transferred by the serial port to MCU. A connection was between MCU and WiFi that enabled transferring data through I cloud to managing room.

### PH sensor

Type SENO161 pH meter (Fig. 1) for water quality test power 5V, range for measuring 0–14 PH accuracy 0.1 PH, response  $\leq 1$  min. Measuring PH in water. The range of PH from 0 to 14, PH=7 means natural, PH less than 7 means acidity, PH greater than 7 means base that measuring amount of free hydrogen in water. According to international standard the save range of PH in drinking water is (6.5 to 8.5).

### Turbidity sensor (Fig. 1)

Type SENO 189 for water quality test work, analog voltage o/p 0 to 4.5v.

Work on 5V DC voltage compatible with Arduino measuring turbidity of water quality.

### Arduino Uno card (Fig. 1)

ATmega 328P microcontroller 8bits AVR family work on 5V, analog I/P pins(A0-A5), Flash memory 32KB, SRAM, 2KB, EPROM:4KB.

### ESP8266 NodeMCU (Fig. 2)

ESP8266 NodeMCU came with USB input it is work with digital Write, digital Read, analog Write, analog Read it is low power consumption. It is a highly integrated chip designed for your network needs and provides a complete Wi-Fi solution.

Features of ESP8266 NodeMCU (Fig. 2) are powerful onboard processing and storage capabilities that allow it to be combined with other sensors and devices. The development board is a true plug- and-play solution for inexpensive projects using Wi-Fi. The IoT board contains an integrated ESP8266 module with every (GPIO) (General purpose input/output) and power supply all in one easy-to-use package (Fig. 3 and 4). The work flow shown in (Fig. 5).

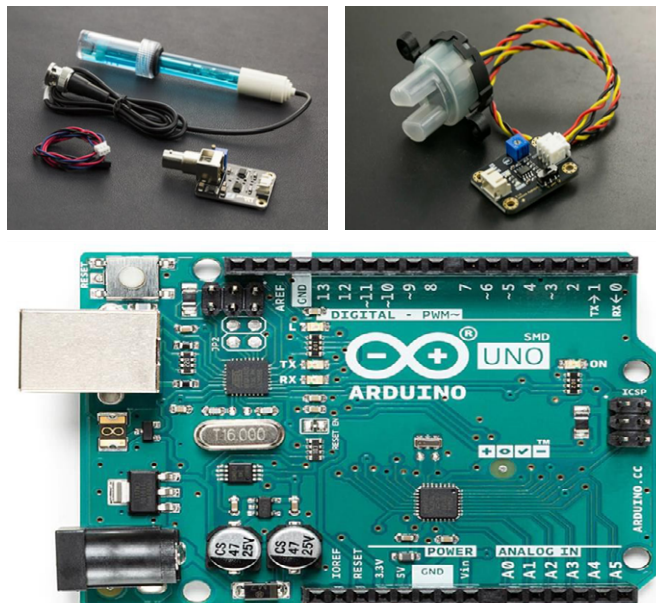


**Fig. 1. pH Sensor, turbidity sensor and Arduino Uno card**

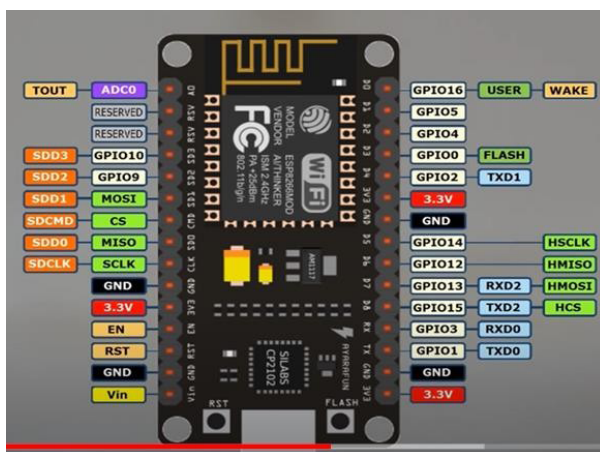


**Fig. 2. ESP8266 NodeMCU**



**Fig. 3. The sample Water quality control using IOT**

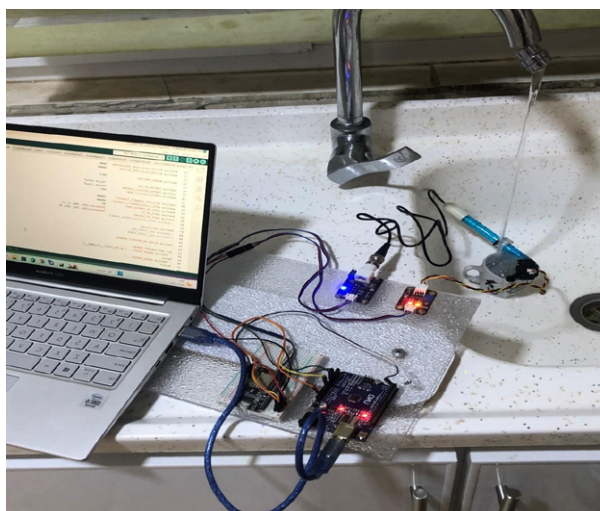


**Fig. 4. On line Water quality control using IOT (in real-time)**

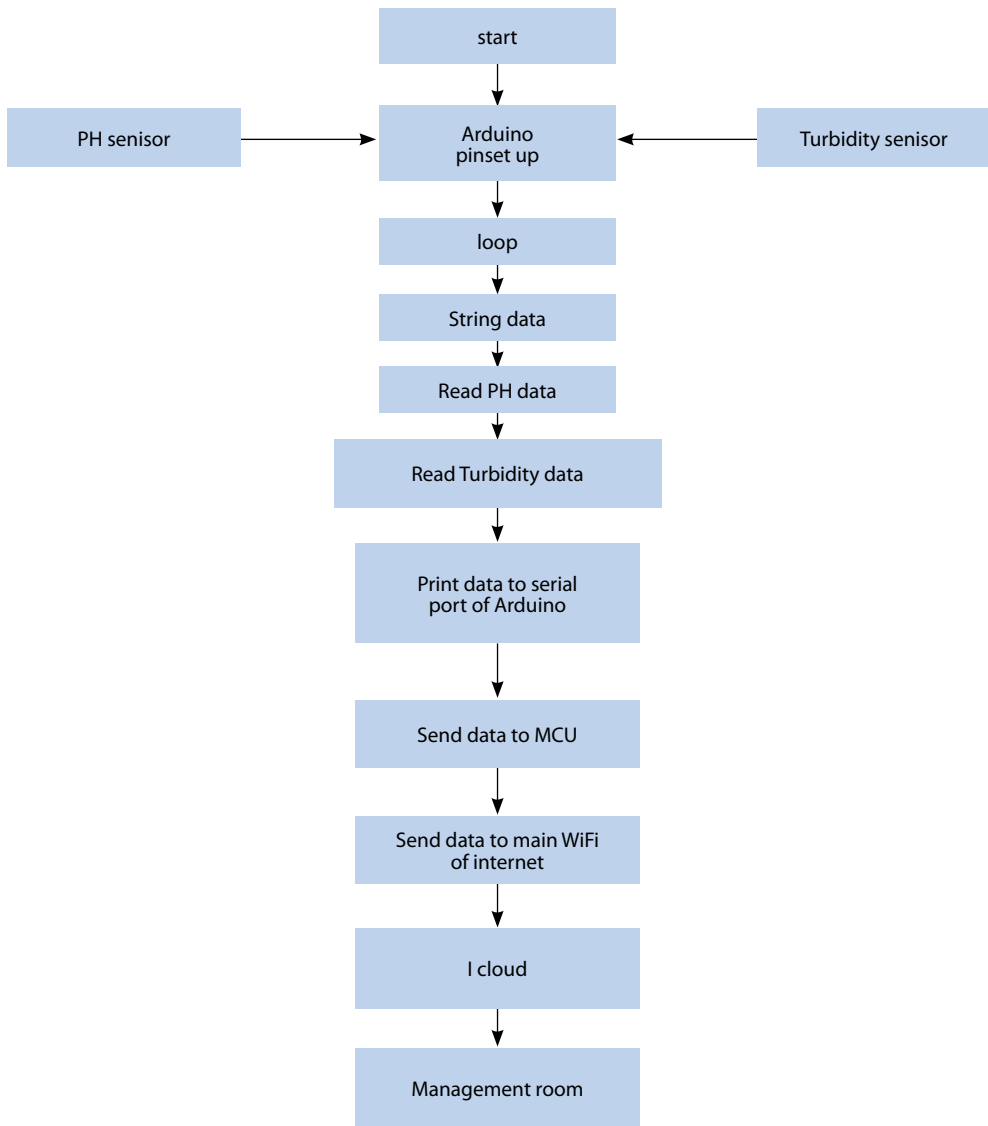


**Fig. 5. Work flow diagram**

## ■ RESULTS

### **PH AND Turbidity test drinking water (Jubaila treatment station)**

Result of testing the PH of (Jubaila treatment station) indicated pH test values varies between 6.97–6.98 within normal range 6.5 to 8.5 while turbidity testing showed 1.71–1.72 ntu outside normal range 0–0.5 ntu (Table 1, 2 and Fig. 6, 7).

**Table 1**  
**PH & Turbidity test drinking water (Jubaila treatment station) (city center) of Basrah In 8/5/2022**

NO	PH(Test)	PH(Standard)	NO	Turbidit (Test) (ntu)	Turbidity(standard) (ntu)
1	6.98905	7	1	1.727349	0.5
2	6.98833	7	2	1.727349	0.5
3	6.98742	7	3	1.727349	0.5
4	6.98800	7	4	1.726121	0.5
5	6.988926	7	5	1.72500	0.5
6	6.988554	7	6	1.72472	0.5
7	6.98800	7	7	1.72420	0.5
8	6.987321	7	8	1.72361	0.5
9	6.98600	7	9	1.72243	0.5
10	6.984823	7	10	1.72000	0.5
11	6.98405	7	11	1.71921	0.5
12	6.98400	7	12	1.71739	0.5
13	6.92967	7	13	1.71642	0.5
14	6.98237	7	14	1.71500	0.5
15	6.98200	7	15	1.71433	0.5
16	6.98120	7	16	1.71397	0.5
17	6.98054	7	17	1.71100	0.5
18	6.98026	7	18	1.71000	0.5
19	6.98000	7	19	1.70938	0.5
20	6.979942	7	20	1.70761	0.5
21	6.975532	7	21	1.70500	0.5
22	6.971689	7	22	1.70462	0.5
23	6.971103	7	23	1.70399	0.5
24	6.98054	7	24	1.70500	0.5
25	6.98400	7	25	1.70623	0.5
26	6.980936	7	26	1.71983	0.5
27	6.97857	7	27	1.72206	0.5
28	6.97857	7	28	1.72734	0.5
29	6.97253	7	29	1.72734	0.5
30	6.97821	7	30	1.72734	0.5

**Table 2**  
**Results for all treatment stations**

NO	Station	PH Test	Turbidity (ntu) Test	PH-Normal (6.5–8.5)	Turbidity-Normal (0–0.5) ntu	Sample date
1	Jubaila in Basra	6.96–6.98	1.71–1.72	Normal	Out of range	12/3/2022
2	Seeb (south-east) Basra 65Km	7.21–7.24	1.67	Normal	Out of range	6/2/2022
3	Qurna (North) Basra 75Km	7.21–7.22	1.6–1.65	Normal	Out of range	17/2/2022
4	Thagair (North) Basra 90Km	7.18–7.19	1.844	Normal	Out of range	17/2/2022
5	Um-Quasar (south-west) Basra 85Km	7.16–7.18	1.798	Normal	Out of range	25/1/2022

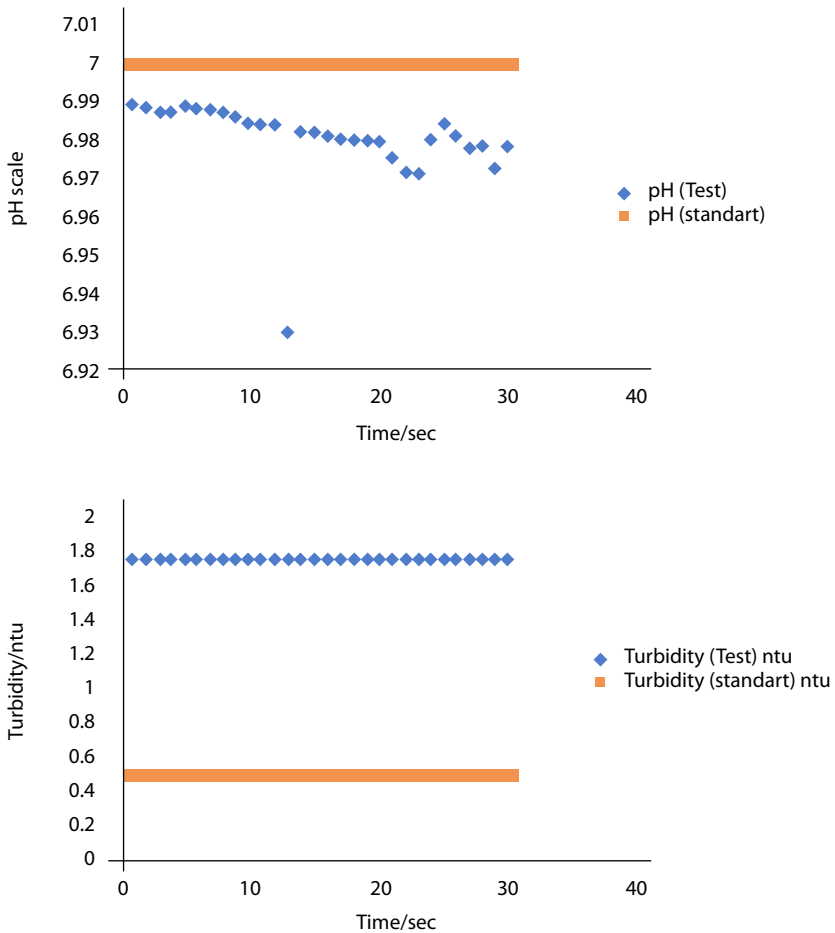


**Fig. 6. Calculation PH and Turbidity in Jubaila water treatment plant**

## ■ DISCUSSION

It is possible to configure a wireless system that adopts the technologies of IoT with high efficiency and low cost and to give results in the real time to give accurate results for testing drinking water quality. This technology can be used now and in the future in smart home that use (IoT) technology in it. A study of water treatment plants such as turbidity data, it was found that the performance is much higher than 98% according to drinking water measurements in Iraq, but now the study showed that the real performance is 68% and in violation of international standards for the environment and this is a matter that deserves consideration. It is better to examine and operate the plants according to modern methods and according to international directives. Results of research found that some of water treatment plants in Basra city the quality of water treatment used only for irrigation not for drinking to improve the treatment process reduce of mixing the

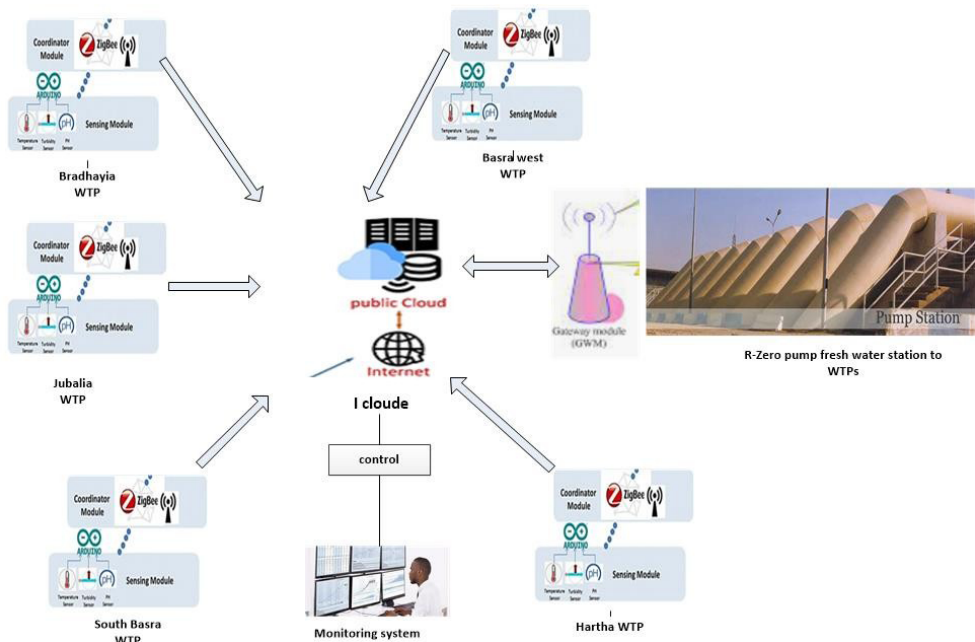


**Fig. 7. Proposal of IoT structure in treatment plants**

R-Zero project)with water come from Shatt Al-Arab river. R-Zero station is connected to a canal that supplies the station from the Al-Badaa project. This canal is the only source that supplies the water treatment plant in Basra with raw water of low salt in relation to the water of the Shatt al-Arab River, which is turbid and has a high salt content. The length of the canal is about 180 km from Basra city. It supplies water from the Tigris River to the R-Zero station). A study in 2012, 2013, 2014 the data result of measuring drinking quality test under the specification of international limit and the drinking water from water treatment not suitable for human used [12]. Through the research listed above, it is clear that the desalination plants that supply water through the liquefaction network of the city of Basra are in a critical condition, due to the adoption of the water supply to the purification stations scattered along the Shatt al-Arab River from the special canal that transports water from the Tigris River in the Al-Badaa region and a length of about 180 km to mix this water with the water of the Shatt al-Arab River and its treatment in desalination plants. Therefore, the percentage of purity and turbidity of the filtered water depends on the mixing ratio and the availability of water transported through the channel. It is evident from this that the treatment plants do not depend mainly on the water of the Shatt al-Arab River, so in our research, and given the critical situation of the drinking water treatment process, it is necessary to find continuous monitoring of data on the quality of drinking water, with low costs and receive data in real time, so we have relied on remote monitoring via the Internet and using IoT structure to get accurate data on water quality instead of the traditional test in lap, which results in slow response and inaccuracy in the

data, adding cost in materials and effort and instead of this a simple electronic circuit with low cost and high speed in reading the data on real-time. The information can be read through the mobile or specific monitoring systems. These systems can be developed in the future to give data and use more sensors to give an integrated program about the systems used for IoT to connect that structure with control network to perform the suitable mixing for water treatment plants in Fig. 7 as well as the use of alternative energy and solar energy in its operation.

## ■ CONCLUSIONS

Using IOT in monitoring drinking water turbidity and pH proved that it is an effective method and can help in control the quality of water. Water treatment plants station via an electronic platform using internet of things due to the critical condition of the Shatt Al-Arab River. It is recommended to connect these systems with solar energy to continue sending data to control points. Connecting these systems with the pumping centers with the treatment and coming from the R-Zero pumping centers to control the amount of mixing with the raw water from the Shatt Al-Arab River to produce water suitable for consumption. Other sensors can be added to control pollutants such as chemicals and hydrogen sulfide gas.

## ■ REFERENCES

1. Kedia N. Water quality monitoring for rural areas – a Sensor Cloud based economical project, 2015 1st International Conference on Next Generation Computing Technologies (NGCT). Dehradun, India, 2015:50–54.
2. WHO (World Health Organization). Drinking-water, 2019. [https://www.essentialneed.org/education/world-water-data?gad\\_source=1&gclid=Cj0KCQjw8-2BhCHARisAF\\_w1gy0QY8FKn0aK0YbTpWmrixaFdi2l2Mjd7y-LVUxuotEILw5eIJtrBcaAuCwEALw\\_wcB](https://www.essentialneed.org/education/world-water-data?gad_source=1&gclid=Cj0KCQjw8-2BhCHARisAF_w1gy0QY8FKn0aK0YbTpWmrixaFdi2l2Mjd7y-LVUxuotEILw5eIJtrBcaAuCwEALw_wcB)
3. Daigavane V, Gaikwad M. Advances in wireless and mobile communications. 2017;10(5):1107–1116.
4. Sachio S, Noertjahyana A, Lim R. 3rd Technology Innovation Management and Engineering Science Int. Conf. 2018;1–5.
5. Khatri P, Gupta KK, Gupta RK. Assessment of Water Quality Parameters in Real-Time Environment. *SN Comput. Sci.* 2020;1:6.
6. Sugapriyaa T, Rakshaya S, Ramyadevi K, et al. Smart water quality monitoring system for real time applications. *Int. J. Pure Appl. Math.* 2018;118:1363–1369.
7. Al Chalabi AS. Assessment of Drinking Water Quality and the Efficiency of the Al-Buradieiah Water Treatment Plant in Basra City. *Nat. Environ. Poll. Technol.* 2020;19:1057–1065.
8. Maher D. IOT for fresh water quality monitoring (PhD Thesis). 2018.
9. Alshattnawi SK. International Conference on New Trends in Computing Sciences (ICTCS)/ *IEEE.* 2017;289–294.
10. Olatinwo S, Joubert T. Enabling communication networks for water quality monitoring applications: A survey. *IEEE Access.* 2019;7:100332–100362.
11. Hasibuan AA, Fahrianto F. International Conference on Cyber and IT Service Management (CITSM 2019). 2019;1–7.
12. Jan F, Min-Allah N, Düşteğör D. IoT Based Smart Water Quality Monitoring: Recent Techniques, Trends and Challenges for Domestic Applications. *Water.* 2021;3(131):729.

<https://doi.org/10.34883/PI.2025.14.1.056>

Layth Yousif Jebur<sup>1</sup>, Mohsen Kadhim Muttaleb<sup>2</sup>, Shaymaa Awad Kadhim<sup>3</sup>,  
Ahmed Alshewered<sup>4</sup> ✉

<sup>1</sup> College of Medical Technology, Islamic University, Najaf, Iraq

<sup>2</sup> College of Science, University of Babylon, Babylon, Iraq

<sup>3</sup> Faculty of Science, University of Kufa, Najaf, Iraq

<sup>4</sup> Misan Radiation Oncology Center, Misan, Iraq

## Dangers of Elevated Radon Gas Concentration in Surface and Ground Waters in Al-Haydaria Agricultural Areas, Al-Najaf, Iraq

**Conflict of interest:** nothing to declare.

**Authors' contribution:** Layth Yousif Jebur – data curation, investigation, methodology, resources, validation, visualization, writing – original draft and writing – review & editing; Mohsen Kadhim Muttaleb – investigation, methodology, resources, validation, visualization, writing – original draft and writing – review & editing; Shaymaa Awad Kadhim – data curation, investigation, methodology, resources, visualization, writing – original draft and writing – review & editing; Ahmed Alshewered – investigation, software, validation, visualization, writing – original draft and writing – review & editing.  
The article is published in author's edition.

Submitted: 20.01.2025

Accepted: 17.03.2025

Contacts: Ahmedsalihdr2008@yahoo.com

### Abstract

**Introduction.** Water is essential element of life, therefore watching water quality is of high necessity. The research in front of us dealing with measurement of <sup>222</sup>Rn concentrations in 40 water samples, of two sources: 20 samples of surface water, and another 20 samples of ground water.

**Materials and methods.** These samples are collected from different spots in agricultural areas, in Al-hayderiah, Al-Najaf governorate, Iraq. This experimental study is done by measuring <sup>222</sup>Rn levels in surface and in ground waters using RAD-7 detectors.

**Results.** The average value of <sup>222</sup>Rn concentrations, in Bq/L, for the two types of water (surface and ground water) samples were: extended from 0.036±0.072 Bq/L to 0.144±0.051 Bq/L and the average value is 0.077±0.042 Bq/L for surface water, while for the ground water samples the concentrations were started from a value of 0.036±0.072 Bq/L to a value of 0.433±0.273 Bq/L and the average value is 0.207±0.125 Bq/L.

**Conclusion.** For both instances the levels were found to be within the internationally acceptable limits, that are complied with the recommendations advised by several notable international organizations and committees, including the EPA, WHO, UNSCEAR, and ICRP. Based on the study's findings, it seems safe to assume that the alpha emitter found in the majority of the water samples in this investigation poses no threat to human health.

**Keywords:** RAD-7 detector, annual effective dose, surface water, ground water

## ■ INTRODUCTION

Radon is one of the rarest radioactive noble gases, usually found in the nature as one of the products of uranium-238 decay process. Radon owns nor odor and is tasteless, as well as it has no colour. This noble radioactive gas undergoes decaying process by emitting alpha particles that are distinguished by having characteristic chunks of energy, leading to formation of a set of briefly-lived radionuclides (for example polonium-218 and polonium-214). The half-life of Radon is (3.82 days), relatively long compared to some of its progenies, and it is sufficiently enough to be detected and measured. The surface of the soil is considered as the most important source of radon gas in the atmosphere. In addition to that, secondary sources contribute to the total concentration of Radon in the nature, like the ground and surface water, natural gases and volcanic eruptions, and other resources [1].

Natural radionuclides in water can be traced to their point of origin and to human activity in certain regions where fertilizers are utilized for agricultural purposes [2]. A number of trace elements found in fertilization products, including radon gas, have the ability to increase the amount of these naturally occurring radionuclides in the soil. Radiation exposure in surface and/or groundwater may increase as a result of industrial activities and processes that include the purification and processing of earth minerals or their by-products.

The surrounding rocks or lithological solid aquifers, which serve as reservoirs for groundwater that is accessed by wells and boreholes, may contain radionuclides. It is well knowledge that geological materials like solid aquifers and rocks contain trace levels of radioactive elements like radon gas. This element dissolves into groundwater due to the interaction of rocks, water, and soil [3–5].

Therefore, in contrast to other parts of the province of Al-Najaf, some chemicals and pesticides are utilized more frequently in these agricultural areas. As such, the measurement of radon levels has risen to prominence as one of the most pressing concerns related to the protection of human health from radioactive sources.

Radon exposure is likely to occur as a result of using contaminated water for common home activities like showering, dishwashing, cooking, and drinking. To measure the radon concentrations, Water samples are handled with the RAD-7 and RAD H20 accessories [6]. Recently, numerous nations have begun to use various procedures for measuring radionuclide amounts in water sources across their territory [7–11].

Radon levels in ground and surface water samples collected in the Al-Hadariah area were analyzed in the current investigation using a RAD-7 detector. In addition, the effective annual dose was determined for each of the water samples in relation to various age groups and lifetime cancer risk.

To that end, this research aims to assess radon concentrations in both groundwater and surface water samples from the Al-Haydariah district in the Najaf Governorate.

The reasons this area was selected for research were:

- First: how underground water has altered the region's rock structure.
- Second: the lack of environmental radiation revisions for this region.
- Third: this location's agricultural significance.

## ■ MATERIALS AND METHODS

The detector of the solid state RAD7 is a very helpful apparatus for this study. Figure 1 reveals a detector of solid-state which is manufactured from a material that has conductivity value lies between a conductor and an insulator (semiconductor silicon substance) that changes the energy of alpha particle radiation emitted because of the decomposition of a radioactive molecule  $^{218}\text{Po}$  or  $^{214}\text{Po}$  and it can distinguish between the two isotopes: the RAD7 can select the type of the isotope passing by the means of the recognition between them, by filtering of different electronic energy corresponding By means of an electrical signal, directly to alpha particles. Radon isotopes, specifically  $^{218}\text{Po}$ , a noble gas, release alpha energy at 6 MeV as  $^{214}\text{Po}$  or 7.97 MeV [12]. The radon gas isotopes  $^{218}\text{Po}$  propel alpha particles with an energy ranging from 6 MeV to 7.97 MeV. The RAD7 cell has a size of 0.7 liters, and may be in the shape of a hemisphere as we can see it in the down image. In the figure 2, it is shown that the specially painted electric connector is supplied with elevated voltage supplier equipment, that exerts the starting high-level voltage of about 2000 to 2500 volts all over the half ball shape (hemisphere). This initiates a field of electricity throughout the place. Because of the charged particles it contains, the detector cell produces a positive electrical field. Inside the cell, as  $^{222}\text{Rn}$  atoms decay, a positive charge  $^{218}\text{Po}$  is produced and interacts with the counter (detector), the detector's innermost core. The degrading atoms,  $^{222}\text{Rn}$ , in the inner side of the cell and creating a positive charge  $^{218}\text{Po}$  has a relatively short lifespan, and upon decomposition, it has an equal probability of 50% to impact the detector. This impact results in the generation of an electrical pulse current in the device along with alpha particle energies [13].

A RAD7 add-on that consistently tests for radon at different levels in water used for household purposes is the RAD H2O. After collecting a water sample, it can provide a radon concentration reading in as little as one hour [14].

The RADH2O employs the standard protocols previously established for the RAD7 to accurately measure the concentration of Radon in the water samples being investigated. Thanks to a consistent conversion coefficient, the quantity or concentration of radon in a water sample can be determined by twice the amount of radon per unit size present in the air loop.

A coefficient of conversion to 4 of a 250 ml water sample vial is calculated by applying the volumes of the air circulation, the sample, and the radon distribution equilibrium coefficient at the usual ambient temperature. A system of closed circulation of air system (closed-loop aeration system) is applied during the procedure. The method in which the liquids (air and water) volumes are preserved at the starting level and unaltered by the flow rate. The Wet 250 water protocol check lasts nearly for half an hour to finish. At the start of the assessment, the RAD7's internal pump initiates automatically, running for a duration of 300 seconds (5 minutes). This process aerates the sample and conveys radon gas, free of other gases, to the RAD7 measurement cell. During the entire 300-second cycle, over 94 percent of the accessible radon is extracted from the water. The pump spontaneously stops working after a 5-minute cycle, then the machine holds on for another 5 minutes. Next, the machine restarts working and counting again. Therefore, the apparatus briefly reports the results in 5 minute cycles. The cycles continue for 30 minutes; Same the race continues for half an hour (half an hour it started operating). After four five-minute measurement cycles, the RAD7 produces a summary that includes the average radon concentration per unit size, or concentration. A cumulative spectrum, as shown

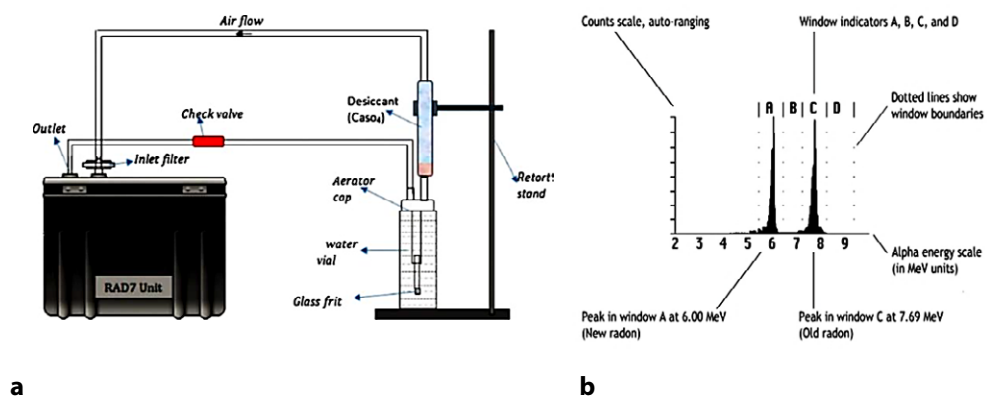


**Fig. 1. Two images presenting the cumulative operational spectrum and measurement of a water sample utilizing the RAD7: a – a visual representation displaying the spectrum of alpha particles and both elements  $^{218}\text{Po}$  and  $^{214}\text{Po}$  in channels A and C, respectively; b – Illustration demonstrating the procedure for assessing a water sample with RAD7 and its RADH2O derivatives**

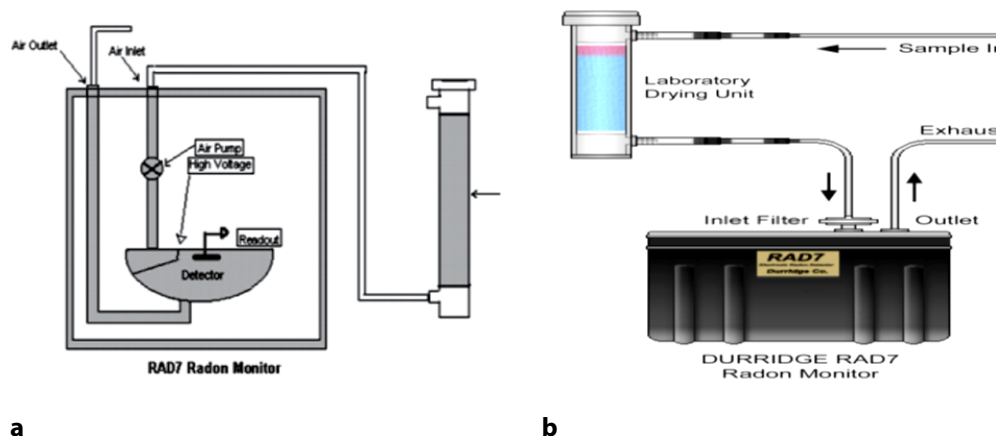


**Fig. 2. The external and internal features of the RAD7 are shown in the image and the schematic: a – the figure displays the internal RAD7; b – The figure displays the diagram in Part a**

in fig. 1a, and a bar chart displaying the measurements from the four cycles are included in this summary [15]. The Radon concentration per unit volume of water (calculated automatically by the RAD7) is depicted in Fig. 1b [16].

### Site of Study

The city of Al-Haydariyah is situated in the northern part of Al Najaf governorate in Iraq, 40 km away from the governorate center, and on the road linking the two sacred cities of Karbala and Najaf. Al-Hydariyah is an administrative sub-district of the Najaf district. Astronomically, it is located between two latitudes ( $32^{\circ}18'28'' - 32^{\circ}20'25''$ ) north and longitudes ( $44^{\circ}14'30'' - 44^{\circ}17'13''$ ) east (Fig. 3).

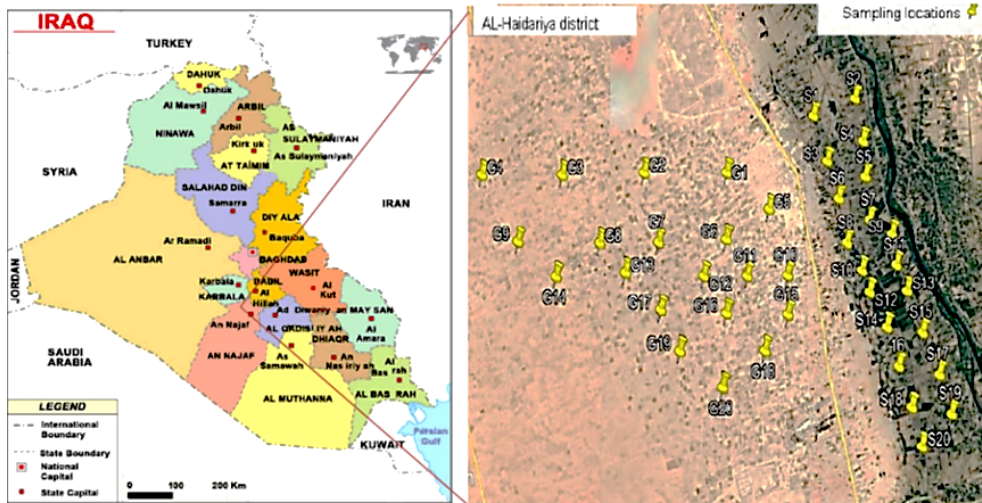


Fig. 3. Map of the study area

## ■ MATERIALS AND METHODS

In this study, 40 water samples were meticulously chosen for examination from two agricultural areas within the Al-Haydariyah region. This selection aimed to provide a comprehensive analysis of the ground and surface waters in the specified area. The sampling techniques employed were as follows: Initially, 20 groundwater samples were obtained from wells at each site, and an additional 20 samples were procured from surface water. Subsequently, each sample was carefully preserved in a 250-ml plastic container.

Moving forward, the radon levels in each sample were measured utilizing a handheld RAD-7 detector. The RAD H<sub>2</sub>O, serving as a companion kit for the RAD-7 reagent, facilitated the measurement of radon in water at concentrations less than 10 pCi/L [17]. This lightweight detector, powered by batteries, delivered precise readings in a short timeframe. The radon content in a water sample could be accurately gauged with this equipment in approximately 60 minutes. Its sensitivity is noteworthy; after about 30 minutes of testing, it can be used to obtain a single reading, matching or even exceeding that of liquid scintillation techniques [18]. After 5 minutes of aeration, the water had removed almost 95% of the radon that was present. RAD-7's inner cell's radon concentration was determined by using the following differential equations:

The following formula was used to estimate an individual's effective dosage (Ed) in (Sv/y) from <sup>222</sup>Rn in groundwater taken as drinking water [19]:

$$Ed = Ac \cdot Ai \cdot Cf \quad (1)$$

Where Ai is the yearly intake of sachet drinking water in liters, Cf is the ingested dosage conversion factor for radionuclides in Sieverts per Becquerel, and Ac is the radioactive activity content in Bq/l of sachet water. In 2000, the United Nations Scientific Committee on the Effects of Atomic Radiations (UNSCEAR) determined that the respective levels for adults, children, and newborns were 3.5 nSv/Bq, 5.9 nSv/Bq, and 23 nSv/Bq [20].

For the age groups of <1, 2–17, and  $\geq 17$  years, the yearly consumption of sachet drinking water was recorded as 230, 330, and 730 liters, respectively [21]. The lifetime cancer risk attributable to radon concentrations in drinking water can be calculated using the following equation [22]:

$$\text{lifetime cancer risk} = \text{Annual effective dose} \times \text{Average lifespan} \times \text{Risk coefficient} \quad (2)$$

Where six age groups' average lifespans were determined [23], and the risk coefficient was determined to be  $0.055 \text{ Sv}^{-1}$  based on public data (ICRP, 2007) [24]. The designated level of cancer risk is set at  $10^{-3}$  [25].

The average radon concentration in the groundwater samples was found to be below what relevant international health organizations or specialized institutions consider to be the acceptable upper limit after the data was analyzed.

## ■ RESULTS

The findings of the radon levels in each of the 20 surface water tests and the 20 ground water samples in these farming areas, which, because they make up a sizable portion of the radiation background, can irradiate a living thing, including humans, and cause a variety of diseases and disorders. When exposed to radon radioisotopes outside of the body, the human skin is thought to act as a barrier, with just two possible entry points inside the body: first by inhalation, or second by ingestion, i.e by drinking polluted water or eating polluted fruits and vegetables that are irrigated by polluted water (so that radon becomes one of the substances involved in the structure position of the fruits and vegetables).

The outcomes of  $^{222}\text{Rn}$  concentrations in this research of the 40 samples (groundwater and surface water using RAD-7) are shown in Table 1, 3, and figure 4, 7. Generally speaking, the prevailed results of radon concentration ranges of ground water 0.109–0.399 Bq/L with the mean of 0.235 Bq/L and the results of surface water 0.036–0.144 Bq/L with the mean of 0.074 Bq/L. The results exposed that radon concentration in the ground water samples have values below than the maximum globally permissible for the health of animals and

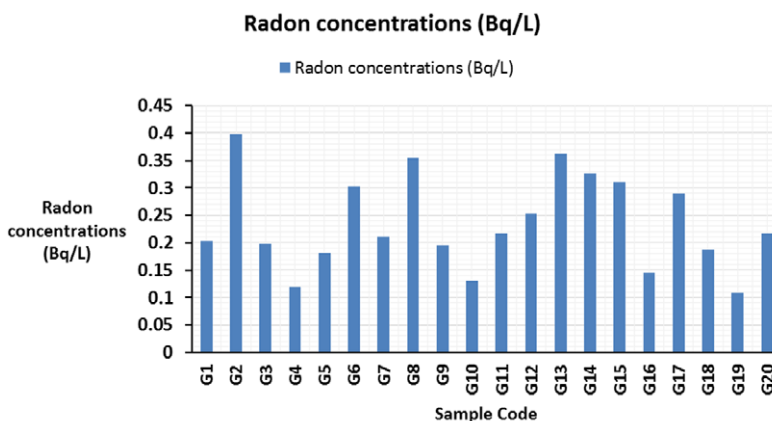


**Fig. 4. Radon concentration of ground water**

human beings. The range of total yearly effective doses that are transferred to babies through ingesting or drinking polluted ground water is 0.031–0.144  $\mu\text{Sv/y}$ , as indicated by Table 2, 4 and Figure 5, 7. The groundwater's radon content for children fell between 0.13 and 2.11  $\mu\text{Sv/y}$ . Additionally, the results obtained for adults varied from 3.07 to 39.42  $\mu\text{Sv/y}$ , with the corresponding mean values being  $27.41\pm 2.06$ ,  $10.08\pm 0.76$ , and  $13.23\pm 0.99$   $\mu\text{Sv/y}$ , respectively. Table 2, 4 shows that the results show substantial differences in the dosage rate between the age groups.

**Table 1**  
**Radon concentrations of ground water**

No.	Sample Code	Radon Concentrations (Bq/L)
1	G1	0.203
2	G2	0.399
3	G3	0.199
4	G4	0.12
5	G5	0.181
6	G6	0.302
7	G7	0.211
8	G8	0.355
9	G9	0.195
10	G10	0.13
11	G11	0.217
12	G12	0.254
13	G13	0.362
14	G14	0.326
15	G15	0.31
16	G16	0.145
17	G17	0.29
18	G18	0.188
19	G19	0.109
20	G20	0.217
Average		0.235 $\pm$ 0.02
WHO		0.5

**Table 2**  
**Annual effective dose of ground water in three age groups**

No.	Sample Code	Annual effective dose ( $\mu\text{Sv/y}$ )		
		$\leq 1$ y	2–17 y	$\geq 17$ y
1	G1	1.074	0.395	0.519
2	G2	2.111	0.777	1.019
3	G3	1.053	0.387	0.508
4	G4	0.635	0.234	0.307
5	G5	0.957	0.352	0.462
6	G6	1.598	0.588	0.772
7	G7	1.116	0.411	0.539

End of table 2

8	G8	1.878	0.691	0.907
9	G9	1.032	0.380	0.498
10	G10	0.688	0.253	0.332
11	G11	1.148	0.422	0.554
12	G12	1.344	0.495	0.649
13	G13	1.915	0.705	0.925
14	G14	1.725	0.635	0.833
15	G15	1.640	0.604	0.792
16	G16	0.767	0.282	0.370
17	G17	1.534	0.565	0.741
18	G18	0.995	0.366	0.480
19	G19	0.577	0.212	0.278
20	G20	1.148	0.422	0.554
Average		1.247±0.103	0.459±0.038	0.602±0.05
UNSCEAR		1m Sv/y		

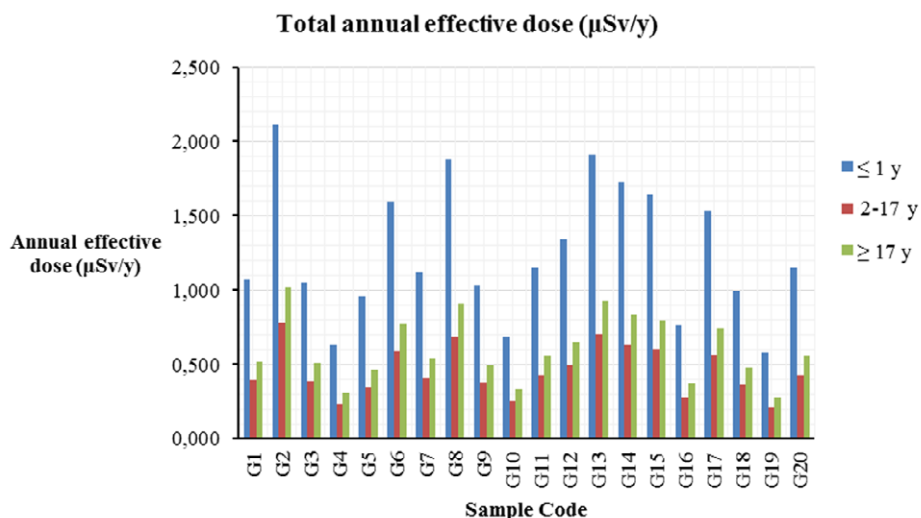


Fig. 5. Annual effective dose of ground water in three age groups

**Table 3**  
Radon concentrations of surface water

No.	Sample Code	Radon concentrations (Bq/L)
1	S1	0.036
2	S2	0.055
3	S3	0.039
4	S4	0.065
5	S5	0.041
6	S6	0.123
7	S7	0.077
8	S8	0.063

End of table 3

9	S9	0.075
10	S10	0.122
11	S11	0.072
12	S12	0.144
13	S13	0.031
14	S14	0.072
15	S15	0.044
16	S16	0.039
17	S17	0.083
18	S18	0.102
19	S19	0.096
20	S20	0.114
Average		0.074±0.008
WHO		0.5

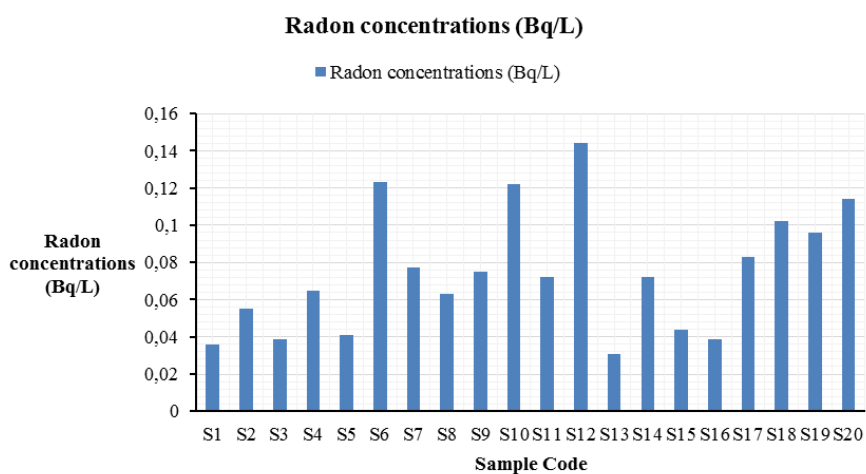


Fig. 6. Radon concentration of Surface water

**Table 4**  
Annual effective dose of surface water in three age groups

No.	Sample Code	Annual effective dose ( $\mu\text{Sv/y}$ )		
		$\leq 1$ y	2–17 y	$\geq 17$ y
1	S1	0.190	0.070	0.092
2	S2	0.291	0.107	0.141
3	S3	0.206	0.076	0.100
4	S4	0.344	0.127	0.166
5	S5	0.217	0.080	0.105
6	S6	0.651	0.239	0.314
7	S7	0.407	0.150	0.197
8	S8	0.333	0.123	0.161
9	S9	0.397	0.146	0.192
10	S10	0.645	0.238	0.312

End of table 4

11	S11	0.381	0.140	0.184
12	S12	0.762	0.280	0.368
13	S13	0.164	0.060	0.079
14	S14	0.381	0.140	0.184
15	S15	0.233	0.086	0.112
16	S16	0.206	0.076	0.100
17	S17	0.439	0.162	0.212
18	S18	0.540	0.199	0.261
19	S19	0.508	0.187	0.245
20	S20	0.603	0.222	0.291
Average		0.394	0.145	0.190
UNSCEAR		1m Sv/y		

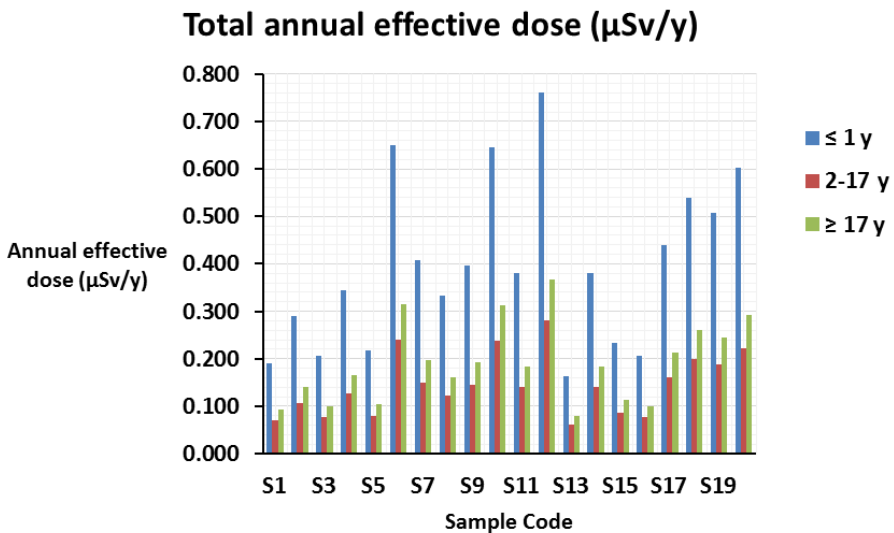


**Fig. 7. Annual effective dose of surface water in three age groups**

## ■ DISCUSSION

The outcomes of the current scientific investigation, encompassing analyses and geographical areas, are presented in Table 1 and Figure 3. Each sample underwent a four-cycle analysis, during which the mean average of the three readings was calculated for all 40 locations where water samples were collected.

According to reports from the World Health Organization (WHO), all of the results for  $^{222}\text{Rn}$  concentrations in water were found to be below the permitted limits set by the organization (0.5 Bq/L or 500 Bq/m<sup>3</sup>) for  $^{222}\text{Rn}$  concentrations in drinking water for human consumption [27, 28]. The present study's groundwater and surface water samples'  $^{222}\text{Rn}$  concentration values varied for a variety of reasons, including the water source used for collection.

Table 1 reveals variations in measurements attributed to localized aqueous testing processes, indicating radon gas levels ranging from 0.120 Bq/L to 0.399 Bq/L for groundwater and 0.036 Bq/L to 0.144 Bq/L for surface water in the selected research area. The primary study conclusion indicates that the readings for groundwater and surface water in the investigated region were, on average, 0.5 Bq/L lower than the recommended levels by major health organizations such as WHO [29]. No universally accepted concentration of radon radiation for safe use by the general population has been established. While various studies on radon concentrations in water have been conducted in Iraq [28], there are currently no defined reference levels for radon gas in water. Even in neighbouring countries to Iraq, safety requirements and standards have not been established, and they continue to rely on the levels set by the World Health Organization and UNSCAER.

## ■ CONCLUSION

The majority of the radon concentrations in the groundwater samples from Agricultural Areas in Al Hayderiah in Al-Najaf Alashraf were found to be below the levels considered to be either harmful or effective by the United States Environmental Protection Agency (EPA), the United Nations Scientific Committee on the Environment (UNSCEAR), the European Union Council (EU Council), and the World Health Organization (WHO). Consequently, it might be stated that the vast majority of samples are suitable for consumption and other household uses. For every location studied, annual effective doses were expected to be less than 100 Sv/y, regardless of age group.

## ■ REFERENCES

1. IAEA. Extent of Environmental Contamination by Naturally Occurring Radioactive Material (NORM) and Technological Options for Mitigation. *Technical Reports Series*. 2003:419.
2. Ghetti F, Checucci G, Bornman JF, editors. Environmental UV Radiation: Impact on Ecosystems and Human Health and Predictive Models: Proceedings of the NATO Advanced Study Institute on Environmental UV Radiation: Impact on Ecosystems and Human Health and Predictive Models Pisa, Italy, June 2001. Springer Science & Business Media; 2006.
3. Ahmed NK. Natural radioactivity of ground and drinking water in some areas of upper Egypt. *Turkish Journal of Engineering and Environmental Sciences*. 2004;28(6):345–54.
4. Bonotto DM, Bueno TO, Tessari BW, Silva A. The natural radioactivity in water by gross alpha and beta measurements. *Radiation Measurements*. 2009;44(1):92–101.
5. Povinec P, Hirose K, Aoyama M. Fukushima accident: radioactivity impact on the environment. *Newnes*; 2013 Jul 9.
6. Malik MF, Rabaiee NA, Jaafar MS. Determination of radon concentration in water using RAD-7 with RAD H2O accessories. In AIP Conference Proceedings. *AIP Publishing*. 2015;1657(1):120005.
7. Saidu A, Bala A. Assessment of the Specific Activity of Alpha-and Beta-emitting Radionuclides in Groundwater, Anka, Nigeria. *Iranian Journal of Medical Physics*. 2018;15(4):285–94.
8. El-Taher A, Al-Turki A. Radon activity measurements in irrigation water from Qassim Province by RAD-7. *Journal of environmental biology*. 2016;37(6):1299.
9. Pourimani R, Nemati Z. Measurement of Radionuclide Concentration in Some Water Resources in Markazi Province, Iran. *Iranian Journal of Medical Physics*. 2016;13(1):49–57.
10. Abojassim AA. Natural Radioactivity and Radon Concentrations in Parenteral Nutrition Samples Utilized in Iraqi Hospitals. *Iranian Journal of Medical Physics*. 2019;16(1):1–7.
11. Parhoudeh M, Khoshgard K, Zare MR, Ebrahimi A. Natural Radioactivity Level of 226Ra, 232Th, and 40K Radionuclides in Drinking Water of Residential Areas in Kermanshah Province, Iran using Gamma Spectroscopy. *Iranian Journal of Medical Physics*. 2019;16(1):98–102.
12. RAD7 Radon Detector. User Manual. (2011). DurrIDGE Company Inc.
13. Manual CAPTURE version 4.7.5. (2011). DurrIDGE Company Inc.
14. RAD7 RAD H2O (2011). Radon in Water Accessory. Owner's Manual. DurrIDGE Company Inc.
15. DurrIDGE Company Inc., Reference Manual, RAD-7 Electronic Radon Detector, (2017).
16. DurrIDGE Company Inc. (2010), Reference Manual version 6.0.1, RAD-7 Electronic Radon Detector.
17. Abojassim AA, Kadhim SH, Mraity A, Abid H, Munim RR. Radon levels in different types of bottled drinking water and carbonated drinks in Iraqi markets. *Water Science and Technology: Water Supply*. 2017;17(1):206–11.
18. Alzurfi SK, Abojassim AA, Mraity HA. Monthly Monitoring of Physicochemical and Radiation Properties of Kufa River, Iraq. *Pakistan Journal of Scientific and Industrial Research Series A: Physical Sciences*. 2018;61(1):43–51.

19. Alam MN, Chowdhury MI, Kamal M, et al. Radiological assessment of drinking water of the Chittagong region of Bangladesh. *Radiation protection dosimetry*. 1999;82(3):207–14.
20. United Nations. Scientific Committee on the Effects of Atomic Radiation. Sources and effects of ionizing radiation: sources. United Nations Publications; 2000.
21. World Health Organization. Guidelines for drinking-water quality: second addendum. Vol. 1, Recommendations. World Health Organization; 2011.
22. Mathews Gladys, et al. Radiological and chemical toxicity due to ingestion of uranium through drinking water in the environment of Bangalore, India. *Journal of Radiological Protection*. 2015;35(2):447]
23. IAEA Safety Series. International basic safety standards for protection against ionizing radiation and for the safety of radiation sources. 1996]
24. Valentin J., et al. Published on behalf of the International Commission on Radiological Protection. 2007]
25. Salman AY, et al. Study the contamination of radioactivity levels of <sup>226</sup>Ra, <sup>232</sup>Th and <sup>40</sup>K in (water) Iraq and their potential radiological risk to human population. in IOP Conference Series: Materials Science and Engineering. 2020. IOP Publishing.
26. World Health Organization, and WHO. Guidelines for drinking-water quality. Vol. 1. World health organization, 2004.]
27. United Nations Scientific Committee on the Effects of Atomic Radiation. Sources and effects of ionizing radiation. UNSCEAR 1996 report to the General Assembly, With scientific annex. 1996.]
28. Ting David S.K. WHO handbook on indoor radon: a public health perspective. 2010;100–102]
29. Environmental Protection Agency. The United States Environmental Protection Agency. A citizen's guide to radon. 2019.

<https://doi.org/10.34883/PI.2025.14.1.058>

Alyaa Hussein Talib , Ihsan Flayyih Hasan AL-Jawhari  
College of Education for Pure Sciences, University of Thi-Qar, Thi-Qar, Iraq

# Biological Decolorization of Congo Red from Textile Effluent and Wastewater by *Aspergillus Terreus*, and *Penicillium Funiculosum*

**Conflict of interest:** nothing to declare.

**Authors' contribution:** Alyaa Talib – conceptualization, data curation, methodology, project administration, resources, software, validation, visualization, writing – original draft and writing – review & editing; Ihsan AL-Jawhari – conceptualization, data curation, investigation, supervision, validation, visualization, writing – original draft and writing – review & editing. The article is published in author's edition.

Submitted: 20.01.2025

Accepted: 17.03.2025

Contacts: Alyaahussin010.bio@utq.edu.iq

## Abstract

**Introduction.** The most prevalent and highly potential to remove Congo Red dye among the isolated fungi were *Aspergillus terreus* and *Penicillium funiculosum*.

**Purpose.** The goal of this study was to isolate several fungus from soil and polluted water samples that were taken from textile facilities.

**Materials and methods.** ITS gene sequencing, morphological and cultural characteristics were used to identify these isolates. The azo dye concentration, pH, carbon source, and nitrogen source were all varied during the dye removal procedure.

**Results.** According to the findings, both fungus were able to break down Congo Red dye at concentrations of 50 and 150 ppm, however the fungi *Penicillium funiculosum* and *Aspergillus terreus* were nearly fatal at 250 ppm. The maximum color removal efficiency of the dye at a concentration of 50 ppm was recorded as (94.33%, 93.33%) for the fungi *Penicillium funiculosum* and *Aspergillus terreus*, respectively, at pH=10. However, at pH=7, the proportion of color removed from *Penicillium funiculosum* and *Aspergillus terreus* respectively, was 88.21% and 79.62%). The reactive dye reached its maximum peak at 489 nm at pH=7 and 490 nm at pH=10, indicating that the fungi's biological activity was the cause of the dye's decolorization.

**Conclusion.** The pH=10 is the ideal value for decolorization, as indicated by the fungi's increased dry weight. For *Penicillium funiculosum* and *Aspergillus terreus*, the dry weight at pH=10 is 2.60 and 2.47 grams, respectively.

**Keywords:** *aspergillus terreus*, *penicillium funiculosum*, azo dye, decolorization, congo red

## ■ INTRODUCTION

Because wastewater contains a wide variety of pigments, some of which are carcinogenic and mutagenic, it is regarded as a hazardous source of pollutants for all living things [1]. Human kidney, liver, brain, reproductive, and central nervous system functioning are among the effects of dyes [2]. Heavy industries include textile paint,

mining chemical dyestuff, and battery manufacture are common sources of wastewater. electroplating, and metal finishing, can release a significant amount of both organic and inorganic pollutants into the atmosphere [3].

In the paper paint culinary cosmetic textile and leather sectors among others dyes are a vital resource. Approximately twenty-five different types of dye groups are available depending on the chromophore's chemical structure [4]. Thousands of dyes have been identified as textile dyes, and they are used to color a wide range of textiles [5]. Precursors to dyes are called dye intermediates. With the help of certain chemical reactions, they can be extracted from unprocessed materials like naphthalene and benzene [6, 7]. With two chromophoric groups (azo groups) in its structure Congo red dye (sodium salt of benzidinediazo-bis-1-naphtylamine-4-sulfonic acid,  $C_{32}H_{22}N_6Na_2O_6S_2$ ) is a classic diazo dye. It, is extremely soluble in water and enduring when released into an untreated natural area [8, 9].

Pollution has a negative impact on the environment and can pose a direct or indirect health risk to all life forms on the planet [10, 11]. Based on their composition and use, dyes can be categorized. Because dyes are highly soluble in water, they are challenging to remove using conventional techniques [12, 13]. Colors used in textile dye can harm artwork and prevent light from diffusing into the water, which lowers the amount of dissolved oxygen and slows down the pace at which aquatic life photosynthesizes [14]. The scientific world has been much more aware of biological approaches in the past few years. Compared to conventional procedures these methods have a number of advantages including reduced costs environmental friendliness, safe operation, and reduced sludge output. Nowadays, bioremediation is regarded as a potential therapy option for the elimination of dye under various circumstances. Because the bioremediation method's operating parameters and design are flexible it can destroy harmful compounds using both natural and recombinant microorganisms. The fact that they can be utilized ex situ, or off-site or in situ or even with plants, as in phytoremediation explains the technique's flexibility. The biologically aided breakdown of a dye molecule into many by-products through the action of different enzymes is known as biodegradation. It's an energy-dependent process [15]. Decolorization and the disintegration of the dye molecules into smaller pieces are the outcomes of dye biodegradation. Many microorganisms, including fungi, bacteria, and algae, are used to break down and decolorize manmade dyes. Numerous dyes can be decolorized by microbes in different ways. When it comes to the biodegradation of synthetic colors, certain types of bacteria have distinct advantages over others. The efficiency of dye bioremediation depends on the activity and adaptability of the microorganisms [16]. The decolorization of dye waste water by fungi has been the subject of extensive investigation in the past few years. As a result, it is beginning to show promise as a replacement or substitute for current therapeutic procedures. The objective of this work is to isolate and characterize fungal strains that can effectively decolorize the textile dye, congo red (RD). The current study set out to find out how well *A. terreus* and *P. funiculosus* removed Congo red dye in different environments.

## ■ MATERIALS AND METHODS

### **Azo dyes and the gathering of samples**

In the Thi Qar province, I gathered sediments and wastewater samples from textile and wool enterprises. Three laboratory stations were used to isolate fungi and three replicate

samples were taken from each station. The same facility provided the congo red (CR) azo dye type that was utilized.

### **Fungi isolation**

The fungi isolated from the sediment and water samples using the dilution method were subjected to one of the techniques after the samples gathered for fungal isolation were inspected. In particular, 9 ml of distilled water and 1 gram of dirt were successively added to 1 ml of waste water or 1 ml of water that had been serially diluted up to 10<sup>-4</sup> [17]. Following homogenization, 1 milliliter of each prior dilution was taken out and placed onto sterile petri plates using the pour-plate method. Next, the antibacterial agent chloramphenicol (250 mg) was added, and then the culture medium potato dextrose agar, or PDA was added. For seven days, the plates were incubated at 25 °C.

### **Molecular identification of fungi that degrade azo dyes**

The internal transcribed spacer (ITS) region was amplified and sequenced in order to perform molecular identification. Using primers (ITS1 and ITS4), the internal transcription space region (ITS1-5.8S-ITS2) was amplified using polymerase chain reaction (PCR) technology. The source of these primers is Macrogen, Korea. Using the genomic DNA as a template and the ITS primers of ITS1 (5'  $\pi$  - TCCGTAGGTGAACCTGCGG -3'  $\text{R}$ ) and ITS4 (5'  $\text{R}$  -TCCTCCGCTTATTGAT ATGC- 3'  $\text{R}$ ), the ITS region was amplified using polymerase chain reaction (PCR). One microliter of isolated fungal genomic DNA, 0.5 micrograms of each primer and 50 microliters of Maxima Hot Start PCR Master Mix (Thermo) made up the PCR mixture. AL Ameen Foundation For Study used a DNA Engine Thermal Cycler to do the PCR. & Research (Najaf, Iraq) with a hot start that lasted for four minutes at 94 °C, thirty cycles of 94 °C, 56 °C, and 72 °C, and a final extension that lasted for seven minutes at 72 °C. At Macrogen Company (Korea), a DNA sequencer was used for the commercial sequencing. The NCBI BLAST tool was used to match the ITS sequence against the Gen Bank database. Then, using BLASTN, sequences were matched with ITS sequences in the Gen Bank database.

### **The capacity of separated fungus to proliferate on solid media enhanced with Congo red dye**

In fifteen 250 ml conical flasks, potato dextrose agar (PDA) was used as the medium. The flasks were autoclaved for 20 minutes at 121 °C and 15 pounds per square inch of pressure. The culture medium was then heated to the proper temperature and three concentrations of the aromatic dye (congo red) were added for each component. 50, 150, 250 ppm each dye in three flasks. In order to provide a control for comparison, one flask was left empty. Subsequently, the 8.5 cm-diameter sanitized Petri dishes were filled with the medium, and they were allowed to dry for 30 minutes.

A 4 mm-diameter disc of pure *Aspergillus terreus* and *penicillium funiculosum*, both at 7 days old, was used to pierce a sterile cork into center of each plate to introduce the fungal inoculum into the dishes. After that, the dishes were incubated for seven days at 25 °C. Three replications of each treatment were used in the experiment, and the colony diameter was used to calculate the fungi's growth rates [18].

### **The capacity of isolated fungus to proliferate in a medium containing mineral salts and added Congo red dye**

The solution of mineral salts was made ready for the growth of fungus. The following chemicals make up one liter of this medium: 1.71 g of  $K_2HPO_4$ ; 1.32 g of  $KH_2PO_4$ ; 0.42 g of  $NaNO_3$ ; 0.42 g of  $MgSO_4 \cdot 7H_2O$ ; and 0.02 g of  $CaCl_2$ . After setting up fifteen 250 ml conical flasks, sterilize the medium in an autoclave for 20 minutes at 121 °C and 15 pounds per square inch of pressure. Once the outside temperature has dropped. Next incorporate the chosen aromatic dyes into the culture medium while lowering the temperature. Methylene blue is the chosen dye, and it is introduced to the medium at concentrations of 50 ppm, 150 ppm, and 250 ppm. Using different pH values 7, 10, repeat the experiment while adding sources of carbon and nitrogen. Once the carbon and nitrogen sources (glucose and  $NH_4Cl$ ) were added, add 0.1 g per liter for each addition. The flasks were then left empty of the material for comparison, and a disc was transferred to inoculate them. Using a sterile Cork Borer, 4 mm of 7-day-old fungal cultures for *Aspergillus terreus* and *Penicillium funiculosum* were examined. Three replications of each treatment were used in this experiment, which was conducted with the flasks incubated for seven days at a temperature of 25 °C. The mycelium was weighed using a sensitive scale after being dried on filter paper for 30 minutes at 50 °C in the oven [18].

### **Maximum detection $\lambda$ for every dye**

Congo red (CR) dye's absorption maxima ( $\lambda$  max) were found using a UV-visible spectrometer (MD 1105 PG instrument Ltd., UK). Every dye solution's optical density in water was measured at various wavelengths between the visible ranges (300–800 nm).

### **Using a fungal isolate, decolorization (%) of congo red in a liquid media**

They were tested for their capacity to decolorize azo dyes in MSM using the procedure outlined in [19]. After the fungal isolates were activated, 900 milliliters of mineral salt medium were ready. After adjusting, the pH was 7, 10. Carbon and nitrogen supplies were provided in the form of glucose and  $NH_4Cl$ . Each of the 250 mL flasks that were created was filled with 90 mL of the prepared mineral salt medium that had been combined with the previously indicated ingredients. Three doses of the aromatic dye Congo Red were applied to each flask 50, 150, 250 ppm. Each flask was supplemented with the study-specific fungal isolates. To achieve decolorization, control flasks with MSM medium and Congo Red dye were made without the presence of fungal isolates. In order to zero the UV-visible spectrometer, blank flasks were made using the same growth media but without fungal isolates and dye. The flasks were kept in an incubator set at 25 °C for seven days. Following the incubation time, 10 mL from each flask were collected and put into a tube. Centrifugation for ten minutes at 5000 rpm, and following the aforementioned additions, the supernatant was scanned in a UV/VIS spectrophotometer at particular wavelengths identified by scanning the dye samples. The following formula was used to calculate the percent decolorization in accordance with [19]:

$$\text{Decolorization (\%)} = [Dy (i) - Dy (1) / Dy (i)] \times 100,$$

where D – decolorization percentage %; Dy (i) – initial absorbance; Dy (1) – final absorbance.

## Statistical analysis

The present study conducted an Anova (analysis of variance) which was performed on all the treatments and done using the SPSS (version 23.0) package to determine whether or not significance difference.

## RESULTS

### Fungal isolation and identification

In the current study, a number of fungi were isolated from water and soil samples of textile wool factories. There were two types of fungi that appeared most prominent among the isolated fungi that were used in the decolorization. The taxonomic status of fungal isolate was defined by sequencing of ITS genes. The morphological culture characteristic as well molecular identification based on ITS sequencing analysis for isolates was similar to *Aspergillus terreus* and *Penicillium funiculosum* as showed in Fig 1, 2.

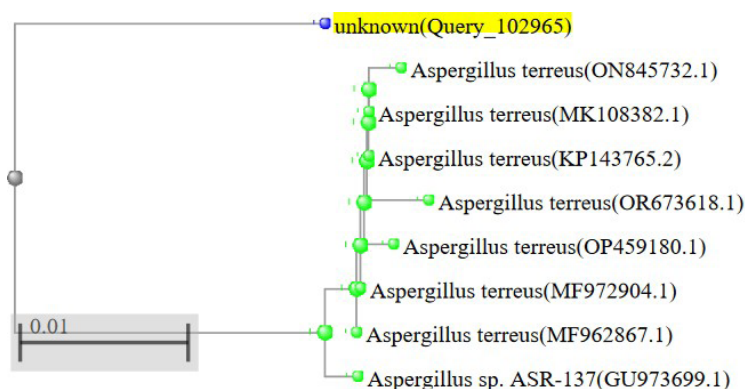


**Fig. 1. Phylogenetic tree of ITS sequences of the fungal isolate with the sequences from NCBI and designated as *Aspergillus terreus***

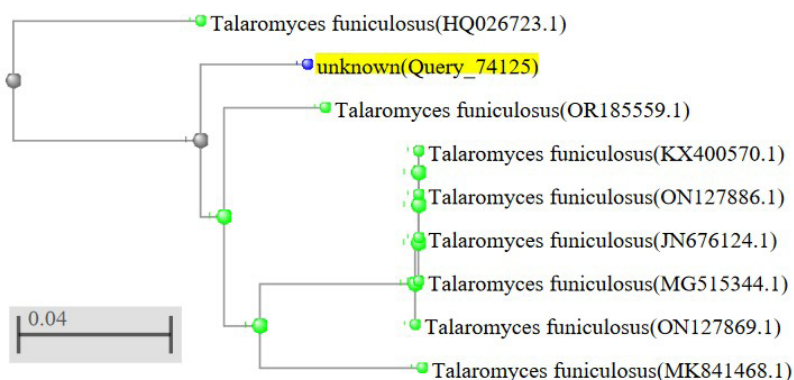


**Fig. 2. Phylogenetic tree of ITS sequences of the fungal isolate with the sequences from NCBI and designated as *Penicillium funiculosum***

### The capacity of separated fungus to proliferate on solid media enhanced with congo red dye

The development of fungi in PDA (Potato Dextrose Agar) medium treated with Congo Red dye is demonstrated by the data shown in (Table 1). The colony diameters of *Penicillium funiculosum* and *Aspergillus terreus* fungi are found to be growing every day. The findings showed that *A. terreus* and *P. funiculosum* were clearly resistant to all of the Congo Red dye doses that were employed. At concentrations of 250, 150, and 50 ppm, respectively, the colony diameter of *A. terreus* reached 8.83, 6.16, 7.00 cm, compared to the control's 9.00 cm. However, *P. funiculosum* shown a higher degree of resistance to the dye, as seen by colony diameters of 8.66, 7.33, and 6.50 cm for the identical concentrations employed, as opposed to 9.00 cm for the control.

The data clearly show that, with the exception of the 250 ppm concentration, which had a minor impact on colony growth, none of the concentrations to which the fungus were exposed caused a substantial change in colony diameter when compared to the control. The fungi *P. funiculosum* and *A. terreus* had colony diameters of 6.50 and 6.16 cm, respectively. The statistical analysis, which revealed no significant variations between fungus and concentrations (Table 1, fig 3, 4).

**Table 1**  
**Ability the growth of *Aspergillus terreus* and *penicillium funiculosum* in solid medium with Congo red**

Fungi	Concentration (ppm)				Mean
	control	50	150	250	
<i>Aspergillus terreus</i>	9.0±0.0	8.83±0.28	7.0±0.50	6.16±0.28	7.75
<i>Penicillium funiculosum</i>	9.0±0.0	8.66±0.28	7.33±0.28	6.50±0.00	7.87

Notes: L.S.D (P<0.05); L.S.D fungi = 0.345.

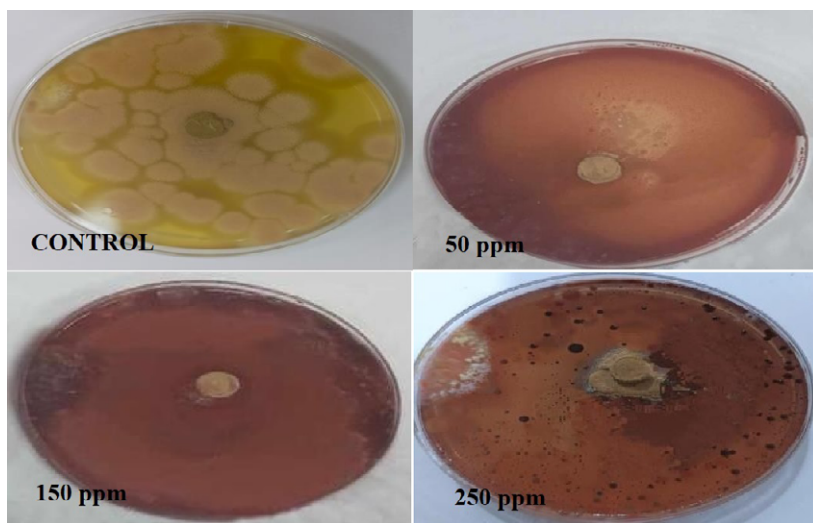


**Fig. 3. Decolorization of Congo red by *Aspergillus terreus* on solid medium**

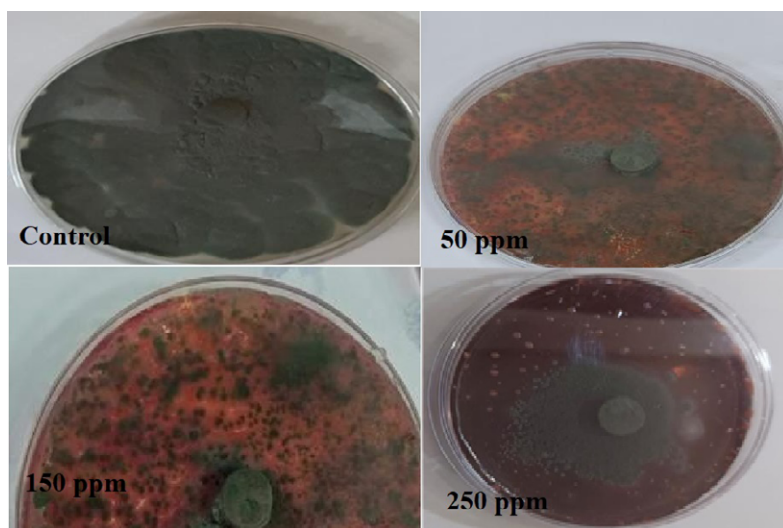


**Fig. 4. Decolorization of Congo red by *Penicillium funiculosum* on solid medium**

#### **The capacity of isolated fungus to proliferate in a solution containing mineral salts and congo red**

The current study's findings show that robust fungal growth can occur in the liquid metal medium SMS at a pH of 7, supplemented with glucose as a carbon source, congo red dye, and  $\text{NH}_4\text{Cl}$  as a nitrogen source. This implies that certain fungi, among the isolated fungal species, are capable of growing in a liquid media with the dye present, at different concentrations and to different degrees. The statistical analysis results, which demonstrated no discernible difference between the fungi and concentration levels (Table 2).

It was discovered that when the fungus's dry weight concentration rose. In contrast to the control, where the dry weight was 1.96 g, the dry weight of the fungus *A. terreus* reached 1.65, 1.82, and 2.10 grammes, respectively, at concentrations of 50, 150, 250 ppm. The fungus *Penicillium funiculosum* was shown to have a higher dry weight increase in comparison to *A. terreus*. At 50, 150, and 250 ppm concentrations, the dry weight was 2.25, 2.30, and 2.53 grams, respectively, while the control had a dry weight of 2.62 grams.

**Table 2**  
**Ability the growth of *Aspergillus terreus* and *Penicillium funiculosum* in mineral salts medium with congo red, pH=7**

Fung	Concentration (ppm)				Mean
	Control	50	150	250	
<i>Aspergillus terreus</i>	1.96±0.00	1.65±0.03	1.82±0.02	2.10±0.01	1.88
<i>Penicillium funiculosum</i>	2.62±0.00	2.25±0.04	0.02±2.30	0.02±2.53	8.10

Notes: L.S.D ( $P < 0.05$ ); L.S.D concentration = 0.041.

Our investigation revealed that, in comparison to fungus at pH=7, the dry weight of fungi at pH= 10 increased. At 50, 150, and 250 ppm concentrations, respectively, the dry weight of

*A. terreus* was 2.21, 2.23 and 2.47 grams, while the control weight was 1.96 grams. Regarding *Penicillium funiculosum*, the dry weights at 50, 150, and 250 ppm concentrations were 2.11, 2.33, and 2.60 grams, respectively, in contrast to the 2.62-gram control weight. The findings show that there are statistically significant variations between the concentrations and the fungus (Table 3).

**Table 3**  
**Ability the growth of *Aspergillus terreu* and *Penicillium funiculosum* mineral salts medium with congo red, PH=10**

Fungi	Concentration (ppm)				Mean
	Control	50	150	250	
<i>Aspergillus terreus</i>	1.96±0.00	2.21±0.02	2.23±0.03	2.47±0.03	2.21
<i>Penicillium funiculosum</i>	2.62±0.00	2.11±0.03	2.33±0.02	2.60±0.05	8.10

Notes: L.S.D (P<0.05), L.S.D fungi = 0.036.

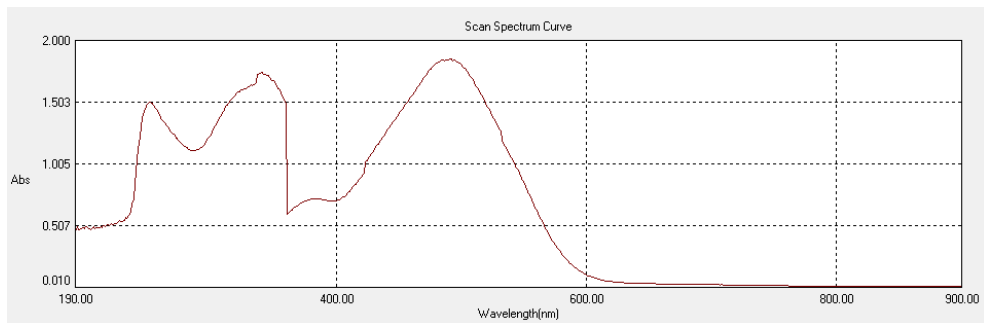


**Fig. 5. The maximum absorption of Congo red when pH=7 by using UV-Visible spectrometer (U.K. / MD 1105 PG instrument Ltd)**

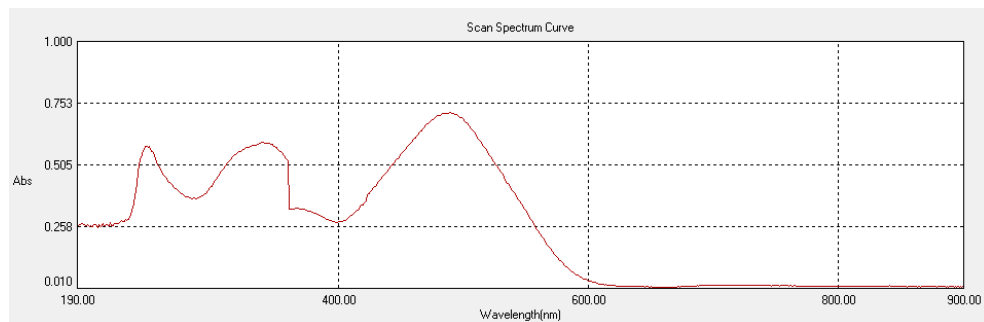


**Fig. 6. The maximum absorption of Congo red when pH=10 by using UV-Visible spectrometer (U.K. / MD 1105 PG instrument Ltd)**

### Determination of absorption maxima ( $\lambda$ max) of congo red dye when pH=7 and pH=10

Using a UV-visible spectrometer (U.K. / MD 1105 PG instrument Ltd.), the maximum absorption for the azo dye employed was found. Each dye's optical density was measured at various wavelengths between 200 and 900 nm when it was dissolved individually in water. The maximum absorbance of the Congo red dye was seen at 489 nm and 490 nm at pH values of 7 and 10 respectively. Consequently, the subsequent optimization procedure employed the identified  $\lambda$  max to determine the percentage of decolorization (Fig. 5, 6).

### Decolorization (%) of congo red in liquid medium using fungal isolate

I have investigated the degrading capacities of *Aspergillus terreus* and *Penicillium funiculosum* fungi at several pH levels and quantities of Congo red dye. The degradation ability of both fungi was shown to diminish in this study when a dye concentration was increased from 50 ppm to 250 ppm and introduced to an SMS medium containing glucose and  $\text{NH}_4\text{Cl}$  as carbon and nitrogen sources. The percentage of *A. terreus* biodegradation at pH=10 was found to drop to 93.33, 80.93, 67.81% at dye doses of 50, 150, 250 ppm, respectively. *P. funiculosum* showed biodegradation percentages of 94.33, 82.90 and 76.83% respectively, at dye concentrations of 50, 150, 250 ppm.

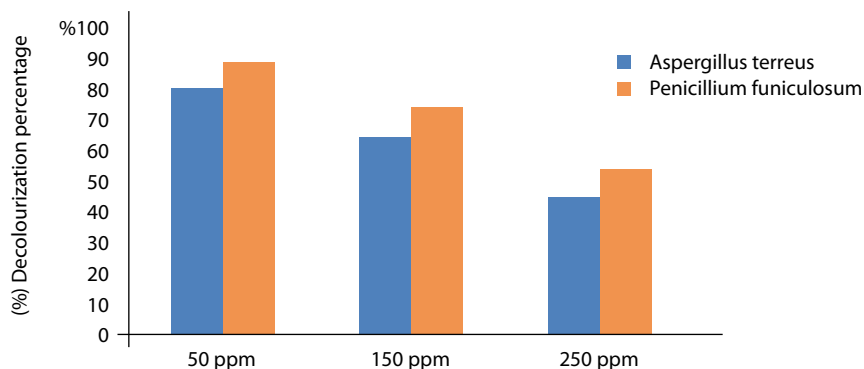


**Fig. 7. Effect of PH=7 on the decolorization percentages treated by *Aspergillus terreus* and *Penicillium funiculosum* through different concentration**

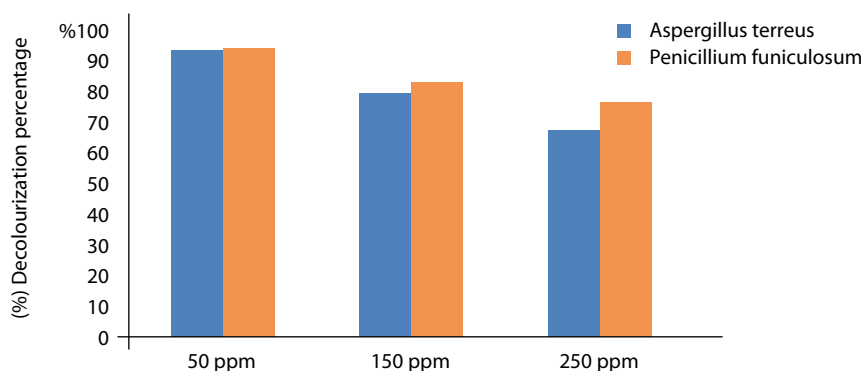


**Fig. 8. Effect of pH=10 on the decolorization percentages treated by *Aspergillus terreus* and *Penicillium funiculosum* through different concentration**

In comparison to pH=10, it was observed that at pH=7, the removal capacity of *P. funiculosum* and *A. terreus* fungus was decreasing, reaching 79.62, 64.46, 43.95% at concentrations of 50, 150, 250 ppm. Regarding *P. funiculosum*, decolorization was attained at the same prior concentrations 88.21, 73.6, 53.92% (fig 7, 8).

## ■ DISCUSSION

The dye's aromatic structure resists deterioration from light, ozone, and other environmental factors. As a result, traditional methods of treating textile sector wastewater are still ineffectual [20]. The development of a single, cost-effective technique for treating dyes in textile wastewater has been attempted by scientists up to this point, but it continues to be a significant difficulty [21]. Most research is focused on biological treatment since it is more environmentally friendly, produces less sludge, and yields consistent results [22]. This study involved the isolation of a number of fungus from soil and polluted water samples that were taken from textile wool companies in the governorate of Thi Qar. The outcomes showed that the most prevalent and highly capable of eliminating Congo Red dye among the isolated fungi were *Aspergillus terreus* and *Penicillium funiculosum*. The azo dye concentration, pH, carbon source, and nitrogen source were all varied during the dye removal procedure. The findings demonstrated that both fungi could break down Congo Red dye at amounts of 50, 150, 250 ppm. As evidenced by the daily increase in colony diameter in solid media, it was found that fungi of the Ascomycetes genus, specifically *A. terreus* and *P. funiculosum*, were clearly growing on all concentrations of red Congo dye. This suggests that the fungi can use the dye as a source of nutrients. These outcomes are in line with those of [18], which demonstrated that *P. funiculosum* had a stronger decolorization activity on solid medium containing CR than other fungi. that dyes might be broken down by fungus into other metabolites. *P. funiculosum*'s dry weight (biomass) was recorded as 1.02 in CR-containing mineral salts medium (MSM). The decolorization of Congo red (CR) dye was investigated in this study using *Aspergillus terreus* GS28 and *Aspergillus flavus* CR500 that were isolated from industrial waste sludge. Because of the ideal pH, temperature, carbon, nitrogen, and heavy metal concentrations, the rate of CR decolorization increased. According to the study, after 120 hours under optimal conditions, *A. terreus* has a greater ability (95%) than *A. flavus* to decolorize CR ( $\approx 100 \text{ mg L}^{-1}$ ) [23]. Regarding the mineral salts medium at pH=7, which is supplemented with glucose as a carbon source,  $\text{NH}_4\text{Cl}$  as a nitrogen source, and congo red dye. The addition of glucose and  $\text{NH}_4\text{Cl}$  increased the dry weight of the fungal mycelium, according to the data. The reason for this is that the most efficient and easily accessible carbon source for microbial metabolism is glucose. A further supply of carbon and nitrogen is also necessary for many bacteria in order to promote growth, cellular development, primary metabolite creation, and enzyme secretion for the process of biodegradation. Azo dyes cannot be the exclusive source of carbon and energy for microorganisms. As a result, for the breakdown of azo dyes, microorganisms typically depend on the kind and presence of a carbon source [24–26].

Based on our research, we found that at pH=10, the dry weight of fungi increased in comparison to that of fungi at pH=7. This is due to the fact that pH has a significant impact on microbial cells because germs lack the ability to control their internal acidity. Every microbe has a pH range, and research has shown that the ideal range is typically between (6 and 10) for the biodegradation of azo dyes [27]. High alkaline conditions cause

reactive azo dyes to lose hydrogen ions, which ionizes the dye and affects its consistency as well as makes it easier to remove from solutions [28]. On the other hand, it was noted in [29] That decolorization of dyes at higher concentrations was accomplished in an acidic environment, which further enables their better removal by enzymatic or fungal cell wall adsorption. Lastly, because most textile wastewater had alkaline pH values and industrial treatments have typically preferred decolorization under alkaline states due to the functionality of reactive azo dye procedures. Our findings are more useful for extensive decolorization procedures. The addition of glucose and  $\text{NH}_4\text{Cl}$  increased the dry weight of the fungal mycelium, according to the data. The reason for this is that the most effective and easily accessible carbon source for microbial metabolism is glucose. This is because many microbes need an extra source of nitrogen and carbon in order to thrive, produce more cells, synthesise primary metabolites, and secrete enzymes for biodegradation. Furthermore, microbes cannot use azo dyes as their only energy and carbon source because they don't usually act as a source of carbon. Thus, to break down azo dyes in general, microbes depend on the kind and presence of a carbon source [25, 26]. The current study's findings were consistent with those of [30]. After three to four days of incubation at 30 °C, the ability of *Coprinus comatus* was examined on potato dextrose agar with dyes at a concentration of 100 ppm. The dye that decolorized the fastest was aniline blue, followed by methyl red and Congo red. According to our findings, *Trichoderma harzianum* can partially and completely decolorize textile dyes (Blue, Yellow, and Red) at low concentrations (50 ppm).

Regarding the investigation on the capacity of *Aspergillus terreus* and *Penicillium funiculosum* fungi to break down Congo red dye at various pH levels and concentrations. The degradation ability of both fungi was shown to diminish in this study when a dye concentration was increased from 50 ppm to 250 ppm and introduced to an SMS medium containing glucose and  $\text{NH}_4\text{Cl}$  as carbon and nitrogen sources. The data shown in Figures 7, 8 demonstrated that a dye concentration of 250 parts per million was below the lethal dose, hence impeding the azo dye's ability to remove dye. In addition to the detrimental effects of high dye concentration on the growth of fungi. There is an instance where the initial dye concentration intensified, leading to a reduction in decolorization [32]. Several reports demonstrated the extreme toxicity.

The removal process is found to diminish at increasing hydrogen ion concentrations, notably at  $\text{pH} = 10$ , in relation to the effect of hydrogen ion concentration on the removal process. Since microorganisms lack a way to control internal acidity, this indicates that hydrogen ion concentration plays a significant role in influencing microbial cells. Every microorganism has a pH range within which it can grow, metabolize, and influence how quickly it degrades. At the ideal pH level, the biodegradation rate rises; at lower or higher pH values, it falls. Generally speaking, the ideal pH range for azo dye biodegradation is between 6–10. The process of dye molecule transport across the microorganism's cell membrane, a stage that restricts the dye's rate of biodegradation, is similarly influenced by hydrogen ion concentration. Furthermore, through altering the structure of dye molecules, hydrogen ion concentration influences the chemistry of the dye in the medium [27, 34, 35]. The current study's findings were consistent with those of [28], who stated that pH 9 was the greatest decolorization of Remazol black. While the ideal pH for the largest azo-reductase enzyme is 7 Maximum decolorization and optimal pH within a range of pH 8 to 9 were demonstrated by some alkali-thermostable azo-reductase

[28, 36]. These findings are consistent with [37], who stated that at pH 5, *Aspergillus ochraceus* NCIM-1146 completely decolorized Reactive Blue-25 (100 ppm). On the other hand, decolorization was achieved at pH 3, 7, 9, and 87%, 81%, and 70%, respectively. This is also consistent with findings from [38], who discovered that for *Aspergillus niger* and *Penicillium* sp. using Reactive Red and Direct Red dyes, the largest percentage of decolorization occurred at pH (4–4.5).

## CONCLUSION

After incubating for seven days, *Aspergillus terreus* and *Penicillium funiculosum* were able to remove the greatest percentage of dye color from Congo red cotton through fungal decolorization. According to the study's findings, the bioremediation method is the best way to lessen the toxicity of dyes in an economical and environmentally responsible way.

## REFERENCES

1. Shojaei S, Khammarnia S, Shojaei S, Sasani M. Removal of reactive red 198 by nanoparticle zero valent iron in the presence of hydrogen peroxide. *Journal of water and environmental nanotechnology*, 2017;2:129–135.
2. Kadirvelu K, Kavipriya M, Karthika C, et al. Utilization of various agricultural wastes for activated carbon preparation and application for the removal of dyes and metal ions from aqueous solutions. *Bioresource technology*, 2003;87:129–135.
3. Olal FO. Biosorption of Selected Heavy Metals Using Green Algae, Spirogyra Species. *Journal of Natural Sciences Research*, 2016;6(14):22–34.
4. Benkhaya S, M'rabet S, El Harfi A. Classifications, properties, recent synthesis and applications of azo dyes. *Heliyon*. 2020;6(1):e03271.
5. Abe FR, Machado AL, Soares AMVM, et al. Life history and behavior effects of synthetic and natural dyes on *Daphnia magna*. *Chemosphere*. 2019;236:124390.
6. Gregory P. Dyes and Intermediates. Kirk-Othmer Encycl. Chem. Technol (Ed.). 2000. <https://doi.org/10.1002/0471238961.0425051907180507.a01.pub2>.
7. Guo Y, Xue Q, Cui K, et al. Study on the degradation mechanism and pathway of benzene dye intermediate 4-methoxy-2-nitroaniline via multiple methods in Fenton oxidation process. *RSC Adv*. 2018;8:10764–10775.
8. Tapalad T, Neramittagapong A, Neramittagapong S, Boonmee M. Degradation of Congo red dye by ozonation. *Chiang Mai. J. Sci*. 2008;35:63–68.
9. Jalandoni – Buan AC, Decena-Soliven ALA, Cao EP, et al. Congo red decolorizing activity under microcosm and decolorization of other dyes by Congo red decolorizing bacteria. *Phillip J Sci*, 2009;138:125–132.
10. Varjani S, Rakholiya P, Ng HY, et al. Microbial degradation of dyes: An overview. *Bioresour Technol*. 2020;314:123728.
11. Bencheqroun Z, Mrabet IE, Kachabi M, et al. Removal of basic dyes from aqueous solutions by adsorption onto Moroccan clay (fez city). *Mediterr. J. Chem*. 2019;8(2):158–167.
12. Dong H, Guo T, Zhang W, et al. Biochemical characterization of a novel azoreductase from *Streptomyces* sp.: Application in eco-friendly decolorization of azo dye wastewater. *Int J Biol Macromol*. 2019;140:1037–1046.
13. Lellis B, Favaro-Polonio CZ, Pamphile JA, Polonio JC. Effects of textile dyes on health and the environment and bioremediation potential of living organisms. *Biotechnol. Res. Innovation*. 2019;3(2):275–290.
14. Ajaz M., Shakeel S., Rehman A. Microbial use for azo dye degradation-a strategy for dye bioremediation. *Int. Microbiol*. 2020;23(2):149–159.
15. Kaushik P, Malik A. Fungal dye decolorization: Recent advances and future potential. *Environ Int*. 2009;35:127–41.
16. Chen KC, Wu JY, Liou DJ, Hwang SC. Decolorization of the textile dyes by newly isolated bacterial strains. *J Biotechnol*. 2003;101:57–68.
17. Al-Nasrawi H. Biodegradation of crude oil by fungi isolated from Gulf of Mexico. *Journal of Bioremediation and Biodegradation*. 2012;3(4):1–6.
18. AL-Jawhari IF, AL-Mansor KJ. Biological removal of malachite green and congo red by some filamentous Fungi. *Int. J. Environ. Agric. Biotechnol*, 2017;2(2):238723.
19. Purnomo A, Mauliddawati V, Khoirudin M, et al. Bio-decolorization and novel bio-transformation of methyl orange by brown-rot fungi. *Int. J. Environ. Sci. Technol*. 2019;16:7555–7564.
20. Joshi M, Bansal R, Purwar R. Colour removal from textile effluents. *Ind J Fibre Textile Res*, 2004;29:239–259.
21. Dos Santos A, Cervantes F, Van Lier J. Review paper on current technologies for decolourisation of textile wastewaters: perspective for anaerobic biotechnology. *Bioresource Technol*, 2007;98:2369–2385.
22. Ramalingam N, Shanmugaparaksh M. Decolorization of textile dyes by *Aspergillus tamari*, mixed fungal culture and *Penicillium purpurogenum*. *J Sci Ind Res*, 2010;69:151–153.
23. Singh G, Dwivedi SK. Biosorptive and biodegradative mechanistic approach for the decolorization of congo red dye by *Aspergillus* species. *Bull Environ Contam Toxicol*. 2022b;108:457–467.
24. Chakraborty S, Basak B, Dutta S, et al. Decolorization and biodegradation of congo red dye by a novel white rot fungus *Alternaria alternata* CMER1 F6. *Bioresour Technol*. 2013;147:662–666.
25. Varjani S, Rakholiya P, Ng HY, et al. Microbial degradation of dyes: An overview. *Bioresour Technol*. 2020;314:123728.
26. Carolin CF, Kumar PS, Joshiba GJ. Sustainable approach to decolorize methyl orange dye from aqueous solution using novel bacterial strain and its metabolites characterization. *Clean Techno. Environ. Policy*. 2021;23:173–181.
27. Jamee R, Siddique R. Biodegradation of synthetic dyes of textile effluent by microorganisms: An environmentally and economically sustainable approach. *Eur. J. Microbiol. Immunol. Bp.*, 2019;9(4):114–118.

28. Hashem RA, Samir R, Essam TM, et al. Optimization and enhancement of textile reactive Remazol black B decolorization and detoxification by environmentally isolated pHolerant *Pseudomonas aeruginosa* KY284155. *AMB Expr.*, 2018;8(1):1–12.
29. Namdhari BS, Rohilla SK, Salar RK, et al. Decolorization of Reactive Blue MR, using *Aspergillus* species Isolated from Textile Waste Water. *ISCA J Biological Sci.* 2012;1(1):24–29.
30. Vantamuri AB, Adhoni SA, Nadaf PD, et al. Isolation and characterization of laccase producing fungi from different environmental samples. *International Journal of Recent Scientific Research.* 2015;6(10):6853–6857.
31. Issa SN. *Biodegradation of some environmental pollutants by laccase produced from Trichoderma harzianum using solid state fermentation.* MSc Thesis, College Of Science, University of Baghdad. 2021.
32. Sadeghi M, Forouzandeh S, Nourmoradi H, et al. Bio decolorization of Reactive Black5 and Reactive Red120 azo dyes using bacterial strains isolated from dairy effluents. *International Journal of Environmental Science and Technology.* 2018;16(7):1–10.
33. Hefnawy MA, Gharieb MM, Shaaban MT, Soliman AM. Optimization of Culture Condition for Enhanced Decolorization of Direct blue Dye by *Aspergillus flavus* and *Penicillium canescens*. *J. App Pharm Sci.* 2017;7(2):83–92.
34. Xi Y, Shen Y, Yang F, et al. Removal of azo dye from aqueous solution by a new biosorbent prepared with *Aspergillus nidulans* cultured in tobacco wastewater. *J. Tai. Inst. Chem. Eng.*, 2013;44:815–820.
35. Ranimol G, Venugopal T, Gopalakrishnan S, Sunkar S. Production of laccase from *Trichoderma harzianum* and its application in dye decolourisation. *Biocatal. Agric. Biotechnol.*, 2018;16:400–404.
36. Kandelbauer A, Erlacher A, Cavaco-paulo A, Gu GM. A new alkali-thermostable azoreductase from *Bacillus* sp. strain SF. *Appl Environ. Microbiol.* 2004;70:837.
37. Parshetti GK, Kalme D, Gomare S, Govindwar P. Biodegradation of Reactive blue-25 by *Aspergillus ochraceus* NCIM-1146. *J. Bioresour Technol.* 2007;98:3638–3642.
38. Husseiniy M. Biodegradation of reactive and direct dyes using Egyptian isolates. *J. Appl Sci Res.* 2008;4:599–606.

<https://doi.org/10.34883/PI.2025.14.1.059>

Narjes Fadhil Abbas, Salih Hassan Jazza, Neran Adnan Abbas Al-Naqeeb ✉  
College of Science, University of Misan, Maysan, Iraq

## Assessment of Water Quality in Al-Musharh River in Maysan Province

**Conflict of interest:** nothing to declare.

**Authors' contribution:** Narjes Fadhil Abbas – conceptualization, data curation, investigation, methodology, project administration, resources, software, visualization, writing – original draft and writing – review & editing; Salih Hassan Jazza – conceptualization, data curation, investigation, methodology, project administration, resources, supervision, validation, writing – original draft and writing – review & editing; Neran Adnan Abbas Al-Naqeeb – conceptualization, methodology, project administration, resources, supervision, validation, visualization, writing – original draft and writing – review & editing. The article is published in author's edition.

Submitted: 20.01.2025

Accepted: 17.03.2025

Contacts: neranecology@uomisan.edu.iq

### Abstract

**Introduction.** Water is essential for life and very important natural resource. Environmental pollution is defined as any change in the basic components of the environment.

**Purpose.** The present study was conducted to assessment of water quality in Al-Musharh River in Maysan province.

**Materials and methods.** Water samples were collected from three sites during the period from July 2022 to January 2023. Ten physical and chemical parameters were analyzed.

**Results.** The values of these factors ranged between 13.5–30 °C, 7.1–8.8, 1108–1415 mg/l, 23–62 NTU, 360–550 mg/l, 5.4–18.67 mg/l, 0.024–0.518 mg/l, 332–422 mg/l, 3.5–6.41 mg/l, 6–11 mg/l for temperature, pH, total dissolved solid, turbidity, total hardness, nitrate, phosphate, sulfate, dissolved oxygen and biological oxygen demand respectively. Our results showed that some of these parameters were within the permissible limit of WHO and Iraqi standards for drinking water such as pH, turbidity, total hardness, nitrate, phosphate and dissolved oxygen, whereas turbidity, total dissolved solid, sulfate and BOD were above the permissible limits according to WHO and Iraqi standards.

**Conclusion.** The parameters are within the permissible limit of WHO and Iraqi standards for drinking water such as pH, total hardness, nitrate, phosphate and dissolved oxygen, whereas turbidity, total dissolved solid, sulfate and BOD are above the permissible limits depending on WHO and Iraqi standards. The water quality of Al-Musharh River is affected by geological nature, agricultural activities, industrial wastes and untreated sewage water.

**Keywords:** Al-Musharh river, water quality, aquatic ecosystem, water pollution, tigris river

## ■ INTRODUCTION

Water is essential for life and very important natural resource, because provides habitat for different aquatic life in surface water such as rivers, lakes and marshes, therefore, must protect water from pollution risks and manage it uses [1, 2]. Environmental pollution is defined as any change in the basic components of the environment, either naturally, or

as a result of human activities [3, 4]. These pollutants can cause a change in biological, chemical and physical properties, which makes it unfit for humans and other living organisms [5]. Aquatic ecosystem exposed too many types of pollutants such as petroleum hydrocarbons, pesticides, heavy metals, detergents, medical wastes in addition to other materials which may be lead to negative effects on human health and biodiversity [6]. This pollution is due to the continued increase in population growth, geological changes, industrial and cultural activities [7]. Water pollution has become one of the important issues nowadays as a result of its impact on all living organisms and various activities [8]. The waters of Tigris river and it branches in Amarh city are exposed to many pollutants due to the increase in population density and discharge of various types of waste containing many chemicals that lead to the deterioration of water quality in this rivers [9]. The physical and chemical properties of water can be used to fully understand and identify the elements that affect water quality as well as to give reliable information in assessing the water quality of rivers [10]. In addition to that provide a good basis for examining and knowing the water sources, water suitability for drinking, industrial and irrigation [11].

## ■ PURPOSE

Determine some physical and chemical properties from Al-Musharh River in Maysan province to assess their suitability for human consumption.

## ■ MATERIALS AND METHODS

### **Description of the study area**

Al-Musharh River is one of the short rivers in Iraq that branches from the northwestern side of the Tigris River in Amarh city, where the Tigris River splits in this location into two branches (Al-Kahlaa and Al-Musharh). Al-Musharh River is 55 km long from its source at its branching point near Al-Nazim to its mouth in the Al-Hawizah marshes [12]. The present study included taking three sites along the Al-Musharh River (Figure 1). These sites were identified by GPS. First site E: 705114 N: 3526471. In the beginning of the River, which branches from the Tigris River near the Al-Majidiyah area in the southeastern part of Amarh city. The second site is E: 730779 N: 3523392. It is located 14 km from the first site in Al-Shabisha area (Bani Hashim village). The area is characterized by agricultural activities. Third site E: 718324 N: 3526844. It is located in the center of Al-Musharh district, this site receive untreated domestic from the city center of Al-Musharh district, it is noted that the river water level is low in third site compared to the first and second sites, and it is noted that there is a large amount of solid waste in this site that is thrown from nearby homes and local markets.

### **Samples collection**

Water samples were collected monthly for the period from July 2022 to January 2023 and expressed during the summer season (July, August), autumn (October, November) and winter (December, January) from three sites distributed along Al-Musharh River in prewashed polyethylene bottles 1 liter capacity from a depth of approximately 10–30 cm for measurement some physical and chemical factors.

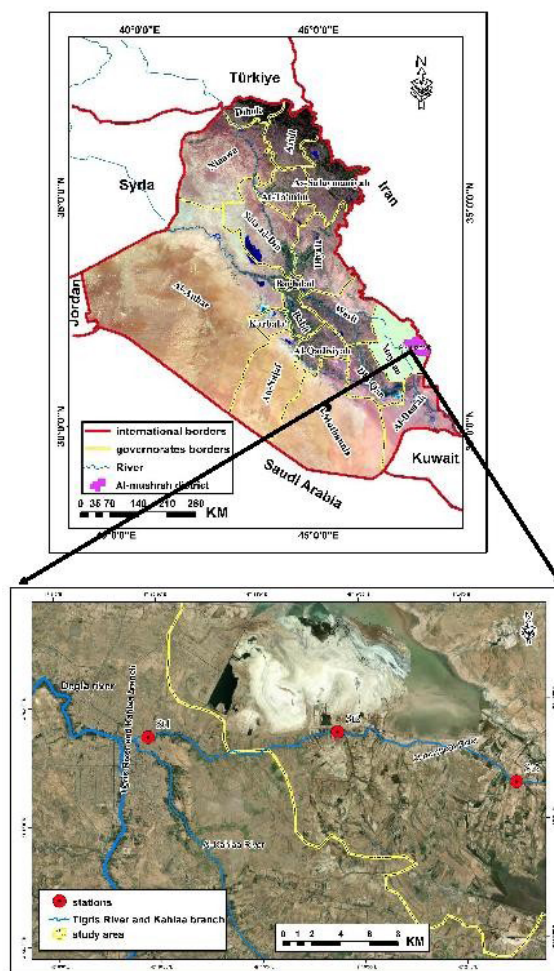


**Fig. 1. The study sites by GIS**

### **Physical and chemical analysis**

The conducted analyses included physical factors which are temperature, turbidity and total dissolved solids TDS, whereas chemical properties are pH, total hardness, nitrate, phosphate, sulfate, dissolved oxygen DO and biological oxygen demand BOD<sub>5</sub>.

The temperature was measured in the field with graduated mercury thermometer (0–100 °C) at the depth 25 cm, the pH was measured in the field by using pH meter and turbidity was measured by using turbidity meter, whereas the concentrations of other parameters such as

TDS, total hardness, nitrate, phosphate were determined according to APHA [13], whereas levels of DO in water samples was determined depending on Azid Modification Winkler method [14], whereas BOD<sub>5</sub>, the water samples put in the dark bottles then incubated in the dark place at 20 °C for 5 days, the dissolved oxygen was fixed and

measured depending on Azid Modification Winkler method by using following equation:  
 $BOD_5 \text{ mg/l} = DO \text{ before incubation} - DO \text{ after incubation}$ .

## ■ RESULTS

The results of the study in figure 2a revealed that there were seasonal variations in the water temperature, which ranged from 13.8 to 30 °C during winter and summer respectively.

The highest of pH value was 8.8 in the site two whereas the lowest 7.1 in the site three during summer (figure 2b). These values were within the permissible limits 6.5–8.5 of WHO and local standards during the period study except in site 2 during summer (table).

Concentrations of TDS was varied from 1108 to 1415 mg/l in the site 3 and 2 during winter and summer respectively (figure 2c).

Results of the current study showed that TDS values were more than the permissible limits (1000 mg/l, table).

Turbidity values were ranged from 23 to 62 NTU in site 2 during winter and autumn respectively (figure 2d).

Results of the current study were more than the local and international standards of the permissible limits (5 NTU, table).

The highest values of total hardness (TH) was 550 mg/L in the site 3 during summer, whereas the 401.5 mg/L in the site 1 during winter (figure 2e).

The hardness values were within the permissible limits of Iraqi standard and WHO except in the site 3 during summer and winter (table).

Nitrate levels were ranged between 5.4 and 18.67 in site 1 and site 3 during summer and winter respectively (figure 2f), these concentrations were lower than the permissible limits of international and local standard limits for drinking water (table).

Phosphate levels were ranged between 0.024 to 0.518 mg/l in site 1 and 3 during autumn and summer respectively.

PO<sub>4</sub> values in all the samples were within the permissible limits of WHO and Iraqi standards (except site 3 during summer) (figure 2g and table).

The values of SO<sub>4</sub><sup>2-</sup> were ranged between 332 and 422 mg/l (figure 2h), concentrations of SO<sub>4</sub><sup>2-</sup> for all samples were more than the permissible limits of international and local standards (table). SO<sub>4</sub><sup>2-</sup> is generally harmless, except its effect on taste.

### Permissible limits of physical chemical factors depending on WHO and Iraqi standards

Parameters	WHO (2017)	Iraqi drinking water standard (2001)
pH	6.5–8.5	6.5–8.5
DO mg/l	>5	>5
BOD <sub>5</sub> mg/l	>5	>5
TUR NTU	5	10
TDS mg/l	1000	1000
TH mg/l	500	500
PO <sub>4</sub> mg/l	0.5	0.10
NO <sub>3</sub> mg/l	50	50
SO <sub>4</sub> mg/l	250	250

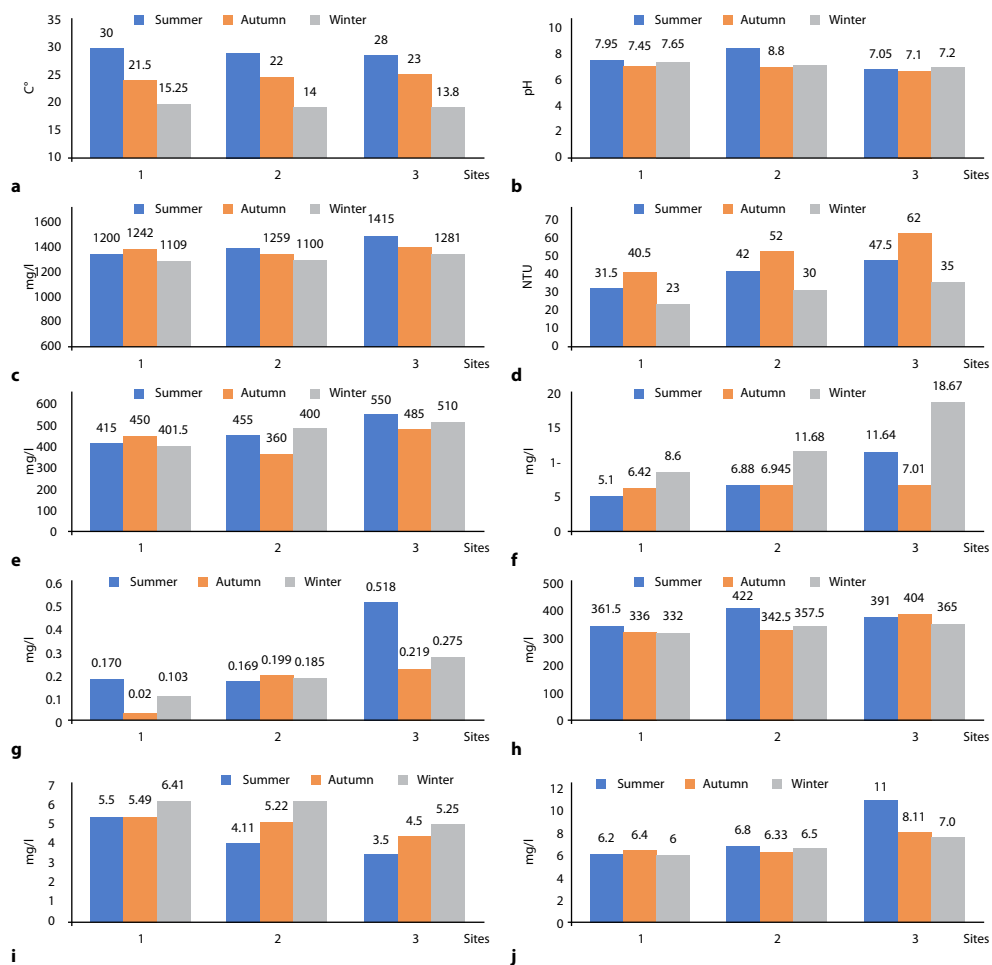


**Fig. 2. Seasonal and spatial variations in a – temperature; b – pH values; c – TDS values; d – turbidity values; e – total hardness values; f – nitrate values; g – phosphate values; h – sulfate values; i – dissolved oxygen levels; j – BOD levels**

Dissolved oxygen levels at the present study are shown in Figure 2i. The lowest value was 3.5 mg/l in summer recorded at site 3, whereas the highest value was 6.41 mg/L in winter 2013 recorded at site 1. Values of DO in most samples were below the permissible standard value as prescribed by WHO and Iraqi standard limits (table). Levels of BOD<sub>5</sub> were varied from 6 to 11 mg/l in site 1 and 3 during autumn and summer respectively (figure 2j).

## ■ DISCUSSION

There are seasonal variations in the water temperature, which ranged from 13.8 to 30 °C during winter and summer respectively, this variation attributed to the nature of Iraq's climate [15].

The highest of pH value is 8.8 in the site two, these spatial variations may be due to amount organic materials which discharge in the river, in addition to other factors such as water temperature and role of bacteria in biodegradation of organic matter [3, 16].

The seasonal variations attributed to changes in water temperature which led to the evaporation process which reflected on TDS levels [4, 17, 18].

The turbidity is a measure of light emitting properties of water and it is mainly caused by solid particles present in the suspended phase [3, 19].

This may be due to soil erosion, water levels in the river and microorganisms (bacteria and plankton), the higher turbidity values may be cause gastrointestinal disease for human and also have negative effects on consumer acceptability of water [20, 21].

The highest values of total hardness (TH) was 550 mg/L in the site 3 during summer, the seasonal and spatial variations may be attributed to the geological nature of the river and soil erosion spatially during winter season, in addition to discharge untreated sewage and industrial water into the rivers [22].

Elevated of hardness values of drinking water is connected with many health problems such as growth retardation, cardiovascular disease and reproductive failure, in addition to that high levels of hardness in water caused a laxative effect [23].

Agricultural runoff and untreated sewage might be the major source of nitrate levels in the river. Nitrate pollution may cause various types of health risks such as blue baby disease [16, 18, 20].

Phosphorus is play a vital role in living organisms, however, excessive phosphorus in aquatic ecosystem are harmful to most aquatic biota which cause a decrease in the dissolved oxygen concentration of water [24].

PO<sub>4</sub> values in all the samples were within the permissible limits of WHO and Iraqi standards. This may be attributed to the domestic sewage which discharged into the river and decreased amount of water during summer [25].

The concentrations of SO<sub>4</sub><sup>2-</sup> for all samples were more than the permissible limits of international and local standards. The major physiological impacts resulting from high levels of SO<sub>4</sub><sup>2-</sup> are gastrointestinal irritation, dehydration and catharsis [3, 19, 26].

The lowest value dissolved oxygen was 3.5 mg/l in summer recorded at site 3, whereas the highest value was 6.41 mg/L in winter 2013 recorded at site 1. This seasonal and spatial variations may be attributed to the consumption of oxygen in the oxidation of organic compounds in the domestic waste discharged into the river specially in the site 3, also, levels of DO may be attributed to many factors such as temperature, photosynthesis, aquatic organisms respiration, good mixing and role of bacteria in degradation of organic matter [22, 27].

Values of DO in most samples were below the permissible standard value as prescribed by WHO and Iraqi standard limits. Levels of BOD<sub>5</sub> were varied from 6 to 11 mg/l in site 1 and 3. The increase in BOD<sub>5</sub> value in site 3 during the present study may be return to excess the effluent of un treatment domestic wastes into the river [28, 29]. BOD<sub>5</sub> concentrations for all samples were more than the permissible limits of WHO [18] and Iraqi drinking water standard [30].

## ■ CONCLUSIONS

The parameters are within the permissible limit of WHO and Iraqi standards for drinking water such as pH, total hardness, nitrate, phosphate and dissolved oxygen,

whereas turbidity, total dissolved solid, sulfate and BOD are above the permissible limits depending on WHO and Iraqi standards. The water quality of Al-Musharh River is affected by geological nature, agricultural activities, industrial wastes and untreated sewage water.

## ■ REFERENCES

1. Ahmed MR, Kheder NK. Determining the Level of Pollution of the River Duhlo in Rahovec, as a Result of Human and Industrial Activity, through Physico-chemical Parameters of Pollution, using Analytical Methods ICP-OES and UV-VIS. *J. Duhok Univ.* 2009;12(1):28–34.
2. Cheepi P. Musi river pollution its impact on health and economic conditions of downstream villages-a study. *Journal of Environmental Science, Toxicology and Food Technology.* 2012;1(4):40-51.
3. Jazza SH, Al-Saad HT. Quality Assessment of Drinking Water in Missan Province, Iraq. *International Journal of Marine Science.* 2016;6(17):1–7.
4. Al-Naqeeb NAA, Jazza SJ. Quality assessment of drinking water by using some Environment Index in Misan Province Eco. *Env. E. Cons.* 2020;26(4):1735–1739.
5. Dadolahi-Sohrab A, Arjonmand F. Water quality index of karoon river as indicator of Khorramshahr soap factory sewage effects. *Journal of Oceanography.* 2011;1(4):21–27.
6. Osibanjo O, Daso AP, Gbadebo AM. The Impact of Industries on Surface Water Quality of River Ona and River Alaro in Oluyole Industrial Estate, Ibadan, Nigeria. *African Journal of Biotechnology.* 2011;10:696–702.
7. Sevda S, Sreekishnan TR, Pous N, Puig S, Pant D. Bioelectro remediation of perchlorate and nitrate contaminated water: a review. *Bioresource technology.* 2018;255:31–339.
8. Packiyam R, Nananan S, Pachaiyappan S, Narayanan U. Effect of Storage Containers on Coliforms in Household Drinking Water. *International Journal of Current Microbiology and Applied Sciences.* 2016;5(1):461–477.
9. Lazim II, Al-Naqeeb NAA. Measuring pollution based on total petroleum hydrocarbons and total organic carbon in Tigris River, Maysan Province, Southern Iraq. *Caspian Journal of Environmental Sciences.* 2021;19(3):535–545.
10. Zhang W, Ma L, Abuduwailli J, et al. Hydrochemical characteristics and irrigation suitability of surface water in the Syr Darya River, Kazakhstan. *Environmental monitoring and assessment.* 2019;191:1–17.
11. Gad M, El Osta M. Geochemical controlling mechanisms and quality of the groundwater resources in El Fayoum Depression, Egypt. *Arabian Journal of Geosciences.* 2020;13:1–23.
12. Saad KS. Qualitative and seasonal assessment of the waters of the Tigris and Euphrates rivers in Thi-Qar and Maysan governorates. Thesis. 2016.
13. APHA (American Public Health Association): Standard Methods for the Examination of Water and Wastewater, 21st Edition. Washington, DC. 2005; 22621 p.
14. Lind OT. Handbook of common method in limnology, 2 nd edition. C.V. Mosby Co., ST. Louis. 1979; 199 p.
15. Al-Atbee RSK. Assessment of some Heavy Elements and Hydrocarbons in the Water, Sediments and Dominant Aquatic Plants at Al-Chibayish marshes. Thesis. 2018.
16. Gaihre S, Dhungel S, Acharya S, et al. Quality appraisal of drinking water from different sources in Nepal. *Scientific World.* 2022;15(15):96–102.
17. Koju NK, Prasai T, Shrestha SM, Raut P. Drinking water quality of Kathmandu valley. *Nepal Journal of Science and Technology.* 2015;15(1):115–120.
18. WHO (World Health Organization): Guidelines for drinking-water quality. WHO. Geneva, Switzerland, 2017.
19. Gupta P, Choudhary R, Vishwakarma M. Assessment of water quality of Kerwa and Kaliasote rivers at Bhopal district for irrigation purpose. *International Journal of Theoretical & Applied Sciences.* 2009;1(2):27–30.
20. Ezeribe AI, Oshieke KC, Jauro A. Physical chemical properties of well samples from some villages in Nigeria cases of stained mottle. *Science World Journal.* 2012;7(1):1–3.
21. Ewaid SH, Abed SA, Al-Ansari N, Salih RM. Development and evaluation of a water quality index for the Iraqi rivers. *Hydrology.* 2020;7(3):67.
22. Al-Yousif MA, Chabuk A. Assessment Water Quality Indices of Surface Water for Drinking and Irrigation Applications – A Comparison Review. *Journal of Ecological Engineering.* 2023;24(5):40–55.
23. Oludairo OO, Aiyedun JO. Contamination of commercially packaged sachet water and the public health implications: an overview. *Bangladesh Journal of Veterinary Medicine.* 2016;13(2):73–81.
24. Bakan G, Özkoc HB, Tülek S, Cüce H. Integrated Environmental Quality Assessment of Kizilirmak River and its Coastal Environment. *Turk. J. Fish. Aquatic. Sci.* 2010;10(4):453–462.
25. Simões F, Moreira AB, Bisnot MC, et al. Water quality index as a simple indicator of aquaculture effects on aquatic bodies. *Ecological Indicator.* 2008;8:476–484.
26. Ghrefat HA. Classification and evaluation of commercial bottled drinking waters in Saudi Arabia. *Research Journal of Environmental and Earth Sciences.* 2013;5(4):210–218.
27. Toma JJ. Limnological study of Dokan, Derbendikhan and Duhok lakes, Kurdistan region of Iraq. *Open J. Eco.* 2013;3(1):23–29.
28. Egai AO, Imasue OI, Torty BB. Quality Assessment of Water Potability in Aguobiri Southern Ijaw Local Government Area Bayelsa State, Nigeria. *J. Appl. Sci. Environ. Manage.* 2013;17(4):493–500.
29. Vaishali P, Punita P. Assessment of seasonal variation in water quality of River Mini, at Sindhrot, Vadodara. *Int. J. Environ. Sci.* 2013;3(5):4396–4402.
30. Iraqi drinking water standard. Central Organization for Quality Control and Standardized. 2001.

<https://doi.org/10.34883/PI.2025.14.1.061>

Alyaa A. Hafed, Muslim Abdulrahman Mohammed, Adnan Issa Al-Badran   
College of Science, University of Basrah, Basrah, Iraq

## Pulmonary Infection with *Acanthamoeba Polyphaga*: Case Report

**Conflict of interest:** nothing to declare.

**Authors' contribution:** all authors made a significant contribution to the writing of the article.

The article is published in author's edition.

Submitted: 03.03.2025

Accepted: 17.03.2025

Contacts: adnan.albadran@uobasrah.edu.iq

### Abstract

**Introduction.** *Acanthamoeba pneumonia* is an infrequent parasitic infection caused by a free-living amoeba found universally in different water sources and soil.

**Case presentation.** *Acanthamoeba* spp. trophozoites and cysts isolated from the sputum of 17 years immune competent old female in Al-Nasiriyah city/Iraq. The patient was presented to the private clinic, she suffering from fatigue, weakness, fever (38.2 °C) for one day ago, short breathing, mild cough, headache, pale skin, nausea and abdominal cramps with loss of appetite. The organism was identified through the detection of amoeba stages by direct microscopic examination.

**Conclusion.** In this case, there are no significant pathological changes as in previous recorded cases of the disease. Most of the inflammatory signs of the infection were normal, in addition to an overlap in symptoms with intestinal symptoms that may have resulted from enteric fever, as the anti-salmonella Ab test was positive.

**Keywords:** Free-living amoebas, *Acanthamoeba keratitis*, *Acanthamoeba pneumonia*, AP, cutaneous *acanthamoebiasis*, trophozoite

### ■ INTRODUCTION

Free-living amoebas (FLAs) are found worldwide in aquatic environments, soil, and air, and they are extensively distributed in a variety of environmental sources [1]. *Acanthamoeba* spp. are free-living amoebas (FLA) broadly dispersed in the different environmental setting, such as: soil and water [2]. They are able to cause cerebral infection (granulomatous amebic encephalitis, GAE) and extra cerebral life-threatening infections (*Acanthamoeba keratitis*, AK; *Acanthamoeba pneumonia*, AP; cutaneous *acanthamoebiasis* and disseminated *acanthamoebiasis*) to human [3]. *Acanthamoeba* spp. be present in two forms: an active (trophozoite) and latent (cyst) forms. The cysts can be stand and resist harsh conditions in several environments for years and convert into trophozoites when the environmental conditions become favor to its growth [4].

Infections caused by *Acanthamoeba* spp. arise commonly among immune-compromised persons, like: HIV patients, organ transplantation recipients, chronic diseases, and patients who received the immunosuppressive therapy. Acanthamoebiasis also recorded in low prevalence rate among immune-competent persons [5, 6]. In spite of low incidence of these infections around the world, the death rate of *Acanthamoeba* spp. infections is extremely high. The pathogenesis of the diseases caused by *acanthamoeba* is not completely understood. *Acanthamoeba* spp. may enter to the body through various ways, such as breaks in the skin or the respiratory tract, resulting in hematogenous spreading to the brain [7]. *Acanthamoeba* spp. infections cases are often underdiagnosed and henceforth strong clinical doubt along with laboratory technical proficiency is required for early diagnosis and managements intervention [8].

So far, 19 case were records of *Acanthamoeba* pneumonia (AP) or disseminated acanthamoebiasis with lung involvement from different countries. Most patients came from the USA, but there were also cases from Poland, Austria, France, Korea, Japan, and India. None of the patients have been survived.

## ■ CASE PRESENTATION

A 17 years immune competent old female from Al-Nasiriyah city/south of Iraq was presented to private clinics with clinical signs including: fatigue, weakness, fever (38.2 °C) for one day ago, short breathing, mild cough, headache, pale skin, nausea and abdominal cramps with loss of appetite. The physician sends the patient to obtain chest X-ray which revealed slightly pathologic changes (mild lung infiltrates). The results of Laboratory diagnostic tests showed table. The patient received various types of medications, including levifloxacin 500 mg twice daily, ceftriaxone (1 g/twice daily), omeprazole 20 mg/1 time daily and a paracetamol 500 mg 3 times/daily were administered.

### Laboratory investigations

Test	Results	Normal value
Blood sugar	5.1	3.1–7.7 mmol/L
Blood urea	25	3.3–7.5 mmol/L
S. creatinine	0.6	62–124 mmol/L
Hb	87	110–160 g/L
HCT	26.8	40–54%
Platelets	300	150–400×10 <sup>9</sup> /L
WBCs	9.2	4.0–11.0×10 <sup>9</sup> /L
Neutrophil	5.33	2.0–7.0×10 <sup>9</sup> /L
Lymphocyte	3.17	0.8–4.0×10 <sup>9</sup> /L
Monocyte	0.62	0.12–1.2×10 <sup>9</sup> /L
Eosinophil	0.06	0.02–0.5×10 <sup>9</sup> /L
Basophil	0.02	0.0–0.1×10 <sup>9</sup> /L
ESR	18	1–20 mm/hr
C-reactive protein	0.2	<5.0 mg/L
AFB staining	Negative	
Anti-salmonella Ab.	IgM: Positive	
TSH	2.308	0.51–4.3 U/L



**Fig. 1. Trophozoite of *Acanthamoeba* spp. From pulmonary infection**



**Fig. 2. Cyst of *Acanthamoeba* spp. From pulmonary infection**

The sputum sample was cultured on Non-Nutrient agar (NNA) medium (1.5% agar) at 30 °C and the media was examined each two to three days microscopically by wet mount for detection of the members of free living amoeba, after 11 days of culture a trophozoite and cyst of *Acanthamoeba* spp. were detected in wet mount preparation as shown respectively in figures 1 and 2. The patient was then transferred by her family for treatment to another province with better health and medical conditions and modern technologies for treating such difficult medical cases.

## ■ DISCUSSION

Pneumonia is one from the most common life-threatening diseases infects millions of peoples annually around the world causing a high number of morbidities and mortalities [9]. *Acanthamoeba* is a more common free living amoeba isolated from different environmental sources such as soil, fresh water, etc., due to its ability to form resistance cyst stage [2, 10]. This amoeba is more common opportunistic amoeba which recorded as an etiologic pathogen of different clinical cases like: granulomatous amebic encephalitis,

Acanthamoeba pneumonia and others which infect immune-compromised patients including: AIDS, cutaneous acanthamoebiasis, disseminated acanthamoebiasis and amebic keratitis that consider as a life-threatening infection [5, 11].

In the previous cases, lungs infections due to Acanthamoeba occur mainly in immune-compromised patients such as organs transplant recipient, cancer and others [12, 13], the pathophysiology of Acanthamoeba pneumonia is not clear and may be greatly complicated interaction of host-specific factors like immune response and may be its undesirable effects, and on the other hand the effects of parasite associated factors such as toxins and various enzymes that may destroyed host tissues and affect their metabolism [14, 15].

## ■ CONCLUSION

In this case, there were no significant pathological changes as in previous recorded cases of the disease. Most of the inflammatory signs of the infection were normal, in addition to an overlap in symptoms with intestinal symptoms that may have resulted from enteric fever, as the anti-salmonella Ab test was positive. The patient's visit to the consultant physician was very early, one day after the first symptoms appeared, which were fever, abdominal pain, and mild cough, which led to the symptoms not being clear in typical images. The delay in the appearance of the microscopic culture result may be due to the low number of amoebas in the sample, which reduced the chances of diagnosing it in the first days of infection.

## ■ REFERENCES

1. Bassad AA, Altooma M, Al-Badran A, Alashkham F. Morphological and Molecular detection of some Opportunistic Free-living Amoebae Isolated From Environmental and clinical Sources in Thi-Qar province/Iraq. *University of Thi-Qar Journal of Science*. 2024;11(1):114–20.
2. Lass A, Guerrero M, Li X, et al. Detection of Acanthamoeba spp. in water samples collected from natural water reservoirs, sewages, and pharmaceutical factory drains using LAMP and PCR in China. *Science of the Total Environment*. 2017;584:489–94.
3. Marciano-Cabral F, Cabral G. Acanthamoeba spp. as agents of disease in humans. *Clinical microbiology reviews*. 2003;16(2):273–307.
4. Juarez MM, Tartara LI, Cid AG, et al. Acanthamoeba in the eye, can the parasite hide even more? Latest developments on the disease. *Contact Lens and Anterior Eye*. 2018;41(3):245–51.
5. Kot K, Lanocha-Arendarczyk NA, Kosik-Bogacka DI. Amoebas from the genus Acanthamoeba and their pathogenic properties. *Annals of parasitology*. 2018;64(4).
6. Kalra SK, Sharma P, Shyam K, et al. Acanthamoeba and its pathogenic role in granulomatous amebic encephalitis. *Experimental parasitology*. 2020;208:107788.
7. Duggal SD, Rongpharpi SR, Duggal AK, et al. Role of Acanthamoeba in granulomatous encephalitis: a review. *J Infect Dis Immune Ther*. 2017;1(1):2.
8. Parija SC, Dinoop KP, Venugopal H. Management of granulomatous amebic encephalitis: Laboratory diagnosis and treatment. *Tropical parasitology*. 2015;5(1):23–8.
9. Thomas K. Global burden of pneumonia. *Int. J. Infect. Dis*. 2016;45(11):1–477.
10. Bunsuwansakul C, Mahboob T, Hounkong K, et al. Acanthamoeba in Southeast Asia—overview and challenges. *The Korean journal of parasitology*. 2019;57(4):341.
11. Król-Turmińska K, Olender A. Human infections caused by free-living amoebae. *Annals of Agricultural and Environmental Medicine*. 2017;24(2):1–4.
12. Im KI, Kim DS. Acanthamoebiasis in Korea: two new cases with clinical cases review. *Yonsei medical journal*. 1998;39(5):478–84.
13. Lanocha N, Kosik-Bogacka D, Maciejewska A, et al. The occurrence Acanthamoeba (free living amoeba) in environmental and respiratory samples in Poland. *Acta Protozoologica*. 2009;48(3):271.
14. Visvesvara GS, Mirra SS, Brandt FH, et al. Isolation of two strains of Acanthamoeba castellanii from human tissue and their pathogenicity and isoenzyme profiles. *Journal of clinical microbiology*. 1983;18(6):1405–12.
15. Kot K, Łanocha-Arendarczyk N, Kosik-Bogacka D. Immunopathogenicity of Acanthamoeba spp. in the Brain and Lungs. *International Journal of Molecular Sciences*. 2021;22(3):1261.

<https://doi.org/10.34883/PI.2025.14.1.050>

Mohamad J. Makki , Waleed K. Ghanim, Muhsin S.G. Al-Moziel  
College of Pharmacy, University of Basrah, Iraq

# Evaluate the Lung-Protective Effects of Hidrosmin and/or Vitamin C in Reducing Lung Fibrosis Caused by Bleomycin in Rats

**Conflict of interest:** nothing to declare.

**Authors' contribution:** Mohamad J. Makki – conceptualization, data curation, investigation, methodology, project administration, resources, software, writing – original draft and writing – review & editing; Waleed K. Ghanim – conceptualization, data curation, investigation, methodology, resources, visualization, writing – original draft and writing – review & editing; Muhsin S.G. Al-Moziel – conceptualization, data curation, methodology, project administration, resources, writing – original draft and writing – review & editing.

The article is published in author's edition.

Submitted: 20.01.2025

Accepted: 17.03.2025

Contacts: pgs.mohamad.jabbar@uobasrah.edu.iq

## Abstract

**Introduction.** Bleomycin is a chemotherapeutic drug categorized as a glycopeptide antibiotic. It is frequently used in the treatment of several types of malignancies. However, it is associated with significant lung injury. Hidrosmin is a synthetic flavonoid that has pleiotropic effects including anti-ischemic, antihypertensive, antioxidant activities, and anti-inflammatory. Vitamin C is a water-soluble vitamin that can reduce unstable species of oxygen, nitrogen, and sulphur radicals and regenerate other antioxidants in the body.

**Purpose.** To investigate the protective effects of hidrosmin and/or vitamin C, and the histology of lung tissue affected by bleomycin.

**Materials and methods.** Forty mature male rats their weight ranged from 250–280 gm were divided into five groups; Group 1: control group, rats with DMSO orally 0.5 ml/kg for twenty days. Group 2: Rats with BLE intratracheally 5 mg/kg on day seven of the experiment. Group 3: Rats with hidrosmin orally 300 mg/kg/day daily for twenty days and BLE intratracheally 5 mg/kg on day seven. Group 4: Rats with vitamin C orally 100 mg/kg/day daily for twenty days and BLE intratracheally 5 mg/kg on day seven. Group 5: Rats with a combination of hidrosmin orally 300 mg/kg/day and vitamin C orally 100 mg/kg/day daily for twenty days and BLE intratracheally 5 mg/kg on day seven.

**Results.** On day twenty, animals were killed for the measurement of TNF- $\alpha$ , TGF- $\beta$ , GSH, and TAS. Group 2 shows a highly significant elevation in TNF- $\alpha$  and TGF- $\beta$  levels, and a highly significant reduction in GSH and TAS levels ( $P < 0.001$ ) compared to Group 1; furthermore, Group 5 shows a highly significant reduction in TNF- $\alpha$  and TGF- $\beta$  levels and a highly significant elevation in GSH and TAS levels ( $P < 0.001$ ), compared to Group 3 and Group 4. Hidrosmin has a lung protective effect against bleomycin-induced lung toxicity by prevented the activation of NF- $\kappa$ B and decreasing the levels of pro-inflammatory cytokines, also Hidrosmin improves histopathological finding when compared with bleomycin alone. Moreover, the combination of hidrosmin and vitamin C produces a synergistic advantage compared to using each alone.

**Conclusions.** Bleomycin stimulates the production of certain pro-inflammatory, such as TNF- $\alpha$  and, TGF- $\beta$  that may lead to lung fibrosis. Additionally, synergistic effects of Hidrosmin and Vitamin C include lung protective effects against BLE-induced lung toxicity.

**Keywords:** hidrosmin, vitamin C, bleomycin, lung fibrosis, rats

## ■ INTRODUCTION

Bleomycin is an antibiotic drug with anticancer properties produced by *Streptomyces verticillus* [1]. Bleomycin (BLE) is the most widely administered antineoplastic agent with a success rate of 60–80% [2]. By demonstrating sequence selective DNA binding and cleavage, resulting in DNA degradation [3, 4]. In addition to inhibiting the incorporation of thymidine into DNA, in vitro, bleomycin-induced DNA degradation is dependent on oxygen and metal ions, such as iron [5]. The major side-effect of the drug is its pulmonary toxicity, which is yet to be overcome, these drugs can lead to significant pulmonary toxicity as a prominent side effect, although it is believed to be triggered by the production of reactive oxygen species (ROS) that give rise to free radical oxidants [6]. Symptoms and signs of BLT include dyspnea, tachypnea, cyanosis, pleural friction, intercostal retraction, and episodes of fever [7]. Hidrosmin is a synthetic flavonoid that has been specifically formulated for the treatment of venous insufficiency [8]. Hidrosmin possesses antioxidant, anti-inflammatory, antihypertensive, and anti-ischemic characteristics [9]. Due to their phenolic structures, have antioxidant activity, and inhibit free radical-mediated processes [8]. Hidrosmin decreases the levels of pro-inflammatory cytokines, such as IL-1, TNF, IL-6, and myeloperoxidase activity [10]. Additionally, Hidrosmin inhibited the activation of NF- $\kappa$ B which led to decreased levels of inflammatory mediators [11]. Vitamin C is a water-soluble vitamin [12] and considered a crucial nutrient with redox properties, a cofactor of numerous enzymes [13]. Vit-C has immunomodulating properties, this is possible by increasing the production of  $\alpha/\beta$  interferons and downregulating the synthesis of pro-inflammatory cytokines [14]. Coadministration of flavonoids with vitamin C may enhance the activity of vitamin C [15]. The synergistic effects of flavonoids and ascorbate on DNA degradation induced by the BLM were observed to be greater with flavonoids [16]. The current study is designed to investigate the protective effects of Hidrosmin and/or vitamin C versus bleomycin-induced lung toxicity.

## ■ MATERIALS AND METHODS

Forty mature male rats were selected to exclude the potential impact of gender differences on the inflammatory and oxidative biomarkers [17, 18]. The animals weighing 250–280 grams at their peak were purchased from the College of Pharmacy at Dhi Qar University. They were thereafter housed in controlled conditions (22 $\pm$ 2 $^{\circ}$ C and 12–12 h/light-dark cycle) in the College of Pharmacy at Basrah University.

The Bleomycin vial was bought from Al-Hikma Company, Jordan, and delivered using the intratracheal route by directly inserting the needle into the trachea. Hidrosmin (200 mg capsule) was purchased from FEAS pharmaceutical company, Bulgaria. It exhibits antioxidant properties that can counteract the oxidative harm caused by bleomycin [19]. Hidrosmin was diluted in dimethyl sulfoxide (DMSO) and administered orally using a gavage technique. The dosage was determined based on the previous research findings

[20]. Vitamin C (500 mg tablet) was provided by Healthy Care, Australia. The stock solution was prepared by dissolving in distilled water and then delivered orally by gavage [16]. Given all the drugs according to the weight of each rat.

### Study design

In the present study, forty mature male rats with weights ranging from 250–280 gm were separated into five groups each one including eight rats:

- Group 1: control group, in which rats with DMSO orally 0.5 ml/kg for twenty days.
- Group 2: Rats with BLE intratracheally (by directly inserting the needle into the trachea) 5 mg/kg on day seven of the experiment.
- Group 3: Rats with Hidrosmin orally 300 mg/kg/day daily for twenty days and BLE intratracheally 5 mg/kg on day seven.
- Group 4: Rats with vitamin C orally 100 mg/kg/day daily for twenty days and BLE intratracheally 5 mg/kg on day seven.
- Group 5: Rats with a combination of Hidrosmin orally 300 mg/kg/day and vitamin C orally 100 mg/kg/day daily for twenty days and BLE intratracheally (5 mg/kg) on day seven.

On day twenty, and 24 hr. after the last dose, rats were anesthetized by chloroform, the chest of the rats was opened, and obtained  $5 \pm 1$  ml of the blood from the vena cava:

- using a rat ELISA kit purchased from Bioassay Technology Laboratory company, USA, inducible Tumour necrosis factor  $\alpha$  (TNF- $\alpha$ ) and Total Antioxidant Status (TAS).
- using a rat ELISA kit purchased from SunLong Biotech Co., LTD Company, USA, inducible transforming growth factor-beta (TGF- $\beta$ ) and glutathione (GSH).

The lungs of the Rats were extracted and stored in formalin for histopathological examination.

### Histopathological examination

For the histopathological study, we extracted the lungs from each animal, washed them with phosphate-buffered saline [20], and then stored them in a 10% formalin solution according to the method of Junqueira [18].

### Statistical analysis

The statistical study was performed using Statistical Package for the Social Sciences (SPSS) version 26. The data were reported as mean  $\pm$  standard error of the mean (SEM). An analysis of variance (ANOVA) was performed to determine the statistical significance of the differences observed among the experimental groups. Statistically significant differences were identified when P-values were  $<0.05$ .

## RESULTS

Table 1 and Figure 1 illustrate that rats were given BLE intratracheally by directly inserting the needle into the trachea with a dose of 5 mg/kg on day 7 (Group 2), which produced a highly significant increase ( $P < 0.001$ ) in the serum level of TNF- $\alpha$  compared to the matching serum level in control (Group 1) rats. Mean  $\pm$  SEM of serum TNF- $\alpha$  levels were respectively,  $451.1250 \pm 0.29505$  and  $61.5000 \pm 0.42258$ .

Additionally, the serum TNF- $\alpha$  level was significantly decreased ( $P < 0.001$ ) in groups treated with Hidrosmin orally 300 mg/kg/day for 20 days to BLE IT 5 mg/kg (Groups 3),

Vitamin C orally 100 mg/kg/day for 20 days to BLE IT 5 mg/kg (Group 4), and combination of Hidrosmin 300 mg/kg/day with vitamin C 100 mg/kg/day prior to BLE IT 5mg/kg (Group 5) compared to the matching serum level in (Group 2) rats with BLE intratracheally 5 mg/kg. Mean±SEM of serum TNF-α levels were respectively, 251.1250±0.29505, 242.5000±1.8898, 182.000±0.46291, 451.1250±0.29505.

Furthermore, a combination of hidrosmin and Vitamin C (Group 5) produced a highly significant reduction ( $P<0.001$ ) in serum TNF-α levels when compared with either use of Hidrosmin or vitamin C alone (Group 3 and Group 4) respectively. Mean±SEM of serum TNF-α levels were respectively, 182.000±0.46291<sup>e</sup>, 251.1250±0.29505<sup>c</sup>, 242.5000±1.8898<sup>d</sup>.

**Table 1**  
**Hidrosmin and Vitamin C's Effects on Serum TNF-α Level**

Groups and Treatment	TNF-α, ng/ml ±SEM
Group 1 (control) / Oral 0.5 ml/kg of DMSO daily for 20 days	61.5000±0.42258 <sup>a</sup>
Group 2 Bleomycin IT (5 mg/kg) on day seven and oral 0.5 ml/kg of DMSO daily for 20 days	451.1250±0.29505 <sup>b</sup>
Group 3 hidrosmin (300 mg/kg/day) for 20 days + Bleomycin IT (5 mg/kg) on day seven	251.1250±0.29505 <sup>c</sup>
Group 4 vitamin C (100 mg/kg/day) for 20 days + Bleomycin IT (5 mg/kg) on day seven	242.5000±1.8898 <sup>d</sup>
Group 5 hidrosmin (300 mg/kg/day) + vitamin C (100 mg/kg/day) for 20 days plus Bleomycin IT (5 mg/kg) on day seven	182.000±0.46291 <sup>e</sup>

Notes:

- Each data is described as mean ± standard error of the mean (SEM).
- The values shown with small letters (a, b, c, d, and e) are highly significantly different ( $P<0.001$ ).
- Each group includes 8 rats.

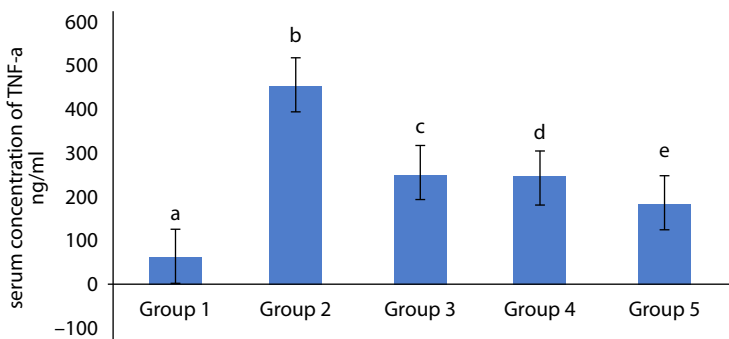


**Fig. 1. Effects of Hidrosmin and Vitamin C on Serum TNF-α Level**

Notes:

- Each value is described as mean ± standard error of the mean (SEM).
- The values shown with small letters (a, b, c, d, and e) are highly significantly different ( $P<0.001$ ).
- Each group includes 8 rats.

Table 2 and Figure 2 illustrate that rats were given BLE intratracheally with a dose of 5 mg/kg on day 7 (Group 2), produced a highly significant increase ( $P<0.001$ ) in the serum

level of TGF- $\beta$  compared to the matching serum level in control (Group 1) rats. Mean $\pm$ SEM of serum TGF- $\beta$  levels were respectively, 255.6250 $\pm$ 0.18298 and 40.6250  $\pm$  0.18298.

Additionally, the serum TGF- $\beta$  level was significantly decreased ( $P<0.001$ ) in groups treated with Hidrosmin orally 300 mg/kg/day for 20 days to BLE IT 5 mg/kg (Groups 3), Vitamin C orally 100 mg/kg/day for 20 days to BLE IT 5 mg/kg (Group 4), and combination of Hidrosmin 300 mg/kg/day with vitamin C 100 mg/kg/day prior to BLE IT 5mg/kg (Group 5) compared to the matching serum level in (Group 2) rats with BLE intratracheally 5 mg/kg. Mean $\pm$ SEM of serum TGF- $\beta$  levels were respectively, 201.1250 $\pm$ 0.29505, 191.8750 $\pm$ 0.44068, 171.1250 $\pm$ 0.29505, 255.6250 $\pm$ 0.18298.

Furthermore, the combination of hidrosmin and vitamin C (Group 5) produced a highly significant reduction ( $P<0.001$ ) in serum TGF- $\beta$  levels when compared with either use of Hidrosmin or Vitamin C alone (Group 3 and Group 4) respectively. Mean $\pm$ SEM of serum TGF- $\beta$  levels were respectively, 171.1250 $\pm$ 0.29505<sup>e</sup>, 201.1250 $\pm$ 0.29505<sup>c</sup>, 191.8750 $\pm$ 0.44068<sup>d</sup>.

**Table 2**  
**Hidrosmin and Vitamin C's Effects on Serum TGF- $\beta$  Level**

Groups and Treatment	TGF- $\beta$ , ng/ml $\pm$ SEM
Group 1 (control)/ Oral 0.5ml/kg of DMSO daily for 20 days	40.6250 $\pm$ 0.18298 <sup>a</sup>
Group 2 Bleomycin IT (5 mg/kg) on day seven and oral 0.5 ml/kg of DMSO daily for 20 days	255.6250 $\pm$ 0.18298 <sup>b</sup>
group 3 hidrosmin (300 mg/kg/day) for 20 days + Bleomycin IT (5 mg/kg) on day seven	201.1250 $\pm$ 0.29505 <sup>c</sup>
Group 4 vitamin C (100 mg/kg/day) for 20 days + Bleomycin IT (5 mg/kg) on day seven	191.8750 $\pm$ 0.44068 <sup>d</sup>
Group 5 hidrosmin (300 mg/kg/day) + vitamin C (100 mg/kg/day) for 20 days plus Bleomycin IT (5 mg/kg) on day seven	171.1250 $\pm$ 0.29505 <sup>e</sup>

Notes:

- Each data is described as mean  $\pm$  standard error of the mean (SEM).
- The values shown with small letters (a, b, c, d, and e) are highly significantly different ( $P<0.001$ ).
- Each group includes 8 rats.

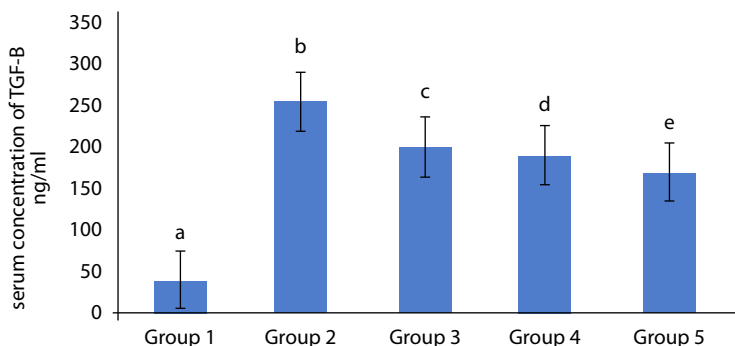


**Fig. 2. Effects of Hidrosmin and Vitamin C on Serum TGF- $\beta$  Level**

Notes:

- Each value is described as mean  $\pm$  standard error of the mean (SEM).
- The values shown with small letters (a, b, c, d, and e) are highly significantly different ( $P<0.001$ ).
- Each group includes 8 rats.

Table 3 and Figure 3 illustrate that rats were given BLE intratracheally with a dose of 5 mg/kg on day 7 (Group 2), produced a highly significant reduction ( $P < 0.001$ ) in the serum level of GSH compared to the matching serum level in control (Group 1) rats. Mean $\pm$ SEM of serum GSH levels were respectively, 154.8750 $\pm$ 0.29505 and 410.0000 $\pm$ 0.26726.

Additionally, the serum GSH level was significantly increased ( $P < 0.001$ ) in groups treated with Hidrosmin orally 300 mg/kg/day for 20 days to BLE IT 5 mg/kg (Groups 3), Vitamin C orally 100 mg/kg/day for 20 days to BLE IT 5 mg/kg (Group 4), and combination of Hidrosmin 300 mg/kg/day with vitamin C 100 mg/kg/day prior to BLE IT 5mg/kg (Group 5) compared to the matching serum level in (Group 2) rats with BLE intratracheally 5 mg/kg. Mean $\pm$ SEM of serum GSH levels were respectively, 233.8750 $\pm$ 0.29505, 266.1250 $\pm$ 0.29505, 312.0000 $\pm$ 0.32733, 154.8750 $\pm$ 0.29505.

Furthermore, a combination of hidrosmin and vitamin C (Group 5) produced a highly significant elevation ( $P < 0.001$ ) in serum GSH level when compared with either use of Hidrosmin or Vitamin C alone (Group 3 and Group 4) respectively. Mean $\pm$ SEM of serum GSH levels were respectively, 312.0000 $\pm$ 0.32733<sup>e</sup>, 233.8750 $\pm$ 0.29505<sup>c</sup>, 266.1250 $\pm$ 0.29505<sup>d</sup>.

**Table 3**  
**Hidrosmin and Vitamin C's Effects on Serum GSH Level**

Groups and Treatment	GSH, ng/ml $\pm$ SEM
Group 1 (control) Oral 0.5ml/kg of DMSO daily for 20 days	410.0000 $\pm$ 0.26726 <sup>a</sup>
Group 2 Bleomycin IT 5 mg/kg on day seven and oral 0.5 ml/kg of DMSO daily for 20 days	154.8750 $\pm$ 0.29505 <sup>b</sup>
Group 3 hidrosmin 300 mg/kg/day for 20 days + Bleomycin IT 5 mg/kg on day seven	233.8750 $\pm$ 0.29505 <sup>c</sup>
Group 4 vitamin C 100 mg/kg/day for 20 days + Bleomycin IT 5 mg/kg on day seven	266.1250 $\pm$ 0.29505 <sup>d</sup>
Group 5 hidrosmin 300 mg/kg/day + vitamin C 100 mg/kg/day for 20 days + Bleomycin IT 5 mg/kg on day seven	312.0000 $\pm$ 0.32733 <sup>e</sup>

Notes:

- Each data is described as mean  $\pm$  standard error of the mean (SEM).
- The values shown with small letters (a, b, c, d, and e) are highly significantly different ( $P < 0.001$ ).
- Each group includes 8 rats.

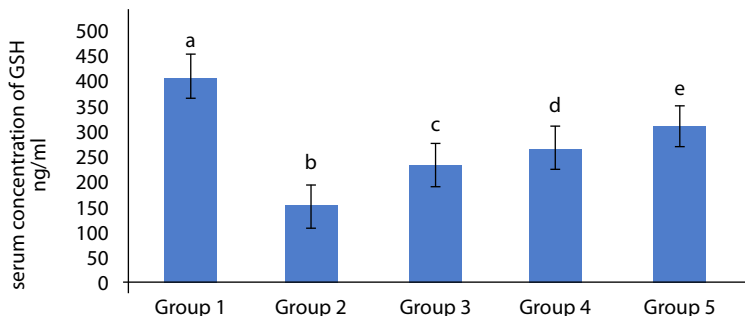


**Fig. 3. Effects of Hidrosmin and Vitamin C on Serum GSH Level**

Notes:

- Each value is described as mean  $\pm$  standard error of the mean (SEM).
- The values shown with small letters (a, b, c, d, and e) are highly significantly different ( $P < 0.001$ ).
- Each group includes 8 rats.

Table 4 and Figure 4 illustrate that rats were given BLE intratracheally with a dose of 5 mg/kg on day 7 (Group 2), produced a highly significant decrease ( $P < 0.001$ ) in the serum level of TAS compared to the matching serum level in control (Group 1) rats. Mean  $\pm$  SEM of serum TAS levels were respectively,  $10.8750 \pm 0.29505$  and  $50.7500 \pm 0.2500$ .

Additionally, the serum TAS level was significantly increased ( $P < 0.001$ ) in groups treated with Hidrosmin orally 300 mg/kg/day for 20 days to BLE IT 5 mg/kg (Groups 3), Vitamin C orally 100 mg/kg/day for 20 days to BLE IT 5 mg/kg (Group 4), and combination of Hidrosmin 300 mg/kg/day with vitamin C 100 mg/kg/day prior to BLE IT 5mg/kg (Group 5) compared to the matching serum level in (Group 2) rats with BLE intratracheally 5 mg/kg. Mean  $\pm$  SEM of serum TAS levels were respectively,  $34.1250 \pm 0.29505$ ,  $38.5000 \pm 0.18898$ ,  $44.1250 \pm 0.29505$ ,  $10.8750 \pm 0.29505$ .

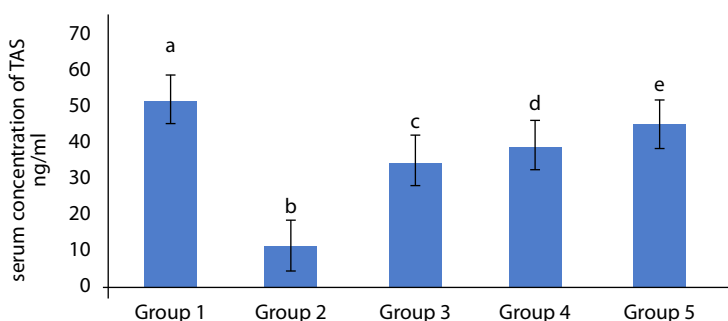
Furthermore, a combination of hidrosmin and vitamin C (Group 5) produced a highly significant elevation ( $P < 0.001$ ) in serum TAS level when compared with either use of Hidrosmin or vitamin C alone (Group 3 and Group 4) respectively. Mean  $\pm$  SEM of serum TAS levels were respectively,  $44.1250 \pm 0.29505^e$ ,  $34.1250 \pm 0.29505^c$ ,  $38.5000 \pm 0.18898^d$ .

**Table 4**  
**Hidrosmin and Vitamin C's Effects on Serum TAS Level**

Groups and Treatment	TAS, ng/ml $\pm$ SEM
Group 1 (control)/ Oral 0.5ml/kg of DMSO daily for 20 days	$50.7500 \pm 0.2500^a$
Group 2 Bleomycin IT (5 mg/kg) on day seven and oral 0.5 ml/kg of DMSO daily for 20 days	$10.8750 \pm 0.29505^b$
Group 3 hidrosmin (300 mg/kg/day) for 20 days + Bleomycin IT (5 mg/kg) on day seven	$34.1250 \pm 0.29505^c$
Group 4 vitamin C (100 mg/kg/day) for 20 days + Bleomycin IT (5 mg/kg) on day seven	$38.5000 \pm 0.18898^d$
Group 5 hidrosmin (300 mg/kg/day) + vitamin C (100 mg/kg/day) for 20 days plus Bleomycin IT (5 mg/kg) on day seven	$44.1250 \pm 0.29505^e$

Notes:

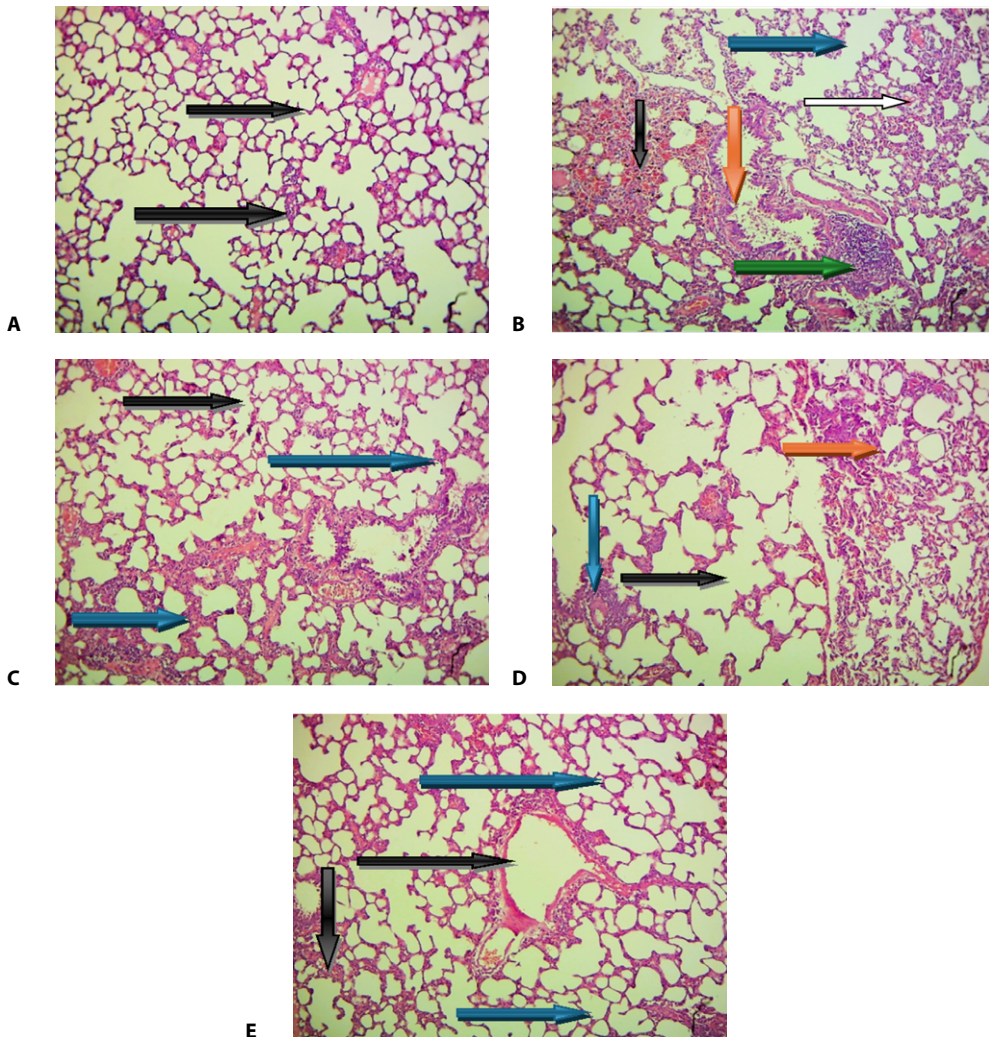
- Each data is described as mean  $\pm$  standard error of the mean (SEM).
- The values shown with small letters (a, b, c, d, and e) are highly significantly different ( $P < 0.001$ ).
- Each group includes 8 rats.



**Fig. 4. Effects of Hidrosmin and Vitamin C on Serum TAS Level**

Notes:

- Each value is described as mean  $\pm$  standard error of the mean (SEM).
- The values shown with small letters (a, b, c, d, and e) are highly significantly different ( $P < 0.001$ ).
- Each group includes 8 rats.

**Histopathological findings of the lung**

**Fig. 5.** Photomicrograph showing lung sections from different experimental groups of rats: A – Which represents Group 1, normal lung tissue appears (control group), where thin alveolar septa were observed (black arrow). B – Which represents Group 2 with bleomycin 5 mg/kg, the alveoli (black arrow) are filled with the pink material characteristic of pulmonary edema as well capillaries within alveolar walls are congested (black arrow), with massive cellular infiltration, also may be fibrosis were observed (green arrow), bronchiolar (orange arrow) epithelium desquamation appears into the lumen, (blue arrow) there is loss of alveolar ducts and alveoli emphysema, the alveolar septum was more thickened (white arrow). C – This represents Group 3, with noticeable improvement in the lung (black arrow) and thickened intra-alveolar septa with cellular infiltration (blue arrow). D – Which represents Group 4, the alveolar septum was more thickened (orange arrow), (black arrow) there is loss of alveolar ducts and alveoli emphysema, inflammatory cell infiltration and congestion may occur (blue arrow). E – This represents Group 5, patent amelioration and clear improvement of effects bleomycin, where most of the alveoli restoration of architecture (blue arrow), and less than other treated groups (Groups 2, 3, and 4). Cellular infiltration and normal appearance of a bronchiole (black arrow). H&E  $\times 10$

## ■ DISCUSSION

In the present study, the results demonstrated that Bleomycin led to a notable increase in the levels of TNF- $\alpha$  and TGF- $\beta$ , and a decrease in the levels of GSH and TAS as shown in (group 2). The observed effects could be explained by the creation of excessive free radicals, leading to an inflammatory reaction, this response involves the secretion of pro-inflammatory cytokines and the stimulation of immune cells, resulting in the simulation of acute lung injury due to pro-inflammatory cytokines, specifically TNF- $\alpha$  and TGF- $\beta$ , have been linked to the formation of fibrosis in animal models treated with bleomycin [21]. In addition to that bleomycin is related to necrosis of pneumocytes type II and release of surfactant, also phagocytosis of surfactant by alveolar macrophages, release of mediators by macrophages, and stimulation of fibroblasts production [22, 23]. Bleomycin initiated the generation of reactive oxygen species (ROS) that resulted in the formation of free radical oxidants [24]. In addition, it causes harm to the thin layer of cells that line small blood vessels and capillaries, resulting in the blockage of blood flow and increased leakage of fluids, which triggers an inflammatory reaction [25]. The onset of bleomycin-induced lung injury occurs when reactive intermediates are generated, resulting in oxidative stress and subsequent damage to the endothelium and epithelial cells. This results in the breakdown of the barrier separating the alveolar and capillary networks, leading to the infiltration of inflammatory cells into the lung tissue. The immune cells release inflammatory mediators and pro-fibrogenic cytokines, which stimulate the growth of myofibroblasts, the deposition of collagen, and ultimately lead to organ failure. This might potentially result in the death of the organism [26].

While rats treated with hidrosmin plus bleomycin (group 3) exhibited a significant reduction in serum levels of TNF- $\alpha$  and TGF- $\beta$ , this can be attributed to the lung-protective and antioxidant properties of hidrosmin, these findings align with prior research that has shown a reduction in serum levels of TNF- $\alpha$  and TGF- $\beta$ , by significantly downregulated the gene expression of inflammatory chemokines and cytokines [9]. In addition to preventing the activation of NF- $\kappa$ B [27]. Additionally, Hidrosmin showed increased levels of GSH and TAS, this is indicated for antioxidant activity.

Furthermore, rats that received vitamin C treatment (group 4) exhibited decreased ROS levels [14] by reduced serum levels of TNF- $\alpha$  and TGF- $\beta$ , compared to group 2, due to vitamin C downregulating the synthesis of inflammatory cytokines [28]. On the other hand, vitamin C increased levels of GSH and TAS due to their antioxidant activity.

While rats that were treated with a combination of hidrosmin and vitamin C (group 5) exhibited a pulmonary-protective benefit against lung damage induced by BLE by showing a significant reduction in serum levels of, TNF- $\alpha$  and TGF- $\beta$ , and significant elevation in serum levels of GSH and TAS compared to hidrosmin or vitamin C (group 3 and group 4, respectively). These effects may be produced from the antioxidant activity of both hidrosmin and vitamin C and additionally the synergistic effects of flavonoids and Vitamin C on the improvement of lung toxicity induced by bleomycin [29].

The histological examination in Figure 5 demonstrates that rats treated with Bleomycin (group 2) revealed the microscopic features of alveolar destruction and pulmonary edema with massive cellular infiltration, in addition to pulmonary fibrosis when compared to the normal architecture of microscopic findings in the control group (group 1). Meanwhile, microscopic findings in (group 3) and (group 4) demonstrate noticeable improvement in the lung.

Additionally clear improvement in the effects of bleomycin and the normal appearance of a bronchiole in (group 5) when compared with group 2. These findings align with previous studies [9] which ensured the lung protective activity of Hidrosmin due to their antioxidant activity.

## ■ CONCLUSIONS

According to the present finding, bleomycin may increase the risk of developing lung injury and stimulate the production of certain pro-inflammatory, such as TNF- $\alpha$  and TGF- $\beta$ , and decrease the levels of GSH and TAS, which may lead to induce lung toxicity. Bleomycin leads to the production of reactive oxygen species and oxidative stress, that are directly associated with lung fibrosis. Hidrosmin has anti-inflammatory and antioxidant activity. In addition to the cooperative effects of Hidrosmin and Vitamin C, which include lung protective effects against BLE-induced lung toxicity through reducing the harmful effects of reactive oxygen.

## ■ REFERENCES

1. Azambuja E, Fleck JF, Batista RG, Menna Barreto SS. Bleomycin lung toxicity: who are the patients with increased risk? *Pulm Pharmacol Ther*. 2005 Oct 1;18(5):363–6.
2. Hussen WM, Facs F, Ali Said FH, Osama Elhassani F. The outcome of Pleurodesis in Malignant Pleural Effusion. *J Fac Med Baghdad* [Internet]. [cited 2024 Feb 26];1(1):2022. Available from: <https://doi.org/10.32007/jfacmedbagdad.6411884>.
3. Suzuki H, Nagai K, Yamaki H, Tanaka N, Umezawa H. On the mechanism of action of bleomycin: scission of DNA strands in vitro and in vivo. *J Antibiot (Tokyo)*. 1969 Sep 25;22(9):446–8.
4. Sugiyama H, Ehrenfeld GM, Shipley JB, Kilkuskie RE, Chang LH, Hecht SM. DNA strand scission by bleomycin group antibiotics. *J Nat Prod* [Internet]. 1985 [cited 2024 Feb 26];48(6):869–77. Available from: <https://asu.elsevierpure.com/en/publications/dna-strand-scission-by-bleomycin-group-antibiotics>
5. Yukio S, Kikuchi T. Formation of superoxide and hydroxy radicals in iron(II)-bleomycin-oxygen system: electron spin resonance detection by spin trapping. *J Antibiot (Tokyo)* [Internet]. 1978 [cited 2024 Feb 26];31(12):1310–2. Available from: <https://pubmed.ncbi.nlm.nih.gov/83984/>
6. Hay J, Shahzeidi S, Laurent G. Mechanisms of bleomycin-induced lung damage. *Arch Toxicol*. 1991;65.
7. Travis WD, Costabel U, Hansell DM, et al. An official American Thoracic Society/European Respiratory Society statement: Update of the international multidisciplinary classification of the idiopathic interstitial pneumonias. *Am J Respir Crit Care Med* [Internet]. 2013 Sep 15 [cited 2024 Feb 26];188(6):733–48. Available from: <https://pubmed.ncbi.nlm.nih.gov/24032382/>
8. Dominguez C, Brautigam I, Gonzalez E, et al. Therapeutic effects of hidrosmin on chronic venous insufficiency of the lower limbs Summary. *Current Medical Research and Opinion*. 1992;12.
9. Jiménez-castilla L, Marin-royo G, Orejudo M, et al. Nephroprotective effects of synthetic flavonoid hidrosmin in experimental diabetic nephropathy. *Antioxidants*. 2021 Dec 1;10(12).
10. Jiménez-Castilla L, Opazo-Ríos L, Marin-Royo G, et al. The Synthetic Flavonoid Hidrosmin Improves Endothelial Dysfunction and Atherosclerotic Lesions in Diabetic Mice. *Antioxidants (Basel)* [Internet]. 2022 Dec 1 [cited 2024 Feb 28];11(12). Available from: <https://pubmed.ncbi.nlm.nih.gov/36552707/>
11. Day AJ, Dupont MS, Ridley S, et al. Deglycosylation of flavonoid and isoflavonoid glycosides by human small intestine and liver beta-glucosidase activity. *FEBS Lett* [Internet]. 1998 Sep 25 [cited 2024 Feb 24];436(1):71–5. Available from: <https://pubmed.ncbi.nlm.nih.gov/9771896/>
12. Castro SM, Guerrero-Plata A, Suarez-Real G, et al. Antioxidant Treatment Ameliorates Respiratory Syncytial Virus-induced Disease and Lung Inflammation. *Am J Respir Crit Care Med* [Internet]. 2006 Dec 12 [cited 2024 Feb 26];174(12):1361. Available from: <https://pubmed.ncbi.nlm.nih.gov/174121361/>
13. Hemilä H, Chalker E. Vitamin C for preventing and treating the common cold. *Cochrane Database Syst Rev* [Internet]. 2013 Jan 31 [cited 2024 Feb 28];2013(1). Available from: <https://pubmed.ncbi.nlm.nih.gov/23440782/>
14. Wu F, Tymk K, Wilson JX. Ascorbate inhibits iNOS expression in endotoxin- and IFN $\gamma$ -stimulated rat skeletal muscle endothelial cells. *FEBS Lett* [Internet]. 2002 [cited 2024 Feb 26];520(1–3):122–6. Available from: <https://pubmed.ncbi.nlm.nih.gov/12044883/>
15. Vitamin C – Health Professional Fact Sheet [Internet]. [cited 2024 Feb 28]. Available from: <https://ods.od.nih.gov/factsheets/VitaminC-HealthProfessional/>
16. Sugihara N, Kaneko A, Furuno K. Synergistic effects of flavonoids and ascorbate on enhancement in DNA degradation induced by a bleomycin-Fe complex. *Free Radic Res*. 2005 Mar;39(3):237–44.
17. Martínez de Toda I, González-Sánchez M, Díaz-Del Cerro E, et al. Sex differences in markers of oxidation and inflammation. Implications for ageing. *Mech Ageing Dev* [Internet]. 2023 Apr 1 [cited 2024 Feb 28];211. Available from: <https://pubmed.ncbi.nlm.nih.gov/36868323/>
18. Jiménez-castilla L, Marin-royo G, Orejudo M, et al. Nephroprotective effects of synthetic flavonoid hidrosmin in experimental diabetic nephropathy. *Antioxidants*. 2021 Dec 1;10(12).
19. Protective Effect of Hidrosmin Against Cisplatin-induced Acute Nephrotoxicity in Rats. *Request PDF* [Internet]. [cited 2024 Feb 28]. Available from: [https://www.researchgate.net/publication/230137833\\_Protective\\_Effect\\_of\\_Hidrosmin\\_Against\\_Cisplatin-induced\\_Acute\\_Nephrotoxicity\\_in\\_Rats](https://www.researchgate.net/publication/230137833_Protective_Effect_of_Hidrosmin_Against_Cisplatin-induced_Acute_Nephrotoxicity_in_Rats)

20. Wu GR, Dai XP, Li XR, Jiang HP. Antioxidant and anti-inflammatory effects of rhamnazin on lipopolysaccharide-induced acute lung injury and inflammation in rats. *African Journal of Traditional, Complementary, and Alternative Medicines* [Internet]. 2017 [cited 2024 May 16];14(4):201. Available from: [/pmc/articles/PMC5471467/](https://pubmed.ncbi.nlm.nih.gov/314671467/)
21. Ishida Y, Kuninaka Y, Mukaida N, Kondo T. Immune Mechanisms of Pulmonary Fibrosis with Bleomycin. *Int J Mol Sci* [Internet]. 2023 Feb 1 [cited 2024 Apr 21];24(4). Available from: [/pmc/articles/PMC9958859/](https://pubmed.ncbi.nlm.nih.gov/4158859/)
22. Peerzada MM, Spiro TP, Daw HA. Pulmonary toxicities of biologics: A review. *Anticancer Drugs*. 2010 Feb;21(2):131–9.
23. Muggia FM, Louie AC, Sikic BI. Pulmonary toxicity of antitumor agents. *Cancer Treat Rev* [Internet]. 1983 [cited 2024 Mar 1];10(4):221–43. Available from: <https://pubmed.ncbi.nlm.nih.gov/6198083/>
24. Hay J, Shahzeidi S, Laurent G. Mechanisms of bleomycin-induced lung damage. *Arch Toxicol*. 1991;65.
25. Hay J, Shahzeidi S, Laurent G. Mechanisms of bleomycin-induced lung damage. *Arch Toxicol* [Internet]. 1991 Feb [cited 2024 Apr 21];65(2):81–94. Available from: <https://pubmed.ncbi.nlm.nih.gov/1711838/>
26. Vats A, Chaturvedi P. The Regenerative Power of Stem Cells: Treating Bleomycin-Induced Lung Fibrosis. *Stem Cells and Cloning: Advances and Applications*. Dove Medical Press Ltd. 2023;16:43–59.
27. Anti-inflammatory effect of hidrosmin in diabetic kidney: (a-d)... *Download Scientific Diagram* [Internet]. [cited 2024 Feb 5]. Available from: [https://www.researchgate.net/figure/Anti-inflammatory-effect-of-hidrosmin-in-diabetic-kidney-a-d-representative-images\\_fig2\\_356638267](https://www.researchgate.net/figure/Anti-inflammatory-effect-of-hidrosmin-in-diabetic-kidney-a-d-representative-images_fig2_356638267)
28. Hemilä H, Chalker E. Vitamin C for preventing and treating the common cold. *Cochrane Database of Systematic Reviews* [Internet]. 2013 Jan 31 [cited 2024 Feb 26];2013(1). Available from: <https://www.cochranelibrary.com/cdsr/doi/10.1002/14651858.CD000980.pub4/full>
29. Sugihara N, Kaneko A, Furuno K. Synergistic effects of flavonoids and ascorbate on enhancement in DNA degradation induced by a bleomycin-Fe complex. *Free Radic Res* [Internet]. 2005 Mar [cited 2024 Feb 26];39(3):237–44. Available from: <https://pubmed.ncbi.nlm.nih.gov/15788228/>

<https://doi.org/10.34883/PI.2025.14.1.060>

Rasha Jawad Kadhim, Basim Hashim Abdullah   
College of Education for Pure Sciences, University of Basrah, Basrah, Iraq

# First Record of Four Species of Trematodes Parasitizing Stray Cat *Felis catus* L.

**Conflict of interest:** nothing to declare.

**Authors' contribution:** Rasha Jawad Kadhim – conceptualization, data curation, investigation, methodology, project administration, resources, software, validation, writing – original draft and writing – review & editing; Basim Hashim Abdullah – conceptualization, data curation, investigation, methodology, supervision, validation, visualization, writing – original draft and writing – review & editing.

The article is published in author's edition.

Submitted: 20.01.2025

Accepted: 17.03.2025

Contacts: basim.abdullah@uobasrah.edu.iq

## Abstract

**Introduction.** Infected cats are a source of infection for humans and other animals. They are also considered an intermediate host, carrier, vector, or reservoir for many parasites. Cats are severely exposed to a variety of parasitic infections. Trematodes are a major group of parasites that infect humans and animals and are distributed throughout the world.

**Materials and methods.** During the current study, 70 loose *Felis catus* L. cats were collected during a period of six months from the beginning of January 2023 until the end of June 2023 from two areas in Basra province, namely the Shatt al-Arab (Al-Jazeera) and the Hay Al-Resala area located in the center of Basrah.

**Results.** The prevalence trematods was 14% Four species of trematodes were recorded for the first time in Iraq, which are (*Brachylaema* sp. 4.2%, *Stictodora* sp. 5.7%, *Proceravium Calderoni* 4.2%, and *Hippocrepis* sp. 1.4%). The mean intensity of infection (*Brachylaema* sp. 166 and *Stictodora* sp. 375, *Proceravium Calderoni* 233, and *Hippocrepis* sp. 5). These trematodes appeared during the summer.

**Conclusion.** Four new types of trematodes were found, recorded for the first time in Iraq, are: *Stictodora* sp., *Hippocrepis* sp., *Brachylaema* sp., and *Procerovum claderoni*.

**Keywords:** *felis catus*, *brachylaema*, *stictodora*, *proceravium calderoni*, *hippocrepis*, trematodes

## ■ INTRODUCTION

Cats are widely spread throughout the world due to their high ability to adapt to live in widely different environments within homes and public places and are a source of many diseases [1].

Infected cats are a source of infection for humans and other animals. They are also considered an intermediate host, carrier, vector, or reservoir for many parasites [2]. Cats are severely exposed to a variety of parasitic infections, and the reason for this is a result of their behavior and habits. They are infected with a wide range of parasites [3]. Comorbidities are a major public health concern and pose a threat to human health and may even lead to death [4].

Trematodes are a major group of parasites that infect humans and animals and are distributed throughout the world. It has a complex life cycle that requires at least two hosts, one of which is usually an invertebrate. Trematodes infect the liver, lung, and intestines. Intestinal trematodes are the largest group, and about seven million people are infected worldwide. Infection occurs when humans eat raw or undercooked foods that contain infectious bacteria [5].

Trematodes parasitize inside various vertebrates and can be transmitted to humans [6]. Cats, dogs, and rats are also important reservoir hosts for many trematodes [7], in addition to being natural hosts for parasitic diseases [8].

The vast majority of invertebrates are intermediate hosts and vertebrates are the definitive hosts of trematodes. Usually trematodes parasitize the digestive system of their hosts, and some of them live in the circulatory system [6].

Adult trematodes parasitize inside various vertebrates and spend the larval stages in the intermediate host, mainly invertebrates such as snails [9]. There are many families of trematodes that infect humans, including Brachylaimiidae and Heterophyidae [5]. The trematodes recorded in the current study belong to three families, including Brachylaimidia, Heterophyidae, and Notocotylidae.

The Brachylaimidia family is a large family, as members of this family parasitize birds, mammals, and even humans [10]. It is considered important from a public health perspective, because it causes diseases in humans such as hemorrhagic enteritis, diarrhea, inflammation of the bile ducts, and anemia [11], and the genus *Brachylaima* is the most important in this family. Its life cycle is represented within intermediate hosts, either from the same species or from two different species of snails [12].

The Heterophyidae family contains small, infective trematodes. The final host becomes infected by eating raw or undercooked fish. Adults also live between the villi in the anterior region of the small intestine and release eggs there, and the eggs are captured by snails (*Melanoides*, *Semisulcospira*, and others). Metacercariae may remain viable for years [13–15].

## ■ MATERIALS AND METHODS

### **Study area**

The stray cats were collected from two areas in Basra Province, which are Shatt al-Arab District (Al-Jazeera) and the Hay Al-Resala located in the center of Basra. I caught 70 loose cats, *Felis catus*, using a special American-made Havahart 1045 trap designed to catch live animals without harming them, during the period extending from the beginning of January 2023 until June 2023.

The caught animals were transported to the laboratory using a bag that was resistant to cats, and they were killed with an overdose of chloroform. A piece of cotton soaked in about 10 milliliters of chloroform was used and they were placed with the cats inside another nylon bag, then closed tightly to prevent air from reaching them.

After anesthetizing the cats, I made an incision along the abdomen towards the chest. I then isolated the digestive tract (from the beginning of the stomach to the end of the rectum), dividing it into five parts, each of which was placed in a glass dish: the stomach, the small intestine with its three parts (the duodenum, the jejunum, and the ileum), and the intestine. The thick one.

The contents and lining of these parts were examined for parasitic worms, which were isolated from infected animals, including trematodes that were prepared for subsequent studies.

Trematodes were diagnosed based on Bray et al. [16] and Yamaguti [17].

Depending on Margolis et al. [18] to define the environmental terms mentioned in this study, especially the incidence of infection and the mean intensity of infection.

## ■ RESULTS

Four new types of trematodes were found, recorded for the first time in Iraq, on trematodes in four infected cats out of 70 examined cats, with the total infection rate reaching 14%.

### **Worms parasitic on cats**

#### **Trematodes**

The prevalence of trematodes was 14%, and four species of trematodes were recorded for the first time in Iraq: *Stictodora* sp., *Hippocrepis* sp., *Brachylaema* sp., and *Procerovum claderoni*.

#### ***Brachylaema* sp.**

More than 500 trematodes of this type were found parasitizing the small intestines of three stray cats caught from the Shatt al-Arab region in Basra. The prevalence was 4.2% and the average infection severity was 166. Below are descriptions and measurements of ten examples of them.

This trematodes is characterized by its flat, cylindrical shape and has a tongue-like body that is round on both ends. Its length ranges between 0.57–0.45 (0.45) and its width is 0.17–0.10 (0.13). The oral sucker is muscular, with a drop of 0.08–0.07 (0.07). The ventral sucker is 0.074–0.072 (0.073) proximal. To the middle of the body from the front end, the pharynx is muscular, with a diameter of 0.036–0.020 (0.028). The testicles are located in the posterior third of the body, one behind the other.

The ovary is usually between the testicles (average location) 0.092–0.080. It is smaller than the testicle, medium in location and overlapping with the testicles. The eggs are many, yellowish-brown in color, 0.04–0.03 (0.003).

#### ***Proceravum calderoni* (Onji et Nishio, 1916)**

More than 700 parasitic trematodes were found in the small intestine of three stray cats caught from the Shatt al-Arab region (Al-Jazeera) in Basra, where the infection rate was 4.2% and the average infection severity was 233. Below are descriptions and measurements of ten examples of them.

This trematode is characterized by being very small and pear-shaped. Its length ranges between 0.35–0.40 (0.37) and its width is 0.19–0.22 (0.20). The body is covered with fine spines.

The oral sucker is terminal, circular, muscular, indistinct, embedded in diameter, 0.048–0.050 (0.047), and the ventral sucker is large, 0.06–0.05 (0.06), the pharynx is oval and has a diameter of 0.03–0.02 (0.02).

The testicle is single and oval at the back end of the body, slightly to the left. Its size ranges from 0.14–0.12 (0.13). The common Genital pore is located in front of the abdominal

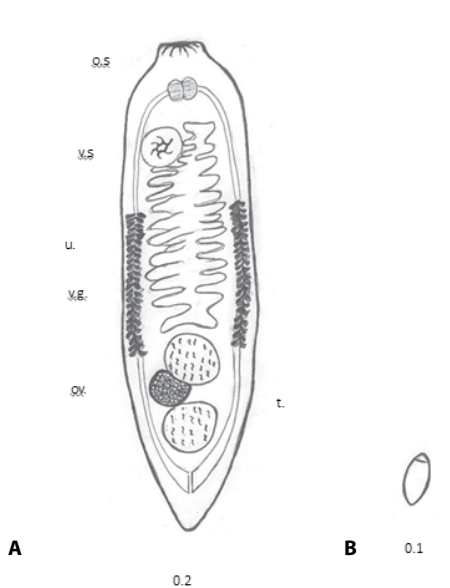


**Fig. 1. *Brachylaema* sp.:** A – adult worm: ov – ovary, os – oral sucker, t – testis, u – uterus, vg – vitelline gland, vs – ventral sucker; B – egg

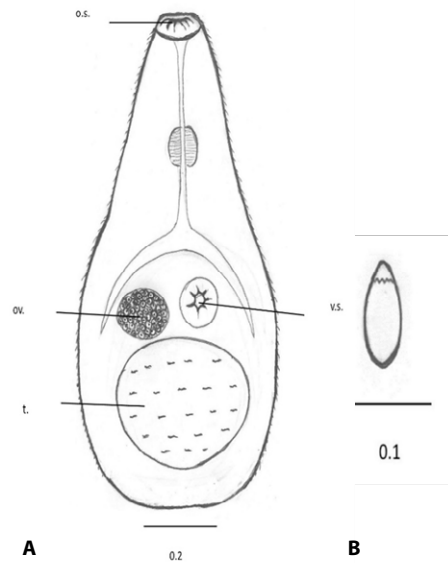


**Fig. 2. *Procerovum claderoni*:** A – worm: ov – ovary, os – oral sucker, t – testis, vg – vitelline gland, vs – ventral sucker, B – egg

retractor. The oviductal area is wide and clear, and the uterus is filled with eggs whose sizes range from 0.026–0.024 (0.025). The excretory sac is funnel-shaped.

### ***Stictodora* sp.**

More than 1,500 parasitic trematodes were found in the small intestines of four stray cats caught from the Shatt al-Arab region in Basra. The prevalence was 5.7% and the mean intensity of infection was 375. Below are descriptions and measurements of ten examples of them.

This trematode is characterized by its pear or club shape. The length of this trematode ranges between 0.41–0.39 (0.40) and its width is 0.20–0.22 (0.21). The cut is covered with soft spines.

The oral sucker is subterminal circular muscular 0.04–0.03 (0.04), the ventral sucker is also circular muscular 0.048–0.043 (0.045), the pharynx is circular in diameter 0.032–0.30 (0.031), the esophagus is short in length 0.032.

The testicles are slanted 0.068–0.060 (0.064), and they do not contain a coma sac, and the reproductive ducts are shaped like the letter eight in Arabic. The uterus is full of eggs whose measurements range between 0.028–0.027 (0.0027).

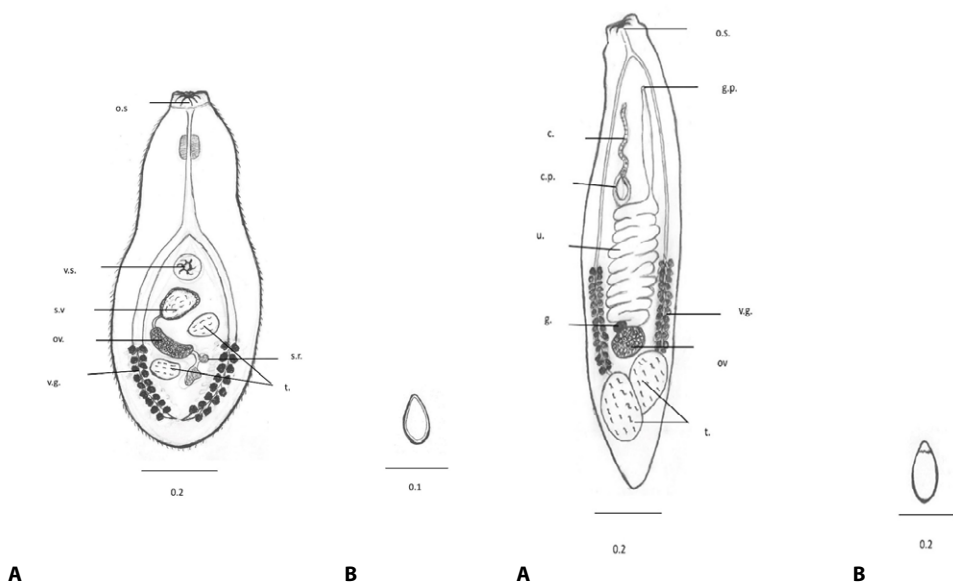


**Fig. 3. *Stictodora* sp.:** A – adult worm: ov – ovary, os – oral sucker, sv – seminal vesicle, sr – seminal receptacle, t – testis, u – uterus, vg – vitelline gland, vs – ventral sucker; B – egg

**Fig. 4. *Hippocercis* sp.:** A – adult worm: c – cecum, cp – cirrus pouch, gp – genital pore, ov – ovary, os – oral sucker, t – testis, u – uterus, vg – vitelline gland, vs – ventral sucker; B – egg

### ***Hippoecrepis* sp.**

Five trematodes of this type were found parasitizing the small intestine in one stray cat caught from the Shatt al-Arab region in Basra. The prevalence was 1.4% and the mean intensity of infection was 5. Below are descriptions and measurements of five models of this perforator. This trematode is characterized by its elongated shape, with a papilla protruding from each side near the front end of the head. This trematode ranges between 0.50–0.40 (0.47) long and 0.12–0.10 (0.011) wide. The body is thin and long. The oral sucker is indistinct, embedded in the form of a subterminal hole, its diameter ranges from 0.09–0.08 (0.07). As for the ventral sucker, 0.04–0.06 (0.05). The body is equal, the front area is the same size as the back area. The testicle is located in the back of the body and has a size of 0.05–0.06. The ovary is located medium in front of the testicle. The uterus is filled with eggs that measure between 0.036–0.032 (0.033).

## ■ DISCUSSION

### **Trematodes**

The trematode recorded in the study belong to three families: Notocotylidae, Heterophyidae, and Brachylaimidia. Four species of trematodes were recorded in the current study, and a decrease in the rate of infection of cats with flukes was observed compared to what was found by Abdullah [19]. as the infection rate reached 22%, during which three species of trematodes were recorded: *Opisthorchis felinus*, *Heterophyes heterophyes*, and *H. aequalis*, as indicated Nasser [2] did not record any fluke infections

in Al- Diwaniyah. In Kirkuk, Hassan and Ghaeib [20] recorded three types of trematodes, with an infection rate of 12%, while in Egypt, Khalaf Al-Allah [21] recorded two types of trematodes, with an infection rate of 3%. The trematodes are less specialized and preferred in choosing the final host than other parasitic worms. Therefore, we find cats harbor large numbers of them, and they share this with other predators. They eat the same intermediate hosts that contain the infective stages, so there is difficulty in determining whether cats represent the true final host for the parasitic trematodes on it [22].

### **Brachylaima sp.**

This trematode belongs to the Brachylaimida family, whose members are characterized by an elongated, flat body, a clear, well-developed oral cavity, and vitelline glands in the middle of the last third of the body [17]. It also includes a large group of species that infect mammals, birds and reptiles. For example, in the genus *Brachylaima*, there are 23 described species that infect rodents all over the world [23]. A number of them are of medical importance because they cause diseases in humans that can even lead to death [24, 25]. The size and shape of the current model agree with the size of the fluke *B. fuscatum*, which was found to infect birds [11].

Butcher et al. [23] described the trematode *B. cribbi*, which they found parasitizing in mammals. The size of this trematode was larger than the model mentioned in the current study. This intestinal trematode has also been reported to infect humans in South Australia, and a laboratory life cycle was established using eggs isolated from human feces. Therefore, the need has increased to study the species of this genus and understand its taxonomic and biological characteristics. It is noteworthy that many species of the genus *Brachylaima* sp. infect mice *Mus musculus* [26].

Waki et al. [27] found in Japan the fluke *B. lignieuhadrae* in snails of the genus *Euhadra*, and the measurements of this model were larger than the measurements mentioned in the current study.

One example of this genus was also found parasitizing the snail *Corn aspersum* (Pulmonata), which is considered the second intermediate host containing metacarcariae. Note that this conch is considered a food in Spain [28]. It also includes the genus *Brachylaima* sp. Many *Brachylaima* species complete their life cycles in mammals and birds around the world [29]. As mentioned Nakao et al., [30] the intermediate host increases the chance of transmitting the parasite to various mammals and birds. It also infects adults in the digestive systems of birds and mammals, and rarely infects amphibians. Its life cycle includes two intermediate hosts, both of which are molluscs [31].

### **Proceravum calderoni**

This trematode is characterized by its small size and pear-shaped shape surrounded by densely distributed spines, in addition to the presence of a single, oval testicle at the back [32]. This trematode belongs to the Heterophyidae family, which includes a number of small trematode, most of which are parasitizing the small intestines of birds and mammals, but the current type has been found. It is parasitic in mammals only [33].

The trematode measurements recorded in this study agree with the trematode measurements recorded by Chen [32]. Another species, *Procerovum varium*, of the same genus was also recorded by Onji and Nishio [34] and the measurements of this species were less than what was recorded in this study.

Cats become infected by eating fish waste or parts thereof that contain metacercariae. Other families who eat infected raw fish are also likely to become infected [22], as the metacercariae settle in the muscles and then transform into adults that shed eggs in the small intestine. Within 8 to 10 days [35].

Species belonging to this genus differ greatly from each other depending on the type of host and their size. The specimens found in birds are smaller than the specimens found in cats. The reason for this is that the internal organs in birds are smaller than they are in cats [32].

### **Stictodora sp.**

This genus of trematodes belongs to the Heterophyidae family, which is characterized by an elongated body and a terminal mouthpiece [22]. Some measurements of this model were lower than those reported by Chai et al. [36]. Abdul-Salam et al. [37] in Kuwait described *S. tridactyla* isolated from kittens that feed on fish, as it is characterized by a pear-shaped body and a terminal circular mouth size with thorns covering the body. These characteristics are consistent with the characteristics mentioned in the current study. As for the measurements, they were slightly larger than the current model's measurements.

Chai et al. [36] was also able to record two species from the Heterophyidae family, which belong to the genus *Stictodora*, which he collected from the droppings of an adult human. Eggs of *Diphyllobothrium latum* and Heterophyids were also found. He also recorded this genus of fish-eating birds and mammals [29].

Chai et al. [38] also recorded another species, *Stictodora lari*, in Korea, but the measurements of this species are larger than what was recorded in the current study. The genus *Stictodora* and the species *S. sawakinensis* were also described by Looss [39] collected from gulls, and *S. sawakinensis* and *S. Thaparai* were also described in Egypt and occupied Palestine as parasitism on cats [40].

Sohn et al. [41] described the fluke *S. fuscatum* and it was noted that the characters were similar in appearance but differed in measurements.

Kinsella and Heard [42] studied the life cycle of *S. cursitans* from squirrels, and it was noted that the models studied were larger than those in the current study. The genus *Stictodora* includes more than 20 species that have been recorded in Korea, of which only two species have been described: *S. fuscatum* and *S. lari* [36].

### **Hippocrepis sp**

This trematode belongs to the family Notocotylidae, which includes species belonging to this family that parasitize birds and mammals. The most important characteristic of this genus is the presence of papillae protruding from each side close to the front end of the head, and the function of these papillae is still mysterious [43].

Rocha et al. [44] recorded a prevalence of 25% and mean intensity of infection 12. The rates were higher than what was recorded in the current study.

Assis et al. [45] found this trematode parasitizing the large intestine of the water pig (*Capybaras*) in Brazil, which is considered one of the largest rodent species that lives near rivers and lakes in South America. As for Rocha et al. [44] the trematode *H. felleborni* was found parasitizing a species of rodent (*Coypu*). The snails are of the genus *Biophalaria* sp. Intermediate hosts for most species of the genus *Hippocrepis* sp. On the other hand, the snail *B. straminea* is the first intermediate host recorded for the

Trematode *H. hippocrepis*, and aspects of the life cycle and pathogenesis of these trematodes are still unknown [45].

## ■ CONCLUSION

Four new types of trematodes were found, recorded for the first time in Iraq, are: *Stictodora* sp., *Hippocrepis* sp., *Brachylaema* sp., and *Procerovum claderoni*.

## ■ REFERENCES

1. Al-Tae ARA, Al-Rubaie ARL. Checklists of parasites stray cats *Felis catus* of Iraq. *Ibn AL-Haitham Journal For Pure and Applied Science*, 2018; IHSCICONF 2017:143–151
2. Hajim NF. *Epidemiological and diagnostic study of external and internal parasites in domestic cats Felis catus in Al-Qadisiyah Governorate*. Master's thesis, College of Science, 2016.
3. Krecek RC, Moura L, Lucas H, Kelly P. Parasites of stray cats (*Felis domesticus* L., 1758) on St. Kitts, West Indies. *Vet Parasitol*. 2010;172(1–2):147–91
4. Grace D, Mutua F, Ochungo P, et al. Mapping of poverty and likely zoonoses hotspots. Zoonoses Project 4. Report to the UK Department for International Development. Nairobi, Kenya: ILRI, 2012.
5. Fürst T, Keiser J, Utzinger J. Global burden of human food-borne trematodiasis: a systematic review and meta-analysis. *Lancet Infect Dis*. 2012;12(3):210–21.
6. Mhaisen FT, Al-Rubaie AL, Al-Sa'adi BA. Trematodes of fishes from the Euphrates River at Al-Musaib City, Mid Iraq. *Amer. J. Biol. Life Sci*, 2015;3(4):91–95
7. Nguyen HM, Tatonova YV, Madsen H. Infections by Hepatic Trematodes in Cats from Slaughterhouses in Vietnam. *J Parasitol*. 2018;104(3):306–309.
8. Farjat JA, Minvielle MC, Pezzani BC, Niedfeld G. Relationship between parasitological inoculum and immunological parameters in experimental toxocarosis. *Zentralbl Bakteriol*. 1995;282(4):465–73.
9. Mhaisen FT, Khamees NR, Ali AH. Checklists of Trematodes of Freshwater and Marine Fishes of Basrah Province, Iraq. *Basrah Journal of Agricultural Sciences*, 2013;26(spe.1):50–77.
10. Lunaschi LI, Drago FB. Digenean parasites of *Cariama cristata* (Aves, Gruiformes) from Formosa Province, Argentina, with the description of a new species of the genus *Strigea*. *Acta Parasitol*. 2012;57(1):26–33
11. Suleman S, Khan MS. First report of the genus *Brachylaema* Dujardin, 1843 (Trematoda: Brachylaimidae) from the small intestine of common myna (*Acridotheres tristis*) of district Swabi, Khyber Pakhtunkhwa, Pakistan. *Turkish Journal of Zoology*, 2016;40(4):595–600
12. Yamaguti S. A synoptical review of the life histories of digenetic trematodes of vertebrates: with special reference to the morphology of their larval forms, Tokyo: Keigaku Publishing Company, 1975;590–575.
13. Fried B, Graczyk TK, Tamang L. Food-borne intestinal trematodiasis in humans. *Parasitol Res*. 2004;93(2):159–70.
14. Sohn WM. Fish-borne zoonotic trematode metacercariae in the Republic of Korea. *Korean J Parasitol*. 2009;47 Suppl(Suppl):S103–13.
15. Toledo R, Esteban JG, Fried B. Immunology and pathology of intestinal trematodes in their definitive hosts. *Adv Parasitol*. 2006;63:285–365.
16. Zdzislaw S, Boyko G. Keys to the Trematoda. Volume 3 (eds. R.A. Bray, D.J. Gibson and A. Jones) CABI Publishing, Wallingford, UK and the Natural History Museum, London, 2008, 824 p. *Acta Parasitologica*, 2009;54(2):186–186.
17. Yamaguti S. 19610800540, English, Book, Systema helminthum. Vol. II. The cestodes of vertebrates (vii +860 pp.), New York & London: Interscience Publishers, Inc. 1959; 860 p.
18. Margolis L, Esch GW, Holmes JC, et al. The use of ecological terms in parasitology (report of an ad hoc committee of the American Society of Parasitologists). *The Journal of parasitology*, 1982;68(1):131–133
19. Abdullah BH. *Some parasitic worms on stray cats Felis catus L. in Basra and epidemiological and biological studies of the cat tapeworm Taenia taeniaformis Batsch, 1786*. Master thesis. College of Education for Pure Sciences, 2007.
20. Hassan HF, Ghaeb SY. Isolation and diagnosis of intestinal worms from stray cats in Kirkuk city. *Kirkuk University Journal for Scientific Studies*, 2022;17(2):36–43.
21. Khalafalla RE. A survey study on gastrointestinal parasites of stray cats in northern region of Nile delta, Egypt. *PLoS One*. 2011;6(7):e20283
22. Bowman DD, Hendrix CM, Lindsay D, Barr SC. *Feline Clinical Parasitology*. Iowa State Univ. Blackwell Science Company. Iowa, USA. 2002; 469 p.
23. Butcher AR, Palethorpe HM, Grove DI. The susceptibility of inbred mice to infection with *Brachylaema cribbi* (Digenea: Brachylaimidae). *Parasitol Int*. 2002;51(1):109–15.
24. Butcher AR, Graham AT, Norton RE, et al. Locally acquired *Brachylaema* sp. (Digenea: Brachylaimidae) intestinal fluke infection in two South Australian infants. *Med. J. Aust*. 1996;164:475–478.
25. Butcher AR, Grove DI. Description of the life-cycle stages of *Brachylaema cribbi* n. sp. (Digenea: Brachylaimidae) derived from eggs recovered from human faeces in Australia. *Syst Parasitol*. 2001;49(3):211–21.
26. Angel LM, Mutze GJ. On the occurrence of *Brachylaema* sp. (Trematoda) in the feral house mouse, *Mus musculus*, in South Australia. *Transactions of the Royal Society of South Australia*. 1987;111:121–122.
27. Waki T, Sasaki M, Mashino K, et al. *Brachylaema lignieuhadrae* n. sp. (Trematoda: Brachylaimidae) from land snails of the genus *Euhadra* in Japan. *Parasitol Int*. 2020;74:101992
28. Gracenea M, Gállego L. Brachylaimiasis: *Brachylaema* spp. (Digenea: Brachylaimidae) Metacercariae Parasitizing the Edible Snail *Cornu aspersum* (Helicidae) in Spanish Public Marketplaces and Health-Associated Risk Factors. *J Parasitol*. 2017;103(5):440–450
29. Yamaguti S. Systema helminthum. Vol. I. The Digenetic Digenetic Trematodes of Vertebrates – Part II. CABI Databases. 1958:981.
30. Nakao M, Sasaki M, Waki T, et al. *Brachylaema asakawai* sp. nov. (Trematoda: Brachylaimidae), a rodent intestinal fluke in Hokkaido, Japan, with a finding of the first and second intermediate hosts. *Parasitol Int*. 2018;67(5):565–574.

31. Gibson DJ, Jones A, Bray RA. Keys to the trematoda. Vol. 1. London: CAB International and Natural History Museum. 2002;349–350]
32. Chen HT. Systematic consideration of some heterophyid trematodes in the subfamilies Haplorchinae and Stellantchasmae. *Annals of Tropical Medicine & Parasitology*, 1949;43(3–4):304–312]
33. Waikagul J. A review of the heterophyid flukes in man. *Chulalongkorn Medical Journal*, 1985;29(10):1131–1138.
34. Onji Y, Nishio T. (On intestinal distomes). *Iji Shimbun*. 1916;949:589–593. (In Japanese)
35. Velasquez CC. Life cycle of *Procerovum calderoni* (Africa and Garcia, 1935), Price, 1940 (Trematoda: Digenea: Heterophyidae). *The Journal of Parasitology*, 1973;813–816]
36. Chai JY, Hong SJ, Lee SH, Seo BS. *Stictodora* sp. (Trematoda: Heterophyidae) recovered from a man in Korea. *The Korean Journal of Parasitology*, 1988;26(2):127–132]
37. Abdul-Salam J, Sreelatha BS, Ashkanani H. Surface ultrastructure of *Stictodora tridactyla* (Trematoda: Heterophyidae) from Kuwait Bay. *Parasitology international*, 2000;49(1):1–7]
38. Chai JY, Park SK, Hong SJ, et al. Identification of *Stictodora lari* (Heterophyidae) metacercariae encysted in the brackish water fish, *Acanthogobius flavimanus*. *The Korean Journal of Parasitology*, 1989;27(4):253–259.
39. Looss A. Weitere BeitrNge sur Kenntniss der Trematoden-Fauna Aegyptens, zugleich Versuch einer natrlichen Gliederung des Genus *Distomum* Retzius. *Zool Jahrb*. 1899;12:521–784.
40. Kuntz RE, Chandler AC. Studies on Egyptian trematodes with special reference to the heterophyids of mammals. I. Adult flukes, with descriptions of *Phagicola longicollis* n. sp., *Cynodiplostomum namrui* n. sp., and a *Stephanoprora* from cats. *J Parasitol*. 1956;42:445–459.
41. Sohn UM, Chae JI, Lee SH. *Stictodora fuscatum* (Heterophyidae) metacercariae encysted in gobies, *Acanthogobius flavimanus*. *Parasites, Hosts and Diseases*. 1994;32(3):143–148.
42. Kinsella JM, Heard III RW. Morphology and life cycle of *Stictodora cursitans* n. comb. (Trematoda: Heterophyidae) from mammals in Florida salt marshes. *Transactions of the American Microscopical Society*, 1974:408–412]
43. Barton DP, Blair D. Family Notocotylidae Luehe, 1909. In Keys to the Trematoda: Volume 2. Wallingford UK: CABI Publishing. 2005; 383–396 p.
44. Rocha AGDS, Gallas M, da Silveira EF. *Hippocrepis fuelleborni* (Digenea, Notocotylidae) parasitizing *Myocastor coypus* (Rodentia, Myocastoridae) in Southern Brazil. *Neotropical Helminthology*, 2012;6(2):185–190]
45. Assis JC, Lopez-Hernandez D, Pulido-Murillo EA, et al. A morphological, molecular and life cycle study of the capybara parasite *Hippocrepis hippocrepis* (Trematoda: Notocotylidae). *PLoS One*, 2019;14(8):e0221662]

<https://doi.org/10.34883/PI.2025.14.1.051>

Shadia Alhamd

College of Education for Pure Science, Basrah University, Basrah, Iraq

## Evaluation of GAPDH and EF1a Genes as Reference Genes in Molly Fish

**Conflict of interest:** nothing to declare.  
The article is published in author's edition.

Submitted: 02.01.2025

Accepted: 17.03.2025

Contacts: shadia.fahid@uobasrah.edu.iq

### Abstract

**Introduction.** The level of mRNA expression varies greatly under different physiological and experimental conditions. Therefore, when conducting gene expression analysis through qPCR, it is essential to employ reference genes for the normalization of RNA quantities.

**Purpose.** Thus, the study deduces that GAPDH may be valid as a reference gene, and excludes EF1a for this purpose in this species.

**Materials and methods.** Two reference genes were selected to determine their validity as reference genes in Molly Fish. The evaluation of genes was performed in three cases; the first was an adult untreated fish, the second was a treated fish by calcitonin drug, and the third was by using different developmental stages of fish. The fish specimens were categorized into two sets. The first group received an injection of 4 microliters of calcitonin. At the experiment end, pregnant fish were anatomized to obtain embryos of successive stages in addition to organs of the adult. The samples were fixed following special methods of RNA extraction. The primers were designed for the studied genes. The RNA was extracted, tested and purified, and cDNA building, amplification, and RT-PCR interactions were performed.

**Results.** After analyzing the data, it was found that the expression of GAPDH gene was twice the EF1a expression. Also found that GAPDH was more stable and consistent than EF1a under the calcitonin influence. It turns out that GAPDH was the most consistent in its expression during the developmental stages. Unlike EF1a, which showed significant differences among some of these stages.

**Conclusion.** The GAPDH gene expression was stronger, more constant and stable than the EF1a gene at all stages studied, and also under the influence of the hormone. Therefore, it is possible that GAPDH may be a suitable reference gene with *P. latipinna*. Exclude the EF1a gene, for lack of basic conditions that qualify it as a suitable reference gene in this species of fish.

**Keywords:** GAPDH, EF1a, Reference Genes, Fish, *Poecilia latipinna*

## ■ INTRODUCTION

In gene expression analysis, reference genes serve the purpose of normalizing total RNA quantities, addressing mechanical errors, compensating for variations in reverse transcription efficiency, Adjusting for variations in RNA integrity across samples, and mitigating the impact of PCR inhibitors [1]. Real-time RT-PCR relies on endogenous controls such as housekeeping genes (HKGs), rRNA, and total RNA as references for estimating the expression levels of target genes. The primary aim of employing these controls is to minimize or alleviate variations introduced during sampling. Specifically, these differences pertain to both the quantity and quality of RNA [2]. HKGs are expected to demonstrate uniform expression across cells, organs, individual organisms, diverse developmental stages, and various experimental conditions. Numerous HKGs are utilized as reference genes in qPCR. However, even HKGs, in the absence of chemical treatment, have a tendency to undergo changes influenced by the tissue type and developmental stage [3]. Undetected and surprising alterations in the expression of housekeeping genes (HKGs) may lead to incorrect conclusions regarding actual biological effects [4]. Several investigations have demonstrated that no single gene universally maintains a consistent expression level across all developmental or experimental conditions. The selection of the optimal reference gene as an endogenous control depends on the specific tissues under examination. Consequently, a diverse set of genes was chosen to normalize mRNA expression data [5, 6]. Thus, the selected HKGs should be validated for each new experimental setup [7]. For expression studies using qPCR, at least two reference genes, must be used [8]. Fish have many characteristics that distinguish species among themselves, and distinguish them from other vertebrates, which has led to interest in them in studies and research. Its importance has also recently been proven in various scientific fields [9, 10]. Real-time RT-PCR has evolved into a crucial instrument for examining gene expression in fish [7].

The study investigates two genes within HKGs to test their suitability as reference genes in fish *Poecilia latipinna*. The first is the GAPDH gene, that holds significance in various cellular processes [2]. The second one is EF1a, the elongation factor, which plays a crucial role in the translation process and participates in a variety of cellular functions [2, 11].

The specificity of the calcitonin hormone in fish has been demonstrated in previous studies [12–14]. This hormone has been chosen as a crucial factor to elucidate the molecular-level mechanisms of its action. Leveraging the sensitivity, speed, simplicity, and specificity of qPCR technologies enables the detection of minute amounts of nucleic acid across a variety of samples. To our knowledge, there is no previous study investigated the validity of reference genes in the studied species, possibly in the genus *Poecilia* in general. This is crucial because reference genes, frequently borrowed from the literature and applied without adequate validation across diverse experimental conditions, are assumed to maintain a consistent expression level [15].

## ■ MATERIALS AND METHODS

### **Laboratory animals**

Fully developed *P. latipinna* fish were acquired from ornamental fish shops and transported to the laboratory. Fish used were average 5 cm lengths and 5 g weight, divided into two groups at a rate of one male for every five females. Each group contained

approximately 50 fish, and they were under the same laboratory conditions. Fish in group 1 received injections of 4 microliters of calcitonin per 5 grams of fish weight, corresponding to 1 IU per 100 grams of fish weight [12]. Group 2 fish were injected with a 0.6% concentration of normal saline and served as the control group. Injections were administered daily for the initial ten days, after which the injected was every two days until the experiment end that took about a month and a half. Pregnant females from both groups, were anatomized at the end of the experiment and embryos and tissue samples were collected in successive stages. The embryos were measured using a dissection microscope. The stages were determined by the lengths because of their small size, starting from 2 mm to 7 mm.

### Sample preparation

The samples were prepared according to the Morel and Raccurt [16] method known as Formalin Fixed Paraffin Embedded (FFPE) for RNA extraction to study gene expression through quantitative real-time polymerase chain reaction (Q-RT-PCR).

### Primers design

The primers of the two studied genes (EF1a and GAPDH) were designed using data in the Data Banks based on Parameters appropriate for Real-Time PCR processes (Table 1).

**Table 1**  
**Primers designed for the studied genes EF1a and GAPDH**

Genes	Primers
EF1a-F	GTTAAGTCCGTTGAGATGCAC
EF1a-rt-R	GATGATGACCTGAGCATTGAAG
GAPDH-F	CACTGTCAAGGCTGAGAACGG
GAPDAH-R	GAGATGATAACACGCTTAGCACCA

### RNA extraction

RNA was extracted from embedded samples in paraffin wax moldings using a special kit from MACHEREY-NAGEL (MN, Germany). The NanoDrop device was used to assess both the quantity and quality of the extracted RNA. The RNA purification and removal of DNA by DNase was performed using a special Deoxyribonuclease I Kit (Invitrogen, Cat # 18068-015).

### CDNA construction, amplification, and RT-PCR reactions

The cDNA was synthesized using BIO-RAD's iScript kit, and subsequent real-time PCR reactions were carried out on the Light Cycler 96 (Roche Co.) utilizing SYBR Green Master Mix (5x).

### Data analysis

[2<sup>-</sup> Ct] equation was adopted in calculating gene expression [13], and the SPSS statistical analysis program was used to analyze the data in the current study, using both T-Test and ANOVA.

## ■ RESULTS

The average Ct values for the EF1a gene ranged from 38.63 – 38.5 for the control group and from 14.14 – 38.19 for the treatment group (Fig. 1). Ct values for the GAPDH gene ranged from 19.31 – 20.84 for control and from 19.06 – 21.09 for the treatment group (Fig. 2). The results showed that the rates variance, among the Ct values of the EF1a gene of the control group, were greater than the rates variance among the Ct values of the GAPDH gene, as the highest rate of the EF1a gene at 3 mm stage (38.5), and the lowest rate at 4 mm stage (34.63) (Fig. 1). Whereas the highest rate of GAPDH gene was at 6 mm stage (20.84), and the lowest rate was at adult (19.31) (Fig. 2). The rate variance among the stages of the EF1a gene was 3.87, which is greater than the rate variance among the stages of the GAPDH gene, whose value was 1.53.

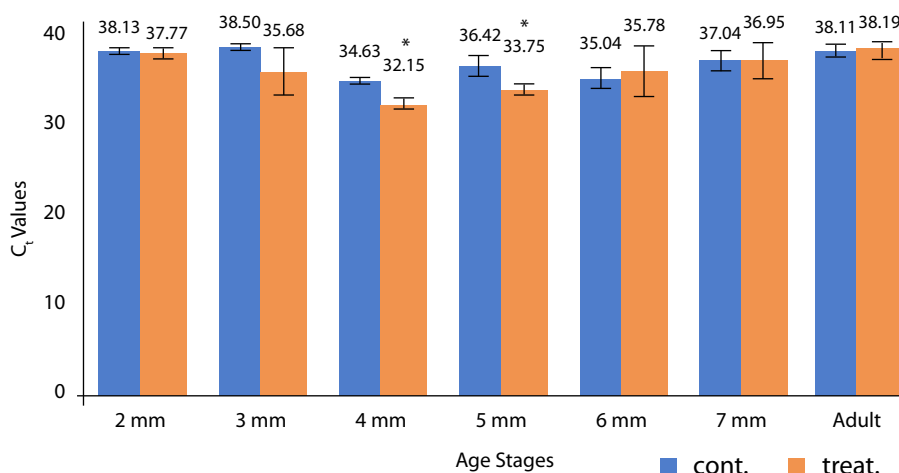


**Fig. 1. Rates of Ct values of the EF1a gene for the control and treatment groups**

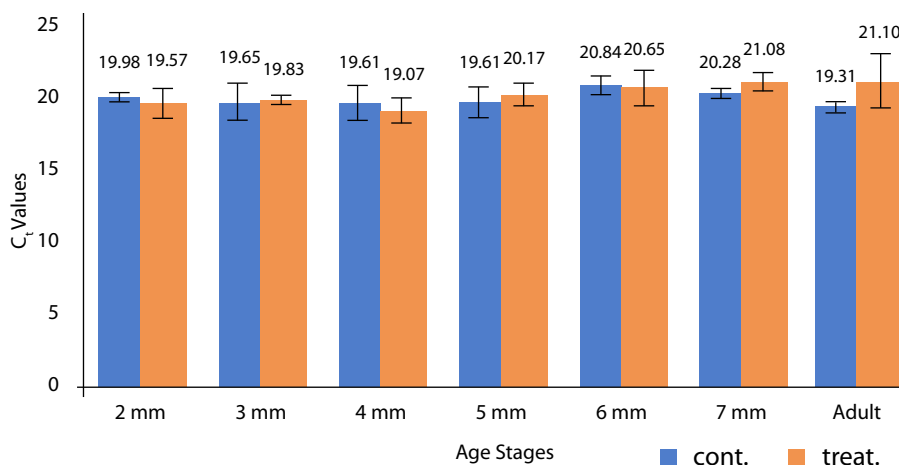


**Fig. 2. Rates of Ct values of the GAPDH gene for the control and treatment groups**

### The effect of calcitonin hormone on gene expression

One: The effect of calcitonin on EF1a

The results of the statistical analysis of the gene expression values for the two genes studied for each stage revealed notable distinctions between the control and treatment groups at the 4 mm and 5 mm stages for the EF1a gene (Fig. 1).

Two: The effect of calcitonin on GAPDH

The results of the statistical analysis did not record significant differences between the groups with any of the GAPDH gene stages (Fig. 2).

### Gene expression among stages

One: The gene expression of EF1a stages.

The results showed that there are clear differences in the Ct values between stages of the EF1a gene and reached the level of significance in some stages. The results of the statistical analysis recorded significant differences between stages (2 & 4 mm), (2 & 6 mm), (3 & 4 mm), (3 & 6 mm), (4 mm & an adult) and (6 mm & an adult) (Table 2, Fig. 3).

Two: The gene expression of GAPDH stages.

Statistical analysis of the Ct values for the GAPDH gene did not show significant differences between stages (Table 3, Fig. 3).

**Table 2**  
Gene expression values between the EF1a gene stages

Ages	P-value	Ages	P-value	Ages	P-value
2 & 3 mm	1.00	3 & 5 mm	0.89	4 mm & Adult	0.02*
2 & 4 mm	0.02*	3 & 6 mm	0.03*	5 & 6 mm	0.26
2 & 5 mm	0.92	3 & 7 mm	0.99	5 & 7 mm	0.99
2 & 6 mm	0.04*	2 mm & Adult	1.00	5 mm & Adult	0.93
2 & 7 mm	0.99	4 & 5 mm	0.16	6 & 7 mm	0.12
2mm & Adult	1.00	4 & 6 mm	1.00	6 mm & Adult	0.04*
3 & 4 mm	0.02*	4 & 7 mm	0.07	7 mm & Adult	0.99

Note: The asterisk marker signifies statistically significant differences.

**Table 3**  
Gene expression values between the GAPDH gene stages

Ages	P-value	Ages	P-value	Ages	P-value
2 & 3 mm	0.97	3 & 5 mm	1.00	4 mm & Adult	1.00
2 & 4 mm	0.96	3 & 6 mm	0.71	5 & 6 mm	0.72
2 & 5 mm	0.97	3 & 7 mm	0.90	5 & 7 mm	0.90
2 & 6 mm	0.99	2 mm & Adult	1.00	5 mm & Adult	1.00
2 & 7 mm	1.00	4 & 5 mm	1.00	6 & 7 mm	1.00
2mm & Adult	0.95	4 & 6 mm	0.69	6 mm & Adult	0.66
3 & 4 mm	1.00	4 & 7 mm	0.88	7 mm & Adult	0.86

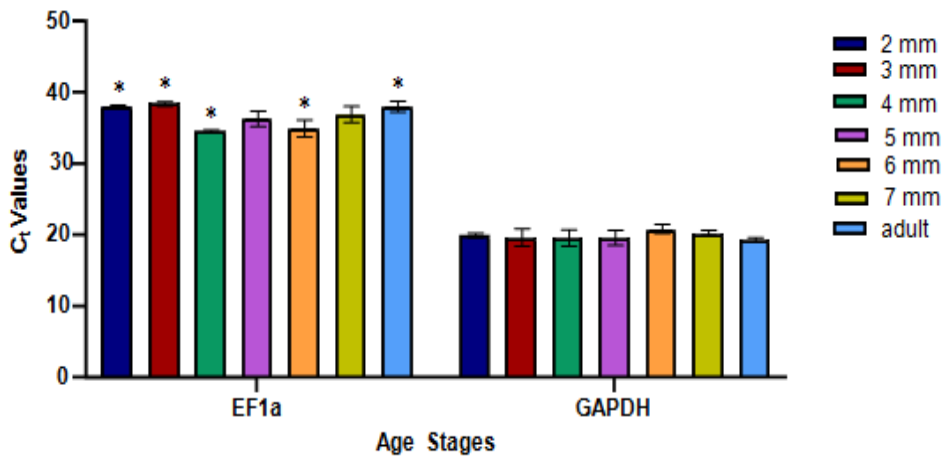


Fig. 3. Rates of Ct values among the stages for the studied genes

## ■ DISCUSSION

Gene expression analysis during qPCR requires proper normalization since the activity of the majority of genes tends to fluctuate based on the physiological state and varying conditions. Hence, it is crucial to identify and validate reference genes that remain stable for the normalization and analysis of data [15].

Reference genes are suitable for adoption when they exhibit consistent expression levels across diverse tissues and throughout all developmental stages of the organism. They remain unaffected by experimental treatments and should ideally be expressed at a level similar to the RNA being studied. Nevertheless, the challenge of data normalization in qPCR persists, especially in the context of absolute quantification [17].

This study was distinguished for testing the validity of two from HKGs, EF1a and GAPDH, as reference genes in *P. latipinna*. The high Ct values for the EF1a gene compared to the Ct values for the GAPDH gene indicate the abundance of the GAPDH gene expression compared to the EF1a in this species. Also, the rates variance of Ct values among the studied stages showed that the GAPDH gene was less different than the EF1a in its expression during those stages. Through the results of the statistical analysis of the gene expression values between the control and treatment groups for the stages studied for the two genes which showed significant differences between the two groups at some stages of the EF1a gene. With no significant differences for the GAPDH gene, it is clarified that the GAPDH gene was the most constant under the influence of the calcitonin hormone. The results of the statistical analysis of the Ct values among the stages resulted in significant differences among some stages of the EF1a gene, whereas no significant differences were recorded among the stages of the GAPDH gene, which indicates the stability of the GAPDH gene expression, and the fluctuation of the EF1a gene expression. During the various developmental stages, from the above, it appears that the EF1a gene is not an ideal candidate for the normalization of the target genes in *P. latipinna*. This conflicts with many studies on various species of fish. EF1a was always at the forefront of the preferred genes being tested as *Dicentrarchus labrax* [8], *Hippoglossus hippoglossus* [7].

As for the GAPDH gene, it appears to be a good candidate to be a reference gene in the studied species. Although, it did not achieve the results obtained by its counterpart except in limited studies and in specific tissues and specific experimental conditions [18, 19].

Most studies that dealt with the two genes together, EF1a gene was the most stable and the GAPDH gene was the least stable among the genes studied in various fish species [2, 20–23].

It is interesting to find here that GAPDH is characterized by constancy and stability at the various stages and under the influence of the hormone. Unlike the EF1a gene, which lost its preference with this species, the results varied in other studies. It was found that both the EF1a and GAPDH genes were suitable as a reference gene in most tissues of *Paralichthys olivaceus* [21], both of which are not suitable in *Ictalurus punctatus* and *Oreochromis niloticus*, respectively [24, 25].

## ■ CONCLUSION

The GAPDH gene expression was stronger, more constant and stable than the EF1a gene at all stages studied, and also under the influence of the hormone. Therefore, it is possible that GAPDH may be a suitable reference gene with *P. latipinna*. Exclude the EF1a gene, for lack of basic conditions that qualify it as a suitable reference gene in this species of fish.

## ■ REFERENCES

1. Bustin SA, Benes V, Nolan T, Pfaffl MW. Quantitative real-time RT-PCR – a perspective. *J Mol Endocrinol*. 2005 Jun;34(3):597–601.
2. Olsvik PA, Lie KK, Jordal AE, et al. Evaluation of potential reference genes in real-time RT-PCR studies of Atlantic salmon. *BMC Mol Biol*. 2005 Nov 17;6:21.
3. Kumari K, Pathakota GB, Annam PK, et al. Characterisation and validation of house keeping gene for expression analysis in *Catla catla* (Hamilton). *Proceedings of the National Academy of Sciences, India Section B: Biological Sciences*, 2015;85(4):993–1000.
4. Dheda K, Huggett JF, Chang JS, et al. The implications of using an inappropriate reference gene for real-time reverse transcription PCR data normalization. *Anal Biochem*. 2005 Sep 1;344(1):141–3.
5. Dheda K, Huggett JF, Bustin SA, et al. Validation of housekeeping genes for normalizing RNA expression in real-time PCR. *Biotechniques*. 2004 Jul;37(1):112–4, 116, 118–9.
6. Radonić A, Thulke S, Mackay IM, et al. Guideline to reference gene selection for quantitative real-time PCR. *Biochem Biophys Res Commun*. 2004 Jan 23;313(4):856–62.
7. Øvergård AC, Nerland AH, Patel S. Evaluation of potential reference genes for real time RT-PCR studies in Atlantic halibut (*Hippoglossus Hippoglossus* L.); during development, in tissues of healthy and NNV-injected fish, and in anterior kidney leucocytes. *BMC Mol Biol*. 2010 May 11;11:36.
8. Mitter K, Kotoulas G, Magoulas A, et al. Evaluation of candidate reference genes for QPCR during ontogenesis and of immune-relevant tissues of European seabass (*Dicentrarchus labrax*). *Comp Biochem Physiol B Biochem Mol Biol*. 2009 Aug;153(4):340–7. doi: 10.1016/j.cbpb.2009.04.009. Epub 2009 May 3. Erratum in: *Comp Biochem Physiol B Biochem Mol Biol*. 2009 Nov;154(3):372.
9. Ribas L, Piferrer F. The zebrafish (*Danio rerio*) as a model organism, with emphasis on applications for finfish aquaculture research. *Reviews in Aquaculture*, 2014;6(4):209–240. <https://doi.org/10.1111/raq.12041>.
10. Bootorabi F, Manouchehri H, Changizi R, et al. Zebrafish as a Model Organism for the Development of Drugs for Skin Cancer. *Int J Mol Sci*. 2017 Jul 18;18(7):1550.
11. Thornton S, Anand N, Purcell D, Lee J. Not just for housekeeping: protein initiation and elongation factors in cell growth and tumorigenesis. *J Mol Med (Berl)*. 2003 Sep;81(9):536–48.
12. Srivastav AK, Singh S, Mishra D, Srivastav SK. Ultimobranchial gland of freshwater catfish, *Heteropneustes fossilis*, in response to calcitonin administration. *Pesquisa Veterinária Brasileira*. 2009;29(12):963–968.
13. Al-Asadi SA. Typical 2-Cys Peroxiredoxins in the Alveolata. PHD. Thesis. Flinders University. 2018; 278 p.
14. Al-Saray ST. Comparative study of the effect of calcitonin hormone on some biochemical parameters in serum for two fish species *Coptodon zillii*, *Astronotus ocellatus*. *International Journal of Psychosocial Rehabilitation*, 2020;24(04):1–5.
15. Faheem M, Jahan N, Khaliq S, Lone KP. Validation of reference genes for expression analysis in a teleost fish (*Catla catla* Hamilton) exposed to an endocrine-disrupting chemical, bisphenol-A. *Rendiconti Lincei. Scienze Fisiche e Naturali*, 2018;29(1):13–22.
16. Morel G, Raccurt M. PCR/RT-PCR in situ: light and electron microscopy. *CRC Press*. 2002. <https://doi.org/10.1201/9781420042535>
17. Bustin SA, Nolan T. Analysis of mRNA expression by real-time PCR. *Real-time PCR. An essential guide*, 2004;125–184.

18. Spinsanti G, Panti C, Lazzeri E, et al. Selection of reference genes for quantitative RT-PCR studies in striped dolphin (*Stenella coeruleoalba*) skin biopsies. *BMC Mol Biol.* 2006 Sep 19;7:32.
19. Pei DS, Sun YH, Chen SP, et al. Zebrafish GAPDH can be used as a reference gene for expression analysis in cross-subfamily cloned embryos. *Anal Biochem.* 2007 Apr 15;363(2):291–3.
20. McCurley AT, Callard GV. Characterization of housekeeping genes in zebrafish: male-female differences and effects of tissue type, developmental stage and chemical treatment. *BMC Mol Biol.* 2008 Nov 12;9:102.
21. Zheng WJ, Sun L. Evaluation of housekeeping genes as references for quantitative real time RT-PCR analysis of gene expression in Japanese flounder (*Paralichthys olivaceus*). *Fish Shellfish Immunol.* 2011;30(2):638–45.
22. Wang E, Wang K, Chen D, et al. Evaluation and Selection of Appropriate Reference Genes for Real-Time Quantitative PCR Analysis of Gene Expression in Nile Tilapia (*Oreochromis niloticus*) during Vaccination and Infection. *Int J Mol Sci.* 2015 Apr 30;16(5):9998–10015.
23. Xia X, Huo W, Wan R, et al. Identification of housekeeping genes as references for quantitative real-time RT-PCR analysis in *Misgurnus anguillicaudatus*. *J Genet.* 2017 Dec;96(6):895–904.
24. Small BC, Murdock CA, Bilodeau-Bourgeois AL, et al. Stability of reference genes for real-time PCR analyses in channel catfish (*Ictalurus punctatus*) tissues under varying physiological conditions. *Comp Biochem Physiol B Biochem Mol Biol.* 2008 Nov;151(3):296–304.
25. Yang CG, Wang XL, Tian J, et al. Evaluation of reference genes for quantitative real-time RT-PCR analysis of gene expression in Nile tilapia (*Oreochromis niloticus*). *Gene.* 2013 Sep 15;527(1):183–92.

<https://doi.org/10.34883/PI.2025.14.1.053>

Mohammed Younus Naji Al Atbee<sup>1</sup> ✉, Hala Sami Tuama<sup>2</sup>, Jawad Ibrahim Rasheed<sup>3</sup>, Ali Jasim Al Saedi<sup>4</sup>

<sup>1</sup> College of Medicine, University of Basrah, Basrah, Iraq

<sup>2</sup> Basrah Primary Health Care, Basrah, Iraq

<sup>3</sup> Baghdad Teaching Hospital, Medical City, Baghdad, Iraq

<sup>4</sup> Baghdad Kidney Transplant Center, Medical City, Baghdad, Iraq

## Prevalence of Peritonitis in Continuous Ambulatory Peritoneal Dialysis Patients: Bacteriology Analysis

**Conflict of interest:** nothing to declare.

**Authors' contribution:** Mohammed Younus Naji Al Atbee – data curation, methodology, project administration, resources, software, supervision, validation, visualization, writing – original draft and writing – review & editing; Hala Sami Tuama – data curation, methodology, resources, software, validation, visualization, writing – original draft and writing – review & editing; Jawad Ibrahim Rasheed – data curation, investigation, resources, validation, visualization, writing – original draft and writing – review & editing; Ali Jasim Al Saedi – data curation, investigation, resources, validation, visualization, writing – original draft and writing – review & editing.

The article is published in author's edition.

Submitted: 20.01.2025

Accepted: 17.03.2025

Contacts: Mohammed.Naji@uobasrah.edu.com

### Abstract

**Introduction.** Peritoneal dialysis (PD) linked with peritonitis is a major risk factor for patients with continuous ambulatory Peritoneal dialysis (CAPD). Factors affecting biochemical characteristics and microbiological data pertinent to PD-related peritonitis (PDRP) are deficient in the Iraq studies. Thus, an observational assessment of patients with CAPD is required to look for susceptible organisms that cause peritonitis and biochemical characteristics outcome.

**Materials and methods.** Blood and peritoneal fluid samples were collected from 100 patients with end-stage chronic kidney disease who underwent CAPD. Different biochemical parameters and microbiological assays of CAPD fluid were analyzed at the laboratory level such as complete blood count (CBC), calcium, phosphate, parathyroid hormone, potassium, sodium, and more factors were included in the current study.

**Results.** A total of 100 CAPD patients, 62 of whom developed at least one attack during the study period. Those developed a total of 301 episodes of peritonitis. The overall peritonitis rate was 3.1 episodes/patient-year. The causative pathogens are gram-positive (*Staphylococcus aureus* and *Enterococcus* sp.) and gram-negative bacteria (*Escherichia coli* and *Klebsiella* sp.). The study revealed that patients developing peritonitis with CAPD have diverse biochemical characteristics.

**Conclusion.** This study showed that peritonitis offers insights into the etiology and outcomes of infectious complications of PD at Basrah Teaching Hospital, nephrology, and dialysis center in Basrah. Thus, critical information was concluded from the study to better manage peritonitis with CAPD and early decision-making.

**Keywords:** CAPD, Diabetes, Peritonitis, Infection, renal replacement therapy

## ■ INTRODUCTION

For patients with end-stage renal disease, renal replacement therapies (RRT) such as dialysis and kidney transplantation represent the sole treatment options to sustain life [1]. Kidney transplantation is a potential and efficient cure, although kidney transplantation surgery is limited by factors such as high-cost surgery, shortage of donors, and transplant failure. Hence patients depend on dialysis for long-term or even life-long.

Worldwide, continuous ambulatory peritoneal dialysis (CAPD) has been accepted as an alternative to RRT which can be even executed at home with proper training. Often peritonitis appears as a serious issue of peritoneal dialysis that causes extension in hospital care, despondency, and even death among CAPD patients [2]. Peritonitis may be caused due to catheter loss and technical failure of the instruments engaged to manage peritonitis [3].

Literature reveals that there are several different forms of microorganisms accountable for the result of peritonitis occurrence such as *Staphylococcus epidermidis*, *Escherichia coli*, *Klebsiella* species, *Proteus* species, *Enterococcus faecalis*, *Pseudomonas* species, *Serratia* sp. and *Corynebacteria* [4]. Peritonitis also depends on various factors like geographical conditions, socio-demographic parameters, and conditional immunity of peritonitis patients [5]. The infection is caused by gram-positive as well as negative bacteria, fungi, and in some cases viruses also an infectious agent. Microbes are inhabitant in the peritoneal fluid at the time of infection and play a crucial role in the results of the varying types of dialysis mode, this state of affairs remains an incumbency among continuous ambulatory peritoneal dialysis patients [3, 5].

Differences in peritonitis occurrence worldwide have resulted in several flexible parameters in which medical practice patterns are also accountable factors [1]. A report on Peritoneal Dialysis Outcomes and Practice Patterns Study (PDOPPS), seven countries viz. Canada, Japan, Australia, New Zealand, Thailand, the UK, and the USA were selected in around 7000 patients across the selected nations subjected to Peritoneal Dialysis have different peritonitis rates [2]. Medical procedures such as higher application of automated peritonitis dialysis (APD), inclusion of antibiotics before and after catheter introduction, and descriptive training of peritonitis liquid exchange are key factors that lower the infection. In several countries, peritonitis results mostly from gram-positive bacteria. A study in 2011, in Australia and New Zealand showed that gram-positive bacteria account for nearly 53% of total peritonitis dominated by *Staphylococci* (27.2%) and *Escherichia coli* (6.3%) and at par, USA, Canada, and India also have dominant gram-positive bacterial infection resulted for peritonitis [6].

Peritonitis connected with PD, microbial infection as well, and consequences have not been yet defined for the CAPD patient population being medicinally treated at Basrah teaching hospital, nephrology, and dialysis center in Basrah. This is a reflective assessment aimed at investigating the local peritonitis rate, the microbiological profiles of causative organisms along with biochemical characteristics associated with peritonitis to draw management protocols.

## ■ MATERIALS AND METHODS

### **Study design**

The study was conducted from March 2019 to March 2024. The samples were collected from the nephrology and dialysis center in Basrah Teaching Hospital. The study

was approved by scientific committees in the College of Medicine, University of Basrah (No.030408-031-2023). Written informed consent was obtained from all the patients who participated in the study.

### **Samples collection**

5 mL of the venous blood sample was drawn from each patient by using disposable syringes in plain tubes without any anticoagulant. Samples were processed immediately which involved the separation of blood serum by centrifuge at 10000 rpm for 5 min at 4° C. The collected samples were also subjected to the biochemical quantitative assessment for urea, blood gases analysis, complete blood count, calcium, phosphate, Parathyroid hormone, potassium, sodium, and bicarbonate.

### **Peritoneal fluid white blood cell (WBC) and Culture and sensitivity**

We collected a sample of peritoneal fluid and sent it for WBC count and WBC differential with culture and sensitivity for all studied patients.

### **Statistical analysis**

The statistical analysis was performed using SPSS software version 20. Calculations of mean values and standard deviation (SD) were made for the characterization of the study population. The statistical significance of the difference in data was assessed by the T-test. P values <0.05 were considered to be statistically significant.

## **■ RESULTS**

### **Demographic and clinical characteristics of the study population**

In the current investigation, one hundred patients (mean age 36.6 years; 60% males, 40% females) per year were examined and the mean duration of peritonitis dialysis treatment was 4.42 per year and the overall peritonitis rate was 3.1 episodes/patient/year. The patients developed 301 episodes of peritonitis (range: 1–6 episodes per patient) of which 32% were non-reverting peritonitis and 68% were recurring peritonitis (Fig.1). The majority of the patients were males (72.06 %) between 10–20 years (specifically 11–13 years age group) followed by post 60 years of male (42.46%) while the maximum female age had peritonitis at the age of 22 years (36.86%) and 34 years (52.63%). The male peritonitis-affected patients were higher accounted for 49%, while female peritonitis-affected affected were reported 19% of the examined population. The peaked age was 66 years and least age was 11 years (Fig. 1).

Only 31 male patients had cardiovascular morbidities, and no malignancies, and 4 females suffered from the genetic disease Thalassemia (Fig. 2). No female reported multiple complications, whereas 60% of males had multiple complications of diabetic mellitus, hypertension, and ischemic heart disease (Fig. 2). The overall morbidity rate was 68% in the current study. The majority of the examined population had diabetic mellitus at a rate of 52% (Males: Females = 31%: 21%). Among the other morbidities, hypertension was second in occurrence with 41%; whereas ischemic heart disease and one genetic disease such as Thalassemia were 31% and 4% respectively. Besides diabetes, other co-morbidity such as hypertension and ischemic heart disease were restricted only to male patients.

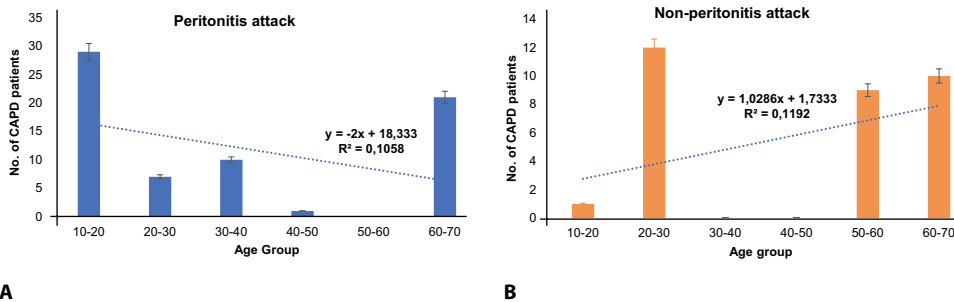


**Fig. 1. Demographical distribution pattern of peritonitis (A) and non-peritonitis patients (B)**

The data showed that 31% of patients were under treatment of continuous ambulatory peritoneal dialysis (CAPD) for more than one year while 69% of the examined population were under CAPD for less than one year. The devices implanted for CAPD in the patients were manufactured by Fresenius (52%) and Baxter (48%). The CAPD catheter was inserted in the body either by surgery or by medical method. The surgical procedure was adopted in 79% of critical patients while 21% were subjected to medical methods. Peritoneal Equilibration Test (PET) revealed that the patient’s peritoneum has a high, average, or low transport rate and the test resulted in relevant information on peritoneum drain volume. The PET selected as the test reflects how much dextrose remains in the fluid sample, and how much 4-hour dialysate/plasma creatinine. The PET result showed that 1% of the population had a low transport rate, 30% of patients of the population required a high transport rate, and 69% of patients required average transport for fluid exchange.

**Causative Organisms of Peritonitis**

The distribution of pathogenic bacteria in the population was mainly Escherichia coli (15), Enterococcus species (12), Staphylococcus aureus (14), and Klebsiella sp. (10).

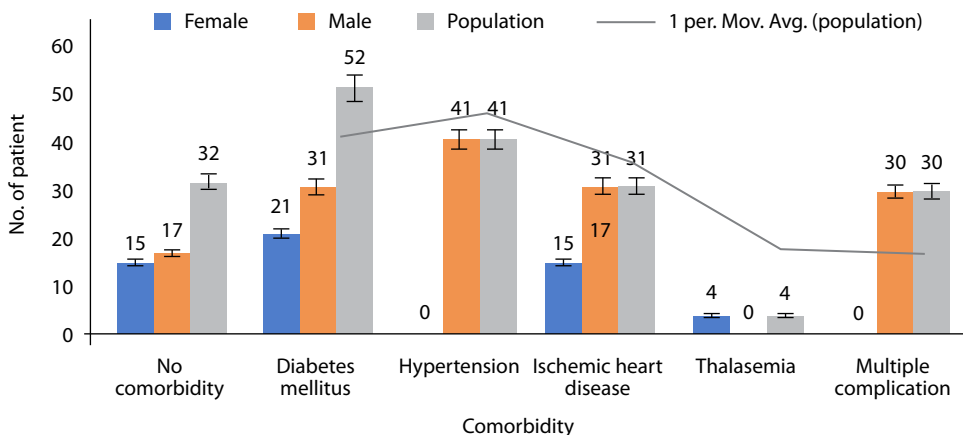


**Fig. 2. Distribution pattern of Co-morbidity in the examined population**

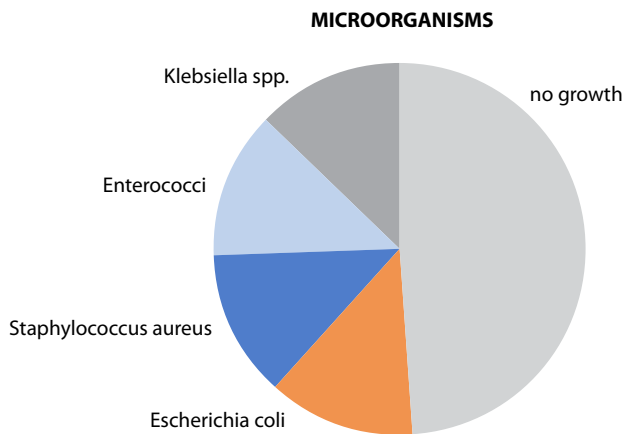


**Fig. 3. Pathological agents accountable for the prevalence of peritonitis**

Most dominant bacterial infection that resulted in peritonitis was *Escherichia coli* with 29% of occurrence among bacterial infection followed by 27% of *Staphylococcus aureus* (27%) and *Enterococcus* species (24%) infection (Fig. 3). The least abundance pathogenic bacteria that were noticed and responsible for peritonitis was *Klebsiella* sp. with 20% presence. The result exhibited that the causative pathogenic peritonitis in the population was equally infected by gram-positive (*Staphylococcus aureus* and *Enterococcus* sp.; 51%) and gram-negative bacteria (*Escherichia coli* and *Klebsiella* sp.; 49%).

### **Biochemical characteristics of the examined population**

The serum of all examined patients was collected and processed for details assessment at the biochemical level. The biochemical analysis comprised of determination of hemoglobin (Hb) count, Albumin, Uric acid, Potassium, Sugar, Sodium, C Reactive protein (CRP), Ferritin, Parathyroid hormone test, Calcium, Phosphate test, and Vitamin D. The mean Hb was 8.72 g/dl with a range of 5–11 g/dl. The female population had slightly elevated Hb near 8.9 mg/dl while the male had 8.4 mg/dl. The mean WBC count of the examined population was  $12.49 \times 10^3/\text{dl}$  and in the range of  $3.5\text{--}30 \times 10^3/\text{dl}$ . The male WBC count ( $10.9 \times 10^3/\text{dl}$ ) is comparatively lower than the female ( $14.9 \times 10^3/\text{dl}$ ).

The mean albumin was 3.07 gm/dl and the range of albumin presence was 2–3.6 gm/dl. The uric acid among the examined population was 4–7.7 mg/dl and the mean occurrence of uric acid in the population was 6.23 mg/dl. The mean male and female uric acid presence was 5.9 mg/dl and 6.7 mg/dl respectively. Higher mean potassium was found in the urine sample of males (3.8 meq/l) compared to females (3.1 meq/l). The mean cumulative potassium was determined within 3.55 meq/l and the normal range in the examined population was 2.2–5.5 meq/l.

The sugar range within the population was 88–400 mg/l with a mean value of 170 mg/l. However, the average serum sugar (149.7 mg/l) of men was near to threshold or safe limit while the females (202.5 mg/l) had 26.4% higher sugar than males. The mean serum sodium, phosphate, and vitamin D were found to be 147.3 meq/l, 5.9 mg/dl,

**Table 1**  
**Mean biochemical characteristics of female and male population under the influence of Peritonitis**

Biochemical characteristics	Female		Male	
	Peritonitis attack	Non-peritonitis attack	Peritonitis attack	Non-peritonitis attack
Hb	8.7	9.0	8.7	8.3
WBCs	19.8	10.5	11.2	9.5
Albumin	2.8	3.3	3.0	3.3
Uric Acid	6.9	6.6	5.9	6.0
Potassium	2.7	3.5	3.7	4.6
Sugar	226.7	180.6	142.7	180.9
Sodium	128.9	135.4	151.4	129.0
C Reactive protein	14.7	8.1	8.5	11.0
Ferritin	247.4	220.0	114.7	146.5
PTH	278.9	222.9	406.7	552.0
Calcium	6.6	8.0	7.0	7.8
Phosphate	6.6	5.4	5.8	5.8
Vitamin D	17.6	19.7	12.2	16.2
Chi-Square test P<0.05%	0.652 (NS*)		0.278(NS*)	
T-Test (p<0.05%)	0.801 (NS*)		0.751 (NS*)	

and 13 ng/ml in males whereas 132.4 meq/l, 6 mg/dl, 18.7 ng/ml in females respectively. The mean serum calcium was between 7.2–7.3 mg/dl in the population. The mean calcium distribution in the population was 7.24 mg/dl and at par in males and females with a normal range of 5–9 mg/dl (Table 2).

**Table 2**  
**Mean biochemical characteristics of investigatory population irrespective of Peritonitis attack**

Biochemical characteristics	Female	Male	Cumulative
Hb	8.9	8.6	8.72
WBCs	14.9	10.9	12.49
Albumin	3.0	3.1	3.074
Uric Acid	6.7	5.9	6.227
Potassium	3.1	3.8	3.556
Sugar	202.5	149.7	170.8
Sodium	132.4	147.3	141.31
C Reactive protein	11.3	9.0	9.9
Ferritin	233.0	120.5	165.5
PTH	249.5	433.3	359.78
Calcium	7.3	7.2	7.24
Phosphate	6.0	5.8	5.9
Vitamin D	18.7	13.0	15.27
Chi-square test P<0.05%	0.0001 (S)		NA
T-Test (p<0.05%)	0.982, (NS*)		NA

Notes: NS\* – Non Significant; NA – Not applicable, S – Significant.

The mean Ferritin and Parathyroid Hormone (PTH) in the testing population were estimated and recorded between the range of 23–400 ng/ml and 80–797 pg/ml, respectively. The mean Ferritin in the female examined population (233 ng/ml) was a 48.28% increase compared with the male-examined population. The PTH was 42.41% elevated in the male population which resulted in 433.3 pg/ml while in mean PTH in the female population was 249.5 pg/ml. The C reactive protein (CRP) in the examined population was measured between 2–30 mg/l with the mean value mean CRP 9.9 mg/l. The elevated CRP above 10 mg/l indicates inflammation in the body. The female population (11.3 mg/l) had 20.90% higher CRP than the male (9 mg/l) population. It has been confirmed by the chi-square test at a significant level (0.05%),  $p < 0.0001$  those overall biochemical characteristics of males and females strongly related to suffering from common peritonitis infection (Table 1). The t-test performed in the population was non-significant (0.05%,  $p = 0.982$ ) and showed that the two groups are different from one another in respect of biochemical characteristics (Table 2).

The biochemical characteristics of peritonitis attack patients and non-peritonitis attack patients within the male and female groups were examined. The chi-square and t-test were performed which resulted in acceptance of the null hypothesis by exhibiting non-significant results ( $p < 0.05\%$ ) that interpret that within the given gender under two different medical conditions, the biochemical characteristics are different in the examined population. The Person's correlation coefficient of biochemical characteristics was among the females having Peritonitis and non-peritonitis attack (Table 3), male Peritonitis and non-peritonitis attack (Table 4), and Overall, between males and females irrespective of peritonitis attack (Table 5). Several biochemical characteristics showed positive and negative correlation coefficients.

**Table 3**  
**Pearson's correlation coefficient ( $R^2$ ) of biochemical characteristics between peritonitis-affected and non-peritonitis-affected female patients under investigation**

	Hb	WBCs	Albumin	Uric Acid	Potassium	Sugar	Sodium	C Reactive protein	Ferritin	PTH	Calcium	Phosphate	Vitamin D
Hb	1.00												
WBCs	-0.83	1.00											
Albumin	0.79	-0.95	1.00										
Uric Acid	0.31	0.15	-0.28	1.00									
Potassium	-0.49	-0.03	0.02	-0.56	1.00								
Sugar	-0.56	0.75	-0.85	0.55	0.10	1.00							
Sodium	0.67	-0.90	0.98	-0.44	0.10	-0.90	1.00						
C Reactive protein	-0.79	0.93	-0.89	0.25	0.16	0.88	-0.87	1.00					
Ferritin	-0.99	0.80	-0.75	-0.39	0.45	0.46	-0.63	0.71	1.00				
PTH	0.33	0.15	-0.27	0.97	-0.56	0.57	-0.43	0.26	-0.42	1.00			
Calcium	0.07	-0.58	0.61	-0.85	0.55	-0.74	0.71	-0.62	0.02	-0.88	1.00		
Phosphate	-0.66	0.94	-0.94	0.44	-0.14	0.89	-0.94	0.95	0.59	0.45	-0.79	1.00	
Vitamin D	0.77	-0.85	0.96	-0.27	-0.12	-0.88	0.96	-0.83	-0.73	-0.26	0.52	-0.85	1

**Table 4**  
**Pearson's correlation coefficient (R<sup>2</sup>) of biochemical characteristics between Peritonitis and non-peritonitis Male patients under investigation**

	Hb	WBCs	Albumin	Uric Acid	Potassium	Sugar	Sodium	C Reactive protein	Ferritin	PTH	Calcium	Phosphate	Vitamin D
Hb	1.00												
WBCs	-0.26	1.00											
Albumin	-0.48	-0.30	1.00										
Uric Acid	0.86	-0.05	-0.35	1.00									
Potassium	-0.09	0.30	0.40	0.38	1.00								
Sugar	-0.07	0.44	0.18	0.42	0.89	1.00							
Sodium	-0.60	0.25	-0.17	-0.61	-0.46	-0.17	1.00						
C Reactive protein	0.03	0.75	-0.09	0.44	0.81	0.85	-0.24	1.00					
Ferritin	0.59	0.28	-0.17	0.88	0.64	0.75	-0.53	0.74	1.00				
PTH	-0.29	-0.55	0.36	-0.35	-0.23	-0.08	0.31	-0.55	-0.32	1.00			
Calcium	0.44	-0.66	0.46	0.35	0.21	-0.14	-0.82	-0.21	0.14	-0.05	1.00		
Phosphate	0.11	0.60	-0.14	0.53	0.63	0.77	-0.01	0.85	0.72	-0.53	-0.25	1.00	
Vitamin D	0.23	-0.86	0.60	0.22	0.16	0.00	-0.44	-0.38	0.06	0.48	0.78	-0.26	1.00

**Table 5**  
**Pearson's correlation coefficient (R<sup>2</sup>) of biochemical characteristics between Peritonitis affected and non-peritonitis investigatory population**

	Hb	WBCs	Albumin	Uric Acid	Potassium	Sugar	Sodium	C Reactive protein	Ferritin	PTH	Calcium	Phosphate	Vitamin D
Hb	1.00												
WBCs	-0.63	1.00											
Albumin	0.43	-0.81	1.00										
Uric Acid	0.53	0.11	-0.23	1.00									
Potassium	-0.23	-0.03	0.19	0.10	1.00								
Sugar	-0.39	0.72	-0.62	0.37	0.24	1.00							
Sodium	-0.25	-0.11	0.08	-0.64	-0.26	-0.27	1.00						
C Reactive protein	-0.42	0.79	-0.57	0.37	0.49	0.81	-0.29	1.00					
Ferritin	-0.35	0.67	-0.54	0.54	0.27	0.58	-0.46	0.69	1.00				
PTH	-0.10	-0.27	0.12	-0.37	-0.06	-0.03	0.35	-0.35	-0.42	1.00			
Calcium	0.23	-0.50	0.51	0.15	0.25	-0.43	-0.55	-0.38	0.10	-0.20	1.00		
Phosphate	-0.29	0.72	-0.58	0.46	0.34	0.75	-0.12	0.89	0.61	-0.31	-0.46	1.00	
Vitamin D	0.46	-0.46	0.60	0.28	-0.16	-0.25	-0.31	-0.42	-0.02	0.00	0.60	-0.38	1.00

## ■ DISCUSSIONS

Peritoneal dialysis patients most frequently experience procedure failure and morbidity due to peritonitis. To use the local empirical antibiotic treatment, the International Society of Peritoneal Dialysis (ISPD) advises each center to track the rates of peritonitis and the etiological agent [7]. Previous research has found that the risk of peritonitis is comparable across age groups, including advanced age [8, 9], greater BMI, and lower blood albumin levels [10]. Age as a risk factor for peritonitis may be explained by physical and cognitive deficits such as diminished dexterity and vision, hand tremors, and dementia in elderly patients, which might make the procedure difficult to execute [11]. Earlier studies showed higher BMI was related to an increased risk of early-onset peritonitis [12]. Obesity was thought to increase the risk of peritonitis during PD catheter implantation.

As compared to our findings, an Indian-based study reported rates of gram-positive culture varied between 30–72% [13, 14] and gram-negative bacteria were accountable for 60–66% of the peritonitis infection, while *E. coli* is the most common pathogen [14, 15]. A study conducted by Prasad et al. (2004) reported the occurrence of fungal peritonitis with an infection rate of 13.5% in its examined population, however, no such observation was reported in the current investigation in the examined population [16].

In the present study, the overall morbidity rate was 31% and the results correspond to the studies conducted by Jhobta et al. (2006) reported a morbidity rate of 50%, whereas Memon et al. (2012) mentioned morbidity 48.5% in their investigation. The co-morbidity was higher in the male population with multiple complications such as hypertension, diabetes, and ischemic heart disease [17, 18]. Paryani et al. (2013) acknowledged that important parameters such as parameters that have an important effect on mortality are heart rate, blood pressure, and relatively high blood sugar [19].

The comparatively lower Hb concerning the normal range in the examined population was recorded. Kunin et al. (2023) reported that WBC increased during the peritonitis infection and similar results were observed in the current examined population [20]. Ascites, a pathological accumulation of fluid in the peritoneal cavity may come with several diseases. Serum ascites albumin gradient (SAAG) is calculated as the difference between the albumin level of serum and ascitic fluid and albumin that should be less than 6 gm/dl fluid. However, our result indicates a safe level of albumin in the population, and albumin was at par in females and males. The elevated SAAG indicates portal hypertension while a lower dose indicates the absence of portal hypertension [21].

In the current scenario, the safe range of uric acid in the serum is accepted as 3–7 mg/dl and our results corroborate with the other findings. The interpreted data related to the sugar level of examined patients were higher and observed that females were more diabetic than male patients. However, a study by van Diepen et al., (2015) confirmed there was no correlation between glucose exposure during the first year of PD and the subsequent time to peritonitis had been noticed [22]. The critical serum potassium and sodium levels were  $4.47 \pm 0.35$  mEq/L and  $142.67 \pm 2.64$  mEq/L, respectively [23]. Mokhber Dezfouli et al. (2012) reported that peritonitis causes a reduction in Na ions because of the inflammation process. The K and Na were observed in a safe range in the examined population which corresponds with the result of Nakai et al. (2017) [24, 25].

The C-reactive protein (CRP) frequently gets elevated within a short period of hours after the tissue is exposed to injury or due to the presence of microbial infection [26]. In a healthy body, CRP is normally available at less than 6 mg/l [27]. Elevated CRP has

been marked as an indicator of inflammation in a patient with infections or injuries [28]. Elevated CRP was reported due to the cause of *Escherichia coli*, *Proteus spp.*, *Klebsiella pneumoniae*, *Staphylococcus aureus*, and others [29]. The CRP in the female population was 52.16% increased than the normal range while male patients had 71% higher than the normal value. The commutatively CRP in the population was higher by 66.66% (9.9 mg/l) and it was inferred from the that the examine population had severe tissue inflammations of patients.

Serum ferritin reflects total body iron stores; thus, a low serum ferritin is used as a parameter of iron deficiency. Clinically, higher ferritin level was pointedly linked with an additional rapid residual renal function decline in patients undergone PD [30]. The data of the current study revealed that females had normal levels of ferritin but exceptionally lower in males. Patients with high iron status were positively linked with the treatment failure of peritonitis [31].

Abnormal mineral bone metabolism in PD patients with low serum parathyroid hormone levels, coupled with either high Ca levels or low/normal P levels, could be new potential risk factors of PD pertinent to peritonitis [32]. In the blood, the delicate process of calcium and phosphate homeostasis is regulated firstly by the parathyroid gland. The gland secretes parathyroid hormone (PTH) when low calcium concentration is detected in the blood as the hormones assist in the manufacturing of Vitamin-D and calcitriol in the kidney. Further, PTH coupled with calcitriol controls calcium and phosphate in bones, kidneys, and small intestines [33]. Further, biochemical parameters within the population showed significant differences, however comparison of non-peritonitis and peritonitis patients showed non-significant differences.

## ■ CONCLUSIONS

The study has a rather low peritonitis rate, elderly individuals had a higher risk of peritonitis episodes. Gram-positive and gram-negative bacteria were the most common causes of peritonitis in CAPD patients. In conclusion, the investigation revealed a wide range of information pertinent to PD patients with CAPD. The biochemical features revealed a broad range of variability among the investigated group.

## ■ REFERENCES

1. Perl J, Fuller DS, Bieber BA, et al. Peritoneal Dialysis-Related Infection Rates and Outcomes: Results From the Peritoneal Dialysis Outcomes and Practice Patterns Study (PDOPPS). *Am J Kidney Dis.* 2020 Jul;76(1):42–53.
2. Bello AK, Okpechi IG, Osman MA, et al. Epidemiology of peritoneal dialysis outcomes. *Nat Rev Nephrol.* 2022 Dec;18(12):779–793.
3. Vikrant S, Guleria RC, Kanga A, et al. Microbiological aspects of peritonitis in patients on continuous ambulatory peritoneal dialysis. *Indian Journal of Nephrology.* 2013;23(1):12.
4. Koulouzidis A, Bhat S, Karagiannidis A, et al. Spontaneous bacterial peritonitis. *Postgraduate medical journal.* 2007;83(980):379–83.
5. Prasad N, Gupta A, Sharma RK, et al. Impact of nutritional status on peritonitis in CAPD patients. *Peritoneal dialysis international.* 2007 Jan;27(1):42–7.
6. Wu H, Yi C, Zhang D, et al. Changes of antibiotic resistance over time among *Escherichia coli* peritonitis in Southern China. *Perit Dial Int.* 2022;42(2):218–222.
7. Moola Y, Musoke J, Bailey A, et al. The prevalence and bacterial distribution of peritonitis amongst adults undergoing continuous ambulatory peritoneal dialysis at Universitas hospital. *Southern African Journal of Infectious Diseases.* 2020;35(1):1–5.
8. Kotsanas D, Polkinghorne KR, Korman TM, et al. Risk factors for peritoneal dialysis-related peritonitis: can we reduce the incidence and improve patient selection? *Nephrology.* 2007;12(3):239–245.
9. Lobo JV, Villar KR, de Andrade Júnior MP, et al. Predictor factors of peritoneal dialysis-related peritonitis. *J Bras Nefrol.* 2010; 32(2):156–164.
10. Fan X, Huang R, Wang J, et al. Risk factors for the first episode of peritonitis in Southern Chinese continuous ambulatory peritoneal dialysis patients. *PLoS One.* 2014;9(9):e107485.

11. Brown EA, Finkelstein FO, Iyasere OU, et al. Peritoneal or hemodialysis for the frail elderly patient, the choice of 2 evils? *Kidney Int.* 2017;91(2):294–303.
12. Wu H, Huang R, Yi C, et al. Risk factors for early-onset peritonitis in Southern Chinese peritoneal dialysis patients. *Perit Dial Int.* 2016;36(6):640–646.
13. Sharma RK, Kumar J, Gupta A, Gulati S. Peritoneal infection in acute intermittent peritoneal dialysis. *Renal Failure.* 2003;25:975–80.
14. Keithi-Reddy SR, Gupta KL, Jha V, et al. Spectrum and sensitivity pattern of gram negative organism causing CAPD peritonitis in India. *Perit Dial Int.* 2007;27:205–7.
15. Jha V. Current status of PD in India: Current status and challenges. *Perit Dial Int.* 2008;28:36–41.
16. Prasad KN, Prasad N, Gupta Amit, et al. Fungal peritonitis in patients on continuous ambulatory peritoneal dialysis: a single centre Indian experience. *J Infect.* 2004;48:96–101.
17. Jhobta RS, Attri AK, Kaushik R, et al. Spectrum of perforation peritonitis in India – Review of 504 consecutive cases. *World J Emerg Surg.* 2006;1:26.
18. Memon AA, Siddiqui FG, Abro AH, et al. An audit of secondary peritonitis at a tertiary care university hospital of Sindh, Pakistan. *World J Emerg Surg.* 2012;7:6.
19. Paryani JJ, Patel V, Rathod G. Etiology of peritonitis and factors predicting the mortality in peritonitis. *Natl J Comm Med.* 2013;4:145–8.
20. Kunin M, Mini S, Abu-Amer N, Beckerman P. Optimal peritoneal fluid white blood cell count for diagnosis of peritonitis in peritoneal dialysis patients. *Kidney Res Clin Pract.* 2023;42(1):127–137.
21. Shahed FHM, Mamun-Al-Mahtab, Rahman S. The Evaluation of Serum Ascites Albumin Gradient and Portal Hypertensive changes in Cirrhotic Patients with Ascites. *Euroasian J Hepatogastroenterol.* 2016;6(1):8–9.
22. Van Diepen AT, van Esch S, Struijk DG, Krediet RT. The Association Between Glucose Exposure and the Risk of Peritonitis in Peritoneal Dialysis Patients. *Perit Dial Int.* 2016;9–10;36(5):533–9.
23. Xi L, Hao YC, Liu J, et al. Associations between serum potassium and sodium levels and risk of hypertension: a community-based cohort study. *J Geriatr Cardiol.* 2015 Mar;12(2):119–26.
24. Mokhber Dezfouli MR, Lotfollahzadeh S, Sadeghian S, et al. Blood electrolytes changes in peritonitis of cattle. *Comp Clin Path.* 2012 Dec;21(6):1445–1449.
25. Nakai K, Saito K, Fujii H, Nishi S. Impact of hypokalemia on peritonitis in peritoneal dialysis patients: a systematic review. *Renal Replacement Therapy.* 2017;3:1–5.
26. Simon L, Gauvin F, Amre DK, et al. Serum procalcitonin and C-reactive protein levels as markers of bacterial infection: a systematic review and meta-analysis. *Clinical Infectious Diseases.* 2004;39(2):206–217.
27. Chan T, Gu F. Early diagnosis of sepsis using serum biomarkers. *Expert Review of Molecular Diagnostics.* 2011;11(5):487–496.
28. Chacha F, Mirambo MM, Mushi MF, et al. Utility of qualitative C-reactive protein assay and white blood cells counts in the diagnosis of neonatal septicemia at Bugando Medical Centre, Tanzania. *BMC Pediatrics.* 2014;14(1):248.
29. Khan F, Malik M, Afzal K, et al. Renal biometry and serum C-reactive protein levels in the evaluation of urinary tract infections. *Indian J Nephrol.* 2004;14:10–14.
30. Hur SM, Ju HY, Park MY, et al. Ferritin as a predictor of decline in residual renal function in peritoneal dialysis patients. *The Korean journal of internal medicine.* 2014;29(4):489.
31. Diao X, Zheng Z, Yi C, et al. Association of Abnormal Iron Status with the Occurrence and Prognosis of Peritoneal Dialysis-Related Peritonitis: A Longitudinal Data-Based 10-Year Retrospective Study. *Nutrients.* 2022;14(8):1613.
32. Liao CT, Zheng CM, Lin YC, et al. Aberrant serum parathyroid hormone, calcium, and phosphorus as risk factors for peritonitis in peritoneal dialysis patients. *Sci Rep.* 2021;11(1):1171.
33. Zhang Z, Wu L, Wang G, Hu P. Effect of vitamin D deficiency on spontaneous peritonitis in cirrhosis: a meta-analysis. *Prz Gastroenterol.* 2021;16(1):10–14.

<https://doi.org/10.34883/PI.2025.14.1.054>

Naseer Malaky Abbood<sup>1</sup> ✉, Ihsan Hameed Khudhair<sup>2</sup>

<sup>1</sup> Thi-Qar Education Directorate, Ministry of Education, Thi-Qar, Iraq

<sup>2</sup> Thi-Qar University, College of Science, Thi-Qar, Iraq

# The Adulticidal and Repellent Effect of Some Doped Nanoparticles in Southern Cowpea Beetle ((Coleoptera: Bruchidae) *Callosobruchus Maculatus* F)

**Conflict of interest:** nothing to declare.

**Authors' contribution:** all authors made a significant contribution to the writing of the article.

The article is published in author's edition.

Submitted: 03.02.2025

Accepted: 17.03.2025

Contacts: Naseer.abood@sci.utq.edu.iq

## Abstract

**Introduction.** The southern cowpea beetle *Callosobruchus maculatus* was treated with doped nanoparticles (N-doped  $TiO_2$ , P-doped  $TiO_2$ , Sb-doped  $TiO_2$ , Bi-doped  $TiO_2$ ) to determine the most efficient in its effect on some biological parameters of the insect such as the percentage of mortality and the repellent effect.

**Results.** For the first parameter, Bi-doped  $TiO_2$  had the highest rate of Percentage of mortality (44.57%) and its  $LC_{50}$  (4389.50 ppm) and Toxicity index (100%) followed by Sb-doped, P-doped  $TiO_2$  and N-doped  $TiO_2$  with rate of percentage of mortality (42.59%, 36.51%, 36.46%) and  $LC_{50}$  4623.77, 5693.75 and 5855.68 ppm and Toxicity index 94, 77 and 74% respectively, but they did not differ significantly ( $p \leq 0.05$ ) between them, but the treatments of interaction between concentration and the four doped nanoparticles differed significantly ( $p \leq 0.05$ ) with control. As for the repellent effect of these particles, N-doped  $TiO_2$  had the highest rate of repellency percentage (16.41%), followed by Sb-doped  $TiO_2$ , Bi-doped  $TiO_2$  and P-doped  $TiO_2$  with a repellency percentage rate (10.39%, 10.26%, 1.27%).

**Conclusion.** The southern cowpea beetle, *Callosobruchus maculatus*, can be controlled using doped nanoparticles (Bi-doped  $TiO_2$ , Sb-doped  $TiO_2$ , P-doped  $TiO_2$ , N-doped  $TiO_2$ ).

**Keywords:** crops, beetle, radiation, *Tribolium castaneum*, adulticidal

## ■ INTRODUCTION

One of the main pests of leguminous grains, such as green gram, cowpeas, lentils, and black gram, is *Callosobruchus maculatus* (F.) [1, 2]. Both in the field and in storage, *C. maculatus* damages crops, although the infestation is particularly severe when crops are stored [2]. Pulse beetle causes losses of roughly 100% when storage conditions are not managed [3]. Additionally, by feeding on the seeds, the larvae contaminate them and render them unfit for human consumption [1–3]. Currently, synthetic pesticides, fumigants, ionizing radiation, and certain botanicals are the main methods used to control storage pests [1]. Due to unintended consequences like food poisoning, health risks, insecticide

resistance and environmental contamination, insecticidal treatment to manage stored product pests is neither practical nor appropriate, Metal phosphides, hydrogen cyanide, methyl bromide and sulfur dioxide, which are very harmful to human health, are components of several fumigants [4]. Ionizing radiations have drawn significant interest for the control of storage insect pests, however they can have negative effects on human health and the environment [5]. Using nanoparticles as pesticides to protect crops is the focus of the newly emerging trend of nanopesticide research, the use of nanoparticles to control insect pests has gained momentum internationally and is predicted to revolutionize pest management in the future [6]. The preparation and use of nanoparticles would be used as an alternate way for protecting stored goods due to the limitations of various insect pest management techniques. Insect pests such as moths, beetles, and mosquitoes have all been tested using a variety of nanoparticles [7–9]. The use of polyethylene glycol-coated nanoparticles loaded with garlic essential oil for controlling adult *Tribolium castaneum* has been the subject of numerous studies [10], and different types of nanoparticles have been used against rice weevil *Sitophilus oryzae* [11]. Silica, silver, and aerosol nanoparticles have all been employed to shield cowpea seeds from *C. maculatus* infestation [12]. Recently, *Callosobruchus maculatus* has been managed using hydrophobic silica nanoparticles on the seeds of *Cajanus cajan* [13] and *Pongamia pinnata* ZnO NPs (Pp-ZnO NPs) on *Vigna radiata* [9]. Nanoparticles are generally characterized by their great efficiency in insect control compared to pesticides due to their small size, which facilitates their access to the insect's body and penetration of its defenses [14]. Among the advantages of using Nanoparticles in insect control do not affect or have a limited effect on non-target organisms such as beneficial insects and fish [15]. The use of these particles in general in insect control will contribute significantly to reduce the damage resulting from the use of chemical pesticides, as the amount used from these pesticides around the world is estimated at 2.8 million tons a year, which reaches pests a little about 0.1%, while the rest goes to water and soil sources [16]. In view of the above, this study was conducted to Study The adulticidal and repellent effect in southern cowpea beetle *Callosobruchus maculatus*.

## ■ MATERIALS AND METHODS

### **Collection and breeding**

The insect was raised on chickpea seeds in a large glass bottle, 20 cm long and 6 cm in diameter. The nozzles were covered with medical gauze patches. The culture was raised at a temperature ( $28 \pm 2$  °C) and a relative humidity ( $70 \pm 5\%$ ). The culture was constantly renewed in order to maintain its vitality and to avoid rotting.

### **Synthesis of doped nanoparticles**

In a series of tests, modified-doped TiO<sub>2</sub> was created by using the sol-gel process to dope TiO<sub>2</sub> with a number of atoms (N, P, Sb, and Bi), wherein Doped – TiO<sub>2</sub> was first made by continuously adding 5 ml of a solution (Ammonia 35%) as a source of nitrogen for doping into 10 ml of a solution (Titanium (IV)) as a source of titanium oxide while rotating at a constant rate (400 rpm) with a magnetic stirrer and adding the materials at a temperature of 30 C for the first ten minutes., a white, extremely thick solution that resembles a colloidal material is created. The resulting solution was hydrolyzed as a result of condensation reactions, and this process continued for about an hour while stirring

continuously. Next, a gel powder was obtained, and it was dried in an oven under vacuum pressure at a temperature of 120 °C for an additional hour to remove any reaction sources and some organic products created during the hydration reactions. Recently, N-doped TiO<sub>2</sub> was produced by calcining materials in a blazing oven at temperatures between 300 and 900 C for an entire hour in order to cause thermal disintegration and remove volatile aggregates. Depending on the calcination temperature, the produced N-doped TiO<sub>2</sub> has a wide range of colors [17]. As for the preparation of p-doped TiO<sub>2</sub>, an aqueous solution of PCI<sub>5</sub> was prepared at a concentration of (1M) by dissolving 2.08 g of it in 10 ml of ionic water, and for the purpose of preparing Sb-doped TiO<sub>2</sub>, an aqueous solution of ionic Sb<sub>2</sub>O<sub>3</sub> was prepared at a concentration of (M1) by dissolving 2.91 g of it in 10 ml of ionic water and drops of a 0.1M NaOH solution were added to complete the dissolution process. In the case of preparing Bi-doped TiO<sub>2</sub>, an aqueous solution of Bi(NO<sub>3</sub>)<sub>3</sub> with a concentration of (1M) was prepared by dissolving 3.94 g of it. In 10 ml of ionic water, then 5 ml of each of the three aforementioned solutions were added to 10 ml of Titanium (IV) solution separately, and all the steps mentioned were repeated in the case of preparing N-doped TiO<sub>2</sub>. All doped nanoparticles mentioned above were characterized using techniques; X-ray diffraction, ATR-FTIR spectrophotometry, and atomic force microscopy (AFM), UV-Visible Spectrophotometry.

#### **Concentrations used in the study**

Three concentrations 4000, 6000, 8000 ppm were prepared for each of the doped nanoparticles (Bi-doped TiO<sub>2</sub>, Sb-doped TiO<sub>2</sub>, P-doped TiO<sub>2</sub>, N-doped TiO<sub>2</sub>) by dissolving 400, 600, 800 mg respectively of each of these particles in 100 ml of deionized distilled water.

### **Biological effects of nanoparticles in adults of the southern cowpea beetle *Callosobruchus maculatus***

#### **Percentage of mortality**

10 adults were placed in Petri dishes covered with pieces of perforated cloth, they was sprayed with 1 ml of each of the three concentrations mentioned above for the four nanoparticles separately with three replicates for each treatment. After 24 hours, the mortality percentage was calculated according to the equation Schneider-Orelli:

$$\text{Corrected \%} = \left( \frac{\text{Mortality \% in treated plot} - \text{Mortality \% in control plot}}{100 - \text{Mortality \% in control plot}} \right) \times 100.$$

The method was used to obtain the LC<sub>50</sub>, and the following equation was used to determine the Toxicity Index:

$$100 \times \frac{\text{LC}_{50} \text{ value of the most toxic substance}}{\text{LC}_{50} \text{ value of any other substance}} \text{ TI (Toxicity Index) =}$$

### The repellent effect

As for the repellent effect of nanoparticles, it was calculated using the method of McDonald and modified by Talukder and Howse using Petri dishes with a diameter of 9 cm. The dish was divided into two equal halves and a circle with a diameter of 4 cm was drawn in the middle. Then one half was wiped with a piece of cotton treated with the three concentrations of each nanoparticles separately, with three replicates of each concentration separately. The other half was wiped with a piece of cotton treated with distilled water only with three replicates too. The dish was left to dry in the air, then, 5 larvae (5–7 days old) were placed in the middle of the small circle and a perforated plastic cover was placed over the dish. After 15 minutes, the numbers of larvae in the untreated half (C) were calculated. The percentage of repellency was measured according to the equation:  $PR = 2(C - 50) \%$ .

Where PR = percentage of repellency, C = percentage of larvae in the untreated part, If C is more than 50%, PR becomes positive and the treatment has a repellent effect, but if C is less than 50%, PR becomes negative and treatment has an attractive effect.

### Statistical analysis

Complete randomized design (CRD) was used in all of the studies, and the percentages were transformed into angle numbers. They were then statistically evaluated in the SPSS program using a variance analysis method, and the Least Significant Difference (L.S.D.) was used to examine the statistical differences at the probability level (0.05).

## ■ RESULTS

### Percentage of mortality of doped nanoparticles (Bi-doped $TiO_2$ , Sb-doped $TiO_2$ , P-doped $TiO_2$ , N-doped $TiO_2$ ) in the adults of southern cowpea beetle *Callosobruchus maculatus*

It was clear from Table 1 that the highest rate of percentage of mortality was for Bi-doped  $TiO_2$ , which reached 44.57%, but it did not differ significantly ( $p \leq 0.05$ ) from the rest of the doped nanoparticles: Sb-doped  $TiO_2$ , P-doped  $TiO_2$ , N-doped  $TiO_2$ , where the rate of mortality percentages reached (42.59, 36.51 and 36.46)% respectively, this was also evident from Table 2 where the  $LC_{50}$  for Bi-doped  $TiO_2$  was the lowest (4389.50 ppm) and the Toxicity Index, for this nanoparticle (100%) while the  $LC_{50}$  for the other doped nanoparticles (Sb-doped  $TiO_2$ , P-doped  $TiO_2$ , N-doped  $TiO_2$ ) was 4623.77, 5693.75, 5855.68 ppm, and the toxicity Index for these particles 94, 77, 74% respectively. Regarding the effect of concentration, it was clear from Table 1 that the highest percentage rate of mortality was at concentration 8000 ppm (56.77%) but it did not differ significantly from the other two concentrations (4000, 6000) ppm, while the above three concentrations differed significantly ( $p \leq 0.05$ ) significant with control.

**Table 1**  
**Percentage mortality of doped nanoparticles (Bi-doped TiO<sub>2</sub>, Sb-doped TiO<sub>2</sub>, P-doped TiO<sub>2</sub>, N-doped TiO<sub>2</sub>) in adults of the southern cowpea beetle *Callosobruchus maculatus***

Rate of Conc.	N-doped TiO <sub>2</sub>	P-doped TiO <sub>2</sub>	Sb-doped TiO <sub>2</sub>	Bi-doped TiO <sub>2</sub>	Substance Conc. (ppm)
0.00	0.00	0.00	0.00	0.00*	Control
47.11	38.85	39.23	54.99	55.37	4000
56.30	38.85	56.99	63.43	65.94	6000
56.77	68.16	50.02	51.94	56.99	8000
	36.46	36.51	42.59	44.57	Rate of Substance

Notes: \* The numbers represent an average of three replicates.

LSD<sub>0.05</sub> for effect of Substance = 12.82.

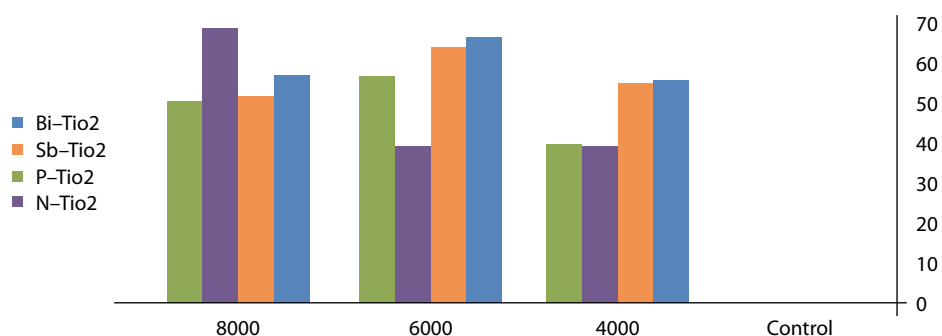
LSD<sub>0.05</sub> for effect of Concentration = 12.82.

**Table 2**  
**LC<sub>50</sub> and Toxicity Index of doped nanoparticles) Bi-doped TiO<sub>2</sub>, Sb-doped TiO<sub>2</sub>, P-doped TiO<sub>2</sub>, N-doped TiO<sub>2</sub>) in adults of the southern cowpea beetle *Callosobruchus maculatus***

Toxicity Index %	LC <sub>50</sub> ppm	Substance
100	4389.50	Bi-doped TiO <sub>2</sub>
94	4623.77	Sb-doped TiO <sub>2</sub>
77	5693.75	P-doped TiO <sub>2</sub>
74	5855.68	N-doped TiO <sub>2</sub>

Note: LSD<sub>0.05</sub> for effect of Substance = 12.82.

From Figure, it appeared that the highest percentage of mortality was 68.16% when adults treated with N-doped TiO<sub>2</sub> at a concentration of 8000 ppm, and the lowest percentage of mortality was 38.85% when treated with the same particle with the two concentrations 6000 ppm and 4000 ppm. The four doped nanoparticles differed significantly ( $p \leq 0.05$ ) in all treatments at the three concentrations with the control.



**Interaction between Substance and concentrations in the mortality percentage of (Bi-doped TiO<sub>2</sub>, Sb-doped TiO<sub>2</sub>, P-doped TiO<sub>2</sub>, N-doped TiO<sub>2</sub>) in adults of southern cowpea beetle *Callosobruchus maculatus***

Note: LSD<sub>0.05</sub> for effect of Interaction (Substance × Concentration) = 25.64.

From Table 3, regarding the effect of the type of substance, it was clear that the treatment with the four doped nanoparticles (Bi-doped  $\text{TiO}_2$ , Sb-doped  $\text{TiO}_2$ , P-doped  $\text{TiO}_2$ , N-doped  $\text{TiO}_2$ ) was repellent, Where the rate of the repellency percentage was 10.26, 10.39, 1.27 and 16.41% respectively, but they did not differ significantly ( $p \leq 0.05$ ) between them, as for the effect of concentration, the effect of the three concentrations 4000, 6000, 8000 ppm was repellent, as the rate of repellency percentage was 2.11, 5.48 and 21.16% respectively, but they did not differ significantly ( $p \leq 0.05$ ) between them, and with regard to the effect of the interaction between the effect of the type of substance and the concentration.

**Table 3**  
Percentage of repellency of doped nanoparticles (Bi-doped  $\text{TiO}_2$ , Sb-doped  $\text{TiO}_2$ , P-doped  $\text{TiO}_2$ , N-doped  $\text{TiO}_2$ ) (in adults of southern cowpea beetle *Callosobruchus maculatus*)

Rate of Conc.	N-doped $\text{TiO}_2$	P-doped $\text{TiO}_2$	Sb-doped $\text{TiO}_2$	Bi-doped $\text{TiO}_2$	Substance Conc. (ppm)
2.11	8.06	-4.63	0.00	5.01*	4000
5.48	2.30	-1.92	4.62	16.92	6000
21.16	38.85	10.37	26.57	8.85	8000
	16.41	1.27	10.39	10.26	Rate of substance

Notes: \* The numbers represent an average of three replicates.

LSD<sub>0.05</sub> for effect of Substance = 48.52.

LSD<sub>0.05</sub> for effect of Concentration = 123.44.

LSD<sub>0.05</sub> for effect of Interaction (Substance × Concentration) = 32.98.

## ■ DISCUSSION

The effectiveness of doped nanoparticles in mortality of insects can be attributed to their size, as a small amount of these particles covers a large surface area of the body of the targeted insects, these particles also have the ability to destroy the wax layer present in the insect's cuticle when they enter this layer through imbibition or friction [18], the damage to the wax layer leads to the dehydration of the insect and thus its death. Vayias and Athanassiou [19] indicated that insect cuticle fat absorbs nanoparticles, including  $\text{TiO}_2$  particles when used in pest control, which leads to the destruction of the insect's defenses. This study may also be consistent with the findings of Atwa et al. [20] who confirmed that the use of silver-doped copper oxide has adulticidal effect against *Spodoptera littoralis*.

It was noted that all treatments had a repellent effect against the adults of the insect, except for the treatment with P-doped  $\text{TiO}_2$  at the two concentrations of 4000 ppm and 6000 ppm, as their effect was attractive to adults, as well as treatment with Sb-doped  $\text{TiO}_2$  at a concentration of 4000 ppm, where the effect against the adults was neutral, this may be close to agreement with Owolade et al. [21], who indicated the repellent effect of silver nanoparticles against insects on food, and it also agrees with Ziaee and Ganji [22], who demonstrated the repellent effect of nanoparticles on warehouse insects.

## ■ CONCLUSION

The southern cowpea beetle, *Callosobruchus maculatus*, can be controlled using doped nanoparticles (Bi-doped  $\text{TiO}_2$ , Sb-doped  $\text{TiO}_2$ , P-doped  $\text{TiO}_2$ , N-doped  $\text{TiO}_2$ ).

These particles didn't differ much from one another and had an adulticidal impact on the insect. Additionally, these nanoparticles demonstrated an insect-repelling impact.

## ■ REFERENCES

1. War AR, Murugesan S, Boddepalli VN, et al. Mechanism of Resistance in Mungbean [*Vigna radiata* (L.) R. Wilczek var. *radiata*] to bruchids, *Callosobruchus* spp. (Coleoptera: Bruchidae). *Front Plant Sci.* 2017;8:1031.
2. Nair RM, Pandey AK, War AR, et al. Biotic and Abiotic Constraints in Mungbean Production-Progress in Genetic Improvement. *Front Plant Sci.* 2019;10:1340.
3. Sonta P, Ammaranan C, Ooi PAC, Srinives P. Inheritance of seed resistance to bruchids in cultivated mungbean (*Vigna radiata*, L. Wilczek). *Euphytica.* 2007;155:47–55.
4. Pieper C, Holthenrich D, Schneider H. Gesundheitliche Risiken durch Schädlingsbekämpfungsmittel [Health risks from pest control products]. *Bundesgesundheitsblatt Gesundheitsforschung Gesundheitsschutz.* 2014;57(5):574–84. (in German).
5. Islam MS, Rahman AK, Laz R. Manipulation of Reproductive Potential of the Pulse Beetles *Callosobruchus* Spp. (Coleoptera: Bruchidae) by Gamma Irradiation. *Univ. j. zool. Rajshahi Univ.* 2001;20:17–24.
6. Bhattacharyya A, Duraisamy P, Govindarajan M, et al. Nano-biofungicides: emerging trend in insect pest control. *Advances and applications through fungal nanobiotechnology.* 2016;307–319.
7. Roni M, Murugan K, Panneerselvam C, et al. Characterization and biotoxicity of Hypnea musciformis-synthesized silver nanoparticles as potential eco-friendly control tool against *Aedes aegypti* and *Plutella xylostella*. *Ecotoxicol Environ Saf.* 2015;121:31–8.
8. Elango G, Roopan SM, Dhamodaran KI, et al. Spectroscopic investigation of biosynthesized nickel nanoparticles and its larvicidal, pesticidal activities. *J Photochem Photobiol B.* 2016;162:162–167.
9. Malaikozhundan B, Vinodhini J. Nanopesticidal effects of *Pongamia pinnata* leaf extract coated zinc oxide nanoparticle against the Pulse beetle, *Callosobruchus maculatus*. *Materials Today Communications.* 2018;14:106–115.
10. Yang FL, Li XG, Zhu F, Lei CL. Structural characterization of nanoparticles loaded with garlic essential oil and their insecticidal activity against *Tribolium castaneum* (Herbst) (Coleoptera: Tenebrionidae). *J Agric Food Chem.* 2009;57(21):10156–62.
11. Goswami A, Roy I, Sengupta S, Debnath N. Novel applications of solid and liquid formulations of nanoparticles against insect pests and pathogens. *Thin solid films.* 2010;519(3):1252–1257.
12. Rouhani M, Samih MA, Kalantari S. Insecticidal effect of silica and silver nanoparticles on the cowpea seed beetle, *Callosobruchus maculatus* F. (Col.: Bruchidae). *Journal of Entomological Research.* 2013;4(4):297–305.
13. Arumugam G, Velayutham V, Shanmugavel S, Sundaram J. Efficacy of nanostructured silica as a stored pulse protector against the infestation of bruchid beetle, *Callosobruchus maculatus* (Coleoptera: Bruchidae). *Applied nanoscience.* 2016;6:445–450.
14. Benelli G. Plant-mediated biosynthesis of nanoparticles as an emerging tool against mosquitoes of medical and veterinary importance: a review. *Parasitology research.* 2016;115(1):23–34.
15. Haldar KM, Haldar B, Chandra G. Fabrication, characterization and mosquito larvicidal bioassay of silver nanoparticles synthesized from aqueous fruit extract of putranjiva, *Drypetes roxburghii* (Wall.). *Parasitology Research.* 2013;112:1451–1459.
16. Ayoub HA, Khairy M, Rashwan FA, Abdel-Hafez HF. Synthesis and characterization of silica nanostructures for cotton leaf worm control. *Journal of Nanostructure in Chemistry.* 2017;7(2):91–100.
17. Li X, Liu Q, Jiang X, Huang J. Enhanced photocatalytic activity of Ga-N Co-doped anatase TiO<sub>2</sub> for water decomposition to hydrogen. *Int. J. Electrochem. Sci.* 2012;7(11):11519–11527.
18. Debnath N, Das S, Seth D, et al. Entomotoxic effect of silica nanoparticles against *Sitophilus oryzae* (L.). *Journal of Pest Science.* 2011;84:99–105.
19. Vayias BJ, Athanassiou CG. Factors affecting the insecticidal efficacy of the diatomaceous earth formulation SilicoSec against adults and larvae of the confused flour beetle, *Tribolium confusum* DuVal (Coleoptera: Tenebrionidae). *Crop Protection.* 2004;23(7):565–573.
20. Atwa AA, Salah NA, Khafagi WE, Al-Ghamdi AA. Insecticidal effects of pure and silver-doped copper oxide nanosheets on Spodoptera littoralis (Lepidoptera: noctuidae). *The Canadian Entomologist.* 2017;149(5):677–690.
21. Owolade OF, Ogunleti DO, Adenekan MO. Titanium dioxide affects disease development and yield of edible cowpea. *Agri. Food. Chem.* 2008;7(50):2942–2947.
22. Ziaee M, Ganji Z. Insecticidal efficacy of silica nanoparticles against *Rhyzopertha dominica* F. and *Tribolium confusum* Jacquelin du Val. *Journal of plant protection research.* 2016;56(3):1–7.

<https://doi.org/10.34883/PI.2025.14.1.055>

Adian A. Dakl , Ikram A. Al-Samraee  
Veterinary Medicine College, University of Baghdad, Baghdad, Iraq

# Histopathological Alterations Caused by *Klebsiella pneumoniae* Infection in Rabbits and the Preventive Effects of Whole Sonicated Killed Antigen and *Albizia Lebbeck* Extract

**Conflict of interest:** nothing to declare.

**Authors' contribution:** all authors made a significant contribution to the writing of the article.  
The article is published in author's edition.

Submitted: 03.03.2025

Accepted: 17.03.2025

Contacts: adian.abd@mu.edu.iq

## Abstract

**Purpose.** To estimate the protective capability of ethanolic *Albizia lebbeck* leaf extract against *Klebsiella pneumoniae* contagion in rabbits.

**Materials and methods.** The animals gathered into three groups each group contain eight albino rabbits were received the following: Subcutaneously group one was received Killed Whole Cell Sonicated Antigen-*Klebsiella pneumoniae* (KWCSAg-KP); group two was orally received ethanolic *Albizia lebbeck* leaf extract and KWCSAg-KP subcutaneously; group three was quit as control group was given PBS subcutaneously. The rabbit groups were orally challenged by  $1.5 \times 10^8$  CFU/ml *Klebsiella pneumoniae* then the rabbit were immolated ten days post-challenge for pathological changes. Spleen, liver, intestine and kidney were examined for histopathological alterations. Intestine, liver, kidney and spleen were examined for pathological changes.

**Results.** The results revealed that the 2<sup>nd</sup> group had the least histopathological alterations with moderate infiltration of inflammatory cells in addition to unabnormality detected in the kidney as well as the liver. The KWCSAg-KP group revealed sloughing with mild superficial inflammation in the lamina propria and mild vacoulation of the hepatocytes in the centrilobuar area in addition to moderate white pulp hyperplasia in the spleen. The control group showed sever changes of inflammation, vacoulation, interstitial hemorrhage and congestion of the hepatic veins as well as hemosiderosis of the red pulp in the spleen.

**Conclusion.** *Albizia lebbeck* leaf extract revealed to give an appropriate protection against inflammation as well as damage of virulent *Klebsiella pneumoniae* contagion in comparison to both of KWCSAg-KP and control groups.

**Keywords:** *Albizia lebbeck*, histopathology, *Klebsiella pneumoniae*, Killed Whole Cell Sonicated Antigen-*Klebsiella pneumoniae*, hemosiderosis

## ■ INTRODUCTION

Klebsiella is an influential microorganism posing a threat to public health due to its transmission as animal-borne bacterial pathogens (zoonosis) [1]. These microorganisms are responsible for a wide range of infections in both humans and animals. These infections can be caused by a variety of initiators, including nosocomial contact, direct or indirect contact with animals that have been infected, and contaminated dairy products [2]. Some of the infections that can be caused by these microorganisms include acute injuries to organs with mucous membranes and infected wounds, bacteremia, meningitis-related infections, and abscesses that are located in different parts of the body [2, 3]. Klebsiella, on the other hand, has been identified from respiratory infections in a variety of domestic animals, including sheep [4] and has the potential to induce sepsis in lambs [5]. Furthermore, it's an essential pulmonary bacteria for camels, calves, horses, foals, sows and horses. It has been linked to a wide range of animal diseases, including a number of systemic infections, as well as diarrhea in calves, mastitis in cattle, metritis in mares, and meningitis in piglets [6]. An investigation into the pathological changes that are brought about by an infection with *Klebsiella pneumoniae* in the urinary organs is conducted by Ibrahim [7]. The resistance character of this bacteria it's belong to a complex structures as antigenic determinants include capsular polysaccharides (CPS) and lipopolysaccharides, enhancing main self-protection against environment, effect of disinfectants, many antibiotics, serum factors as well as multiple forms of capsular K antigens cause different levels of infection severity through phagocytic killing action [8, 9], that explain how Klebsiella promote fatality . Further virulence factors include endotoxin generation, iron acquisition systems as well as adhesins [10].

Several strategies have been followed to evading defense of immune system. Klebsiella hidden techniques are shown by capsular polysaccharides functions in suppressing inflammatory response activation, blocking complement's bactericidal impact through Lipopolysaccharides' function in reducing complement deposition at the surface of the bacteria furthermore the absence porins production to prevent complement activation and therefore eliminating phagocytosis by immune cells. On the other hand, modification its lipid A intermediate structure between the highly antagonistic hexa-acylated and less antagonistic hepta-acylated versions to halt the protracted and excessive immune activation [11].

## ■ PURPOSE

To assessment the protective capability of ethanolic *Albizia lebbek* leaf extract against *Klebsiella pneumoniae* contagion in rabbits.

## ■ MATERIALS AND METHODS

### **Ethics**

Both the experimental design and the procedures that were utilized in this study were examined and authorized by the Scientific Committee of the Department of Microbiology, College of Veterinary Medicine. This was done in compliance with the ethical principles that are concerning animal welfare (No. 2317/2023).

### **Killed Whole Cell Sonicated Antigen-Klebsiella pneumoniae preparation**

The isolate *Klebsiella pneumoniae* was identified and characterized using standard and molecular methods [12, 13] at the Microbiology department, Veterinary medicine college, Baghdad University, on ordinary and HiChrom media to prepare antigen. The Killed Whole-Cell Sonicated Antigen of *Klebsiella pneumoniae* (KWCSA-KP) has been produced in accordance with the procedure described in the references [14, 15].

### **Experiment animals**

There were twenty-four Albino rabbits, both male and female, that were obtained from the animal house of the College of Veterinary Medicine at the University of Baghdad. The rabbits ranged in age from six months to twelve months and weighed between one thousand and one thousand and five hundred grams. The animals were housed under standard circumstances for controlled measurements.

### **Experimental design**

The rabbits were gathered into three groups of eight at random. Group one received a subcutaneous (S/C) injection of 1 mL of KWCSAg-KP at a dosage of 1000 µg/mL. Group two received an oral dose of *Albizia lebbek* leaf extract (300 mg/kg) on alternate days for one week before the first day of the experiment, and subcutaneously, they were immunised with 1 mL of KWCSAg-KP at a dosage of 1000 µg/mL. Group three, which served as a control, 1 mL of PBS was inoculated subcutaneously. Both the first and second groups of KWCSAg-KP S/C recipients got their booster doses on the fourteenth day after the initial injection. In contrast, the second group received an extra dosage of *Albizia lebbek* extract orally equal to 300 mg/kg. On day 21, all groups of rabbits were orally administered the challenge dosage of pathogenic *Klebsiella pneumoniae*, which was ( $1.5 \times 10^8$  CFU/ml) [16]. Organs such as the liver, spleen, kidney, and intestine were taken out for histological examination when the animals were euthanized ten days after the challenge dose, in accordance with [17].

## **■ RESULTS**

### **Histological alterations**

#### **Intestine**

The first group reveals few areas of superficial epithelial sloughing with mild superficial inflammation in the lamina propria (Fig. 1A, B), the second group shows normal epithelium with mild infiltration of inflammatory cells (Fig. 1C, D). Third group shows hyperplasia of the mucosal epithelium with inflammation (Fig. 1E, F).

#### **Liver**

Liver in the first group shows mild vacuolation of the hepatocytes in the centrilobular area otherwise no abnormality was detected (Fig. 2A, B). Hepatocytes in the liver of the second group appear normal as the other components in both centrilobular and portal area (Fig. 2C). Third group shows liver there was congestion of the hepatic veins in the centrilobular and portal area (Fig. 2D, E) with bridging inflammation extending between central and portal area (Fig. 2F).

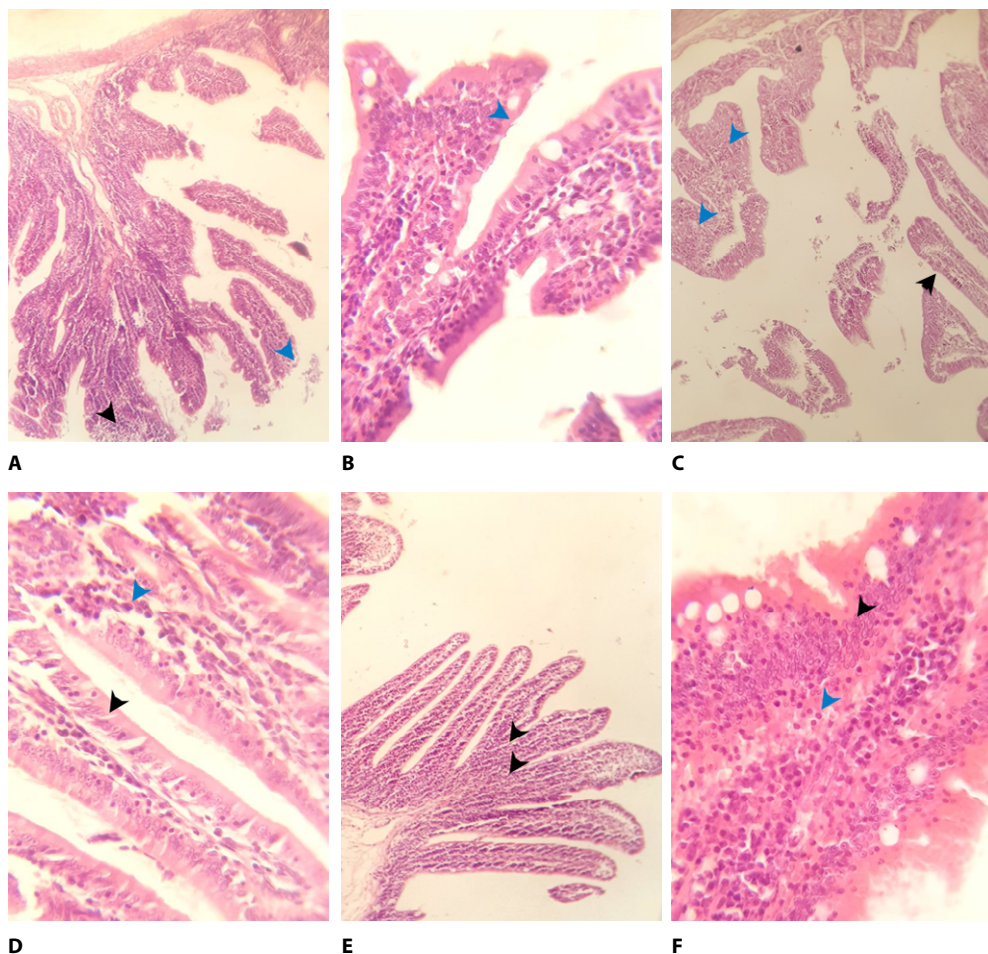


**Fig. 1. A and B – Histopathological sections in the small intestine of adult rabbits immunised with 1000µg/ml of killed whole cell sonicated Antigen-Klebsiella pneumoniae (KWCSAg-KP) revealing mild inflammation in the superficial portion of the villi (black arrow), area of epithelial sloughing (blue arrow) H&E A: 10X, B: 40X; C and D – Histopathological sections in the small intestine of adult rabbits administered Albizia lebbek leaf extract at a dose of 300 mg/kg and immunised with 1000 µg/ml of killed whole cell sonicated Antigen-Klebsiella pneumoniae (KWCSAg-KP) revealing normal epithelium of the intestinal mucosa (black arrow), mild inflammatory infiltration in the lamina propria (blue arrow) H&E C: 10X, D: 40X; E and F – Histopathological sections in the small intestine of adult rabbits of positive control group (inoculated 1 ml PBS) revealing hyperplasia of epithelium of the intestinal mucosa (black arrow) inflammatory, inflammation in the lamina propria (blue arrow) H&E E: 10X, F: 40X**

## Kidney

Histopathological inspection of the organs in the present study showed that kidney in the group 1 appears within normal limits, the glomeruli were normal, renal tubular epithelium were consist of single layer of cuboidal cells in both cortex and medulla (Figure 3 (A, B, C and D)). In group two there was no any abnormality detected in the kidney, as the glomeruli appear of normal architecture as well as the other renal components that

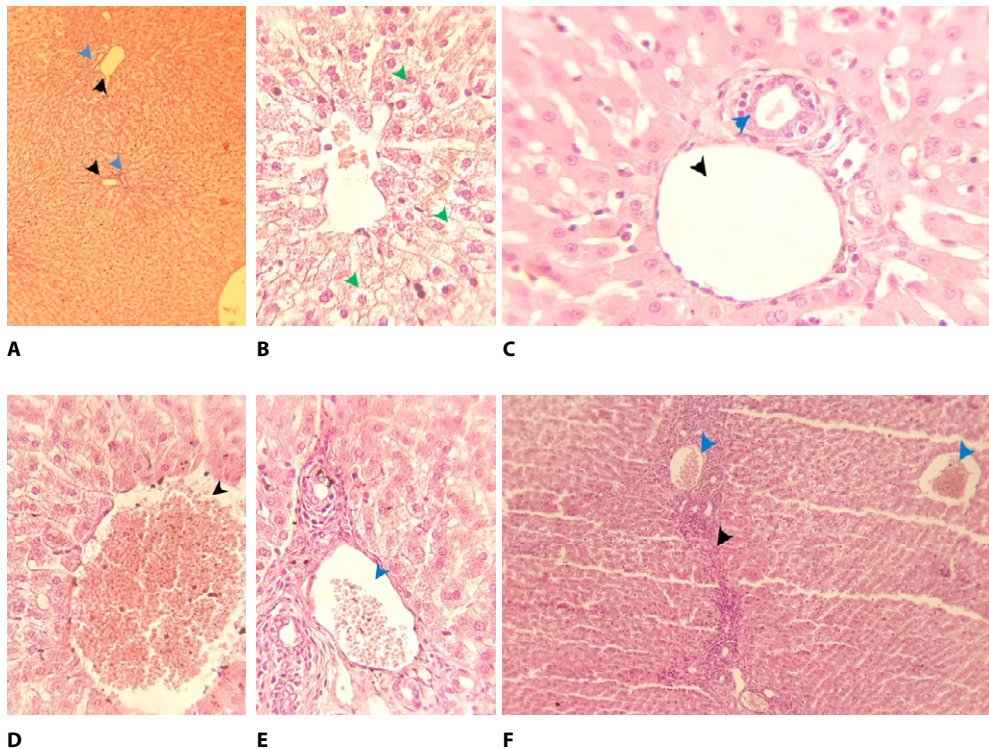


**Fig. 2.** A and B – Histopathological sections in the liver of adult rabbits immunised with 1000µg/ml of killed whole cell sonicated *Antigen-Klebsiella pneumoniae* (KWCSAg-KP) revealing normal liver architecture in the portal area; including portal vein (black arrow), bile canaliculi (blue arrow), mild vacuolation of hepatocytes in the centrilobular area (green arrow) H&E A: 10X, B: 40X; C – Histopathological section in the liver of adult rabbits administered *Albizia lebeck* leaf extract at a dose of 300 mg/kg and immunised with 1000µg/ml of killed whole cell sonicated *Antigen-Klebsiella pneumoniae* (KWCSAg-KP) revealing normal liver architecture in the portal area; including portal vein (black arrow), bile canaliculi (blue arrow) H&E 40X; D and E – Histopathological sections in the liver of adult rabbits of positive control group ( inoculated 1 ml PBS) revealing central vein congestion (black arrow), mild congestion of portal vein (blue arrow). H&E 40X; F – Histopathological section in the liver of adult rabbits of positive control group (inoculated 1 ml PBS) revealing bridge inflammation (black arrow) and vascular congestion (blue arrow). H&E 10X

include renal interstitium, vasculature and the renal tubules in both cortex and medulla (Fig. 3E, F). Group three shows sever changes in the kidney; these are include, marked glomerular atrophy with vacuolation of renal tubular epithelium in cortex and medulla (Fig. 3G, H), marked interstitial hemorrhage and inflammation (Fig. 3I, J).

### Spleen

In the first group spleen shows moderate white pulp hyperplasia with normal red pulp. In the second group spleen shows mild white pulp hyperplasia with normal red pulp. In the third group shows spleen hyprplasia of white pulp was sever with hemosiderosis of the red pulp (Fig. 4A–C).

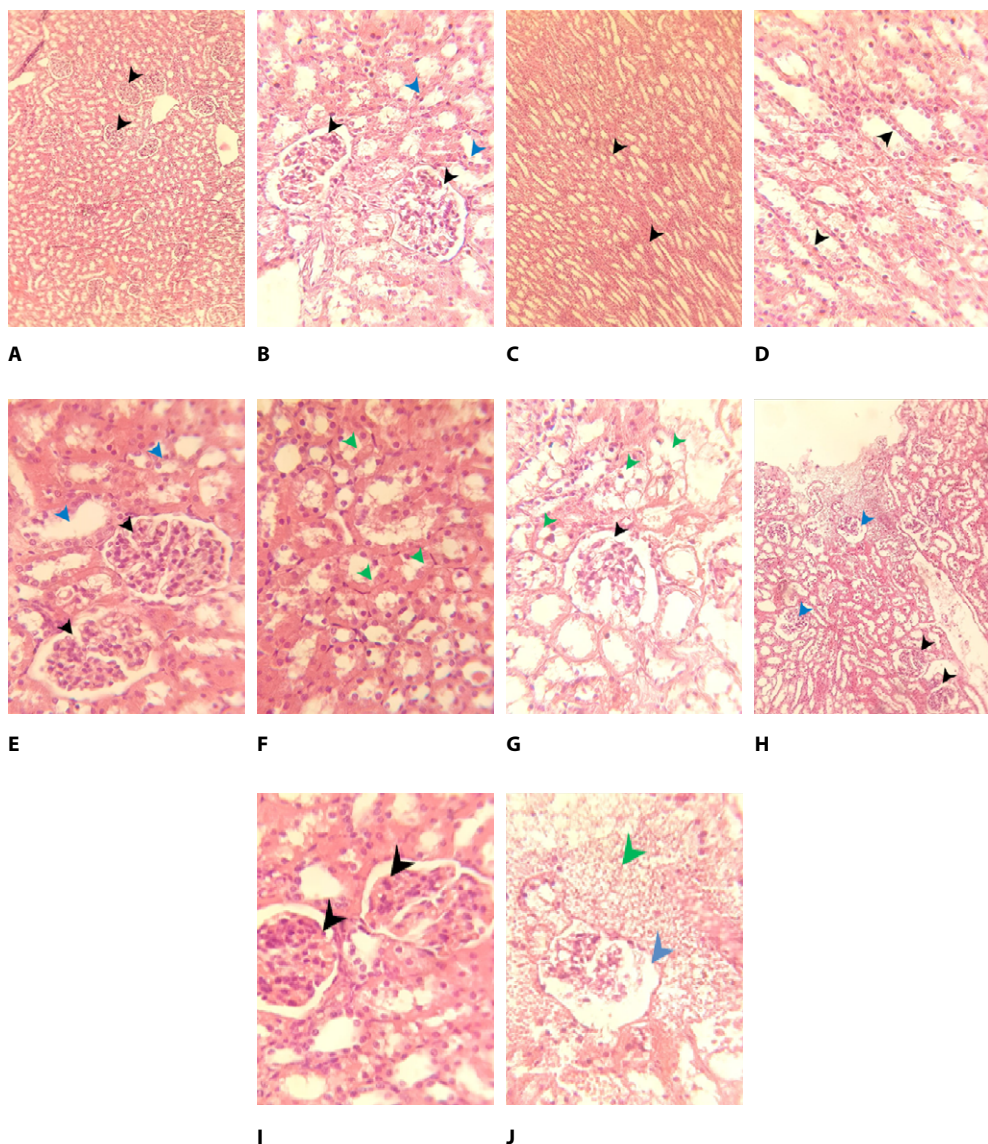


**Fig. 3. A–D – Histopathological sections in the kidney of adult rabbits immunized with 1000 µg/ml of killed whole cell sonicated Antigen-Klebsiella pneumoniae (KWCSAg-KP) revealing normal glomeruli (black arrow) normal renal tubular epithelium in the renal cortex (blue arrow), 10X and 40X and in the medulla (black arrow), H&E, 10X and 40X; E and F – Histopathological sections in the kidney of adult rabbits administered Albizia lebbek leaf extract at a dose of 300 mg/kg and immunized with 1000µg/ml of killed whole cell sonicated Antigen-Klebsiella pneumoniae (KWCSAg-KP) revealing normal glomeruli (black arrow), normal tubules both cortex (blue arrow) and medulla (green arrow), H&E 40X; G and H – Histopathological section in the kidney of adult rabbits of positive control group (inoculated 1 ml PBS) showing normal glomerulus (black arrow), some other atrophied (blue arrow), mild vacoulation renal tubular epithelium (green arrow), H&E, 40X and 10X; I and J – Histopathological section in the kidney of adult rabbits of positive control group (inoculated 1 ml PBS) showing mild glomerular congestion (black arrow), atrophic glomerulus (blue arrow), interstitial hemorrhage (green arrow), H&E 40X**

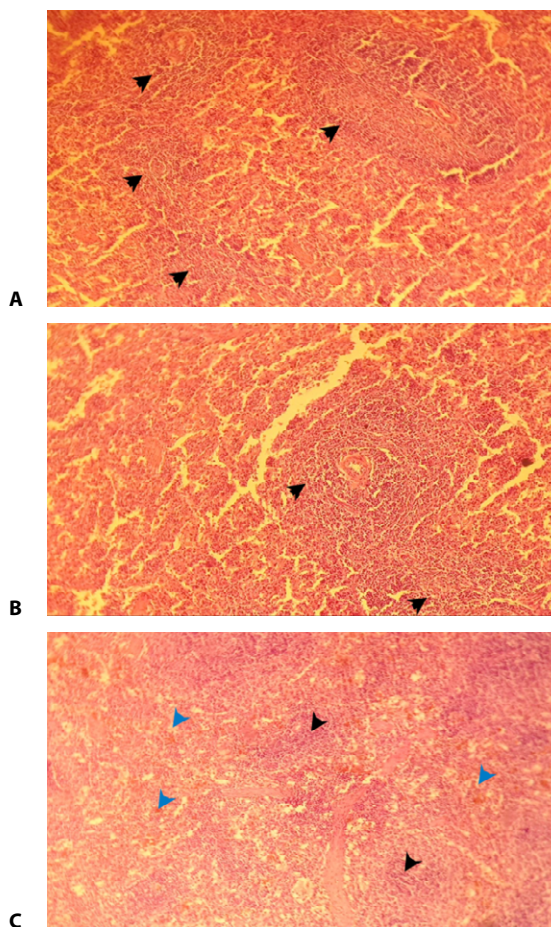


**Fig. 4. A – Histopathological section in the spleen of adult rabbits immunized with 1000 $\mu$ g/ml of killed whole cell sonicated Antigen-Klebsiella pneumoniae (KWCSAg-KP) revealing moderate white pulp hyperplasia with normal red pulp H&E; B – Histopathological section in the spleen of adult rabbits administered Albizia lebbek leaf extract at a dose of 300 mg/kg and immunized with 1000  $\mu$ g/ml of killed whole cell sonicated Antigen-Klebsiella pneumoniae (KWCSAg-KP) revealing hyperplasia of white pulp (black arrow) H&E 10X; C – Histopathological section in the spleen of adult rabbits of positive control group (inoculated 1 ml PBS) showing spleen hyperplasia of white pulp was severe with hem siderosis of the red pulp**

## ■ DISCUSSION

The purpose of this research was to determine whether or not the immunomodulatory Albizia lebbek leaf extract and the killed sonicated Klebsiella pneumoniae antigen could prevent Klebsiella pneumoniae infections.

This study's histopathology results provided more evidence that the Klebsiella pneumoniae vaccine provided some protection against the disease that caused by Klebsiella spp. The first group showed less pathological results compared to the control group, whereas the second group demonstrated less pathological alterations and greater

protection against the viable challenge dosage when injected *Klebsiella pneumoniae* antigen with *Albizia lebbek* leaf extract. This demonstrated that the *Albizia lebbek* leaf extract as anti-inflammatory and preventive capabilities is best than *Klebsiella pneumoniae* antigen alone. In contrast to the moderate inflammatory response shown in the first group treated with the *Klebsiella pneumoniae* antigen, the control group exhibited a wide array of pathological alterations. Because of the high level of protection against the infection, the second group likewise showed the fewest pathogenic alterations.

Other research has debated the importance of synergic action of herbal extract (*Syzygium aromaticum*) combined with killed antigen of (*Salmonella Typhimurium*) in immune modulation and the ability immune response in determining the histopathological changes [18]. These findings are in alignment with previous research that shown pathological symptoms of early infection in mice injected with killed antigen. Specifically, the animals revealed "polymorphonuclear leukocytes in the organs of the reticuloendothelial system", which is indicative of an infection. Vaccinated animals, in contrast to control mice, exhibited mostly small, self-limiting lesions [19].

Humad et al., described in a study the limitation of histopathological alterations of vaccinated mice with *K. pneumoniae* as very low pathological alterations causing no disseminated of infection with a comparatively small vaccine [16]. On the other hand other study revealed inhibition of capsular (k-antigen) for severs histological changes in the intestine following parasitic infection compared with positive control [20].

According to the kind and mode of infection, bacteria of *Klebsiella* spp. may attached and offensive epithelial cells of the upper respiratory tract, cells in gastrointestinal tract, endothelial cells, or uroepithelial cells, followed by colonization of mucosal membranes [21]. Epidemiologic researches demonstrate that gastrointestinal isolates of *K.pneumoniae* correspond liver isolates genotypically and phenotypically (serotype( as well [22], supporting previous hypotheses that most systemic infections seed from the gut primarily [23]. A widely investigated pathogenicity factor is the capsular (serotype k type) component, which impairs phagocytosis and protects against the bactericidal effects of host serum [24]. In addition, as was shown in [25], the type VI secretion system helps with colonization throughout the gastrointestinal tract, and the capsular polysaccharide is essential for large intestine colonization.

## ■ CONCLUSION

*Albizia lebbek* leaf extract revealed to give an appropriate protection against inflammation as well as damage of virulent *Klebsiella pneumoniae* contagion in comparison to both of KWCSAg-KP and control group.

## ■ REFERENCES

1. Cheng F, Li Z, Lan S, et al. Characterization of *Klebsiella pneumoniae* associated with cattle infections in southwest China using multi-locus sequence typing (MLST), antibiotic resistance and virulence-associated gene profile analysis. *Braz. J. Microbiol.* 2018;49:93–100.
2. Paczosa MK, Mecsas J. *Klebsiella pneumoniae*: going on the offense with a strong defense. *Microbiol. Mol. Biol.* 2016;80(3):629–61.
3. Fang C-T, Lai S-Y, Yi W-C, et al. *Klebsiella pneumoniae* genotype K1: an emerging pathogen that causes septic ocular or central nervous system complications from pyogenic liver abscess. *Clin. Infect. Dis.* 2007;45(3):284–93.
4. Mansour AM, Zaki HM, Hassan NA, Al-Humiany AA. Molecular characterization and immunoprotective activity of capsular polysaccharide of *Klebsiella Pneumoniae* isolated from farm animals at Taif Governorate. *Am. J. Infect.* 2014;10(1):1. doi: 10.3844/ajidsp.2014.1.14
5. Hayati M, Indrawati A, Mayasari NLPI, et al. Molecular detection of extended-spectrum  $\beta$ -lactamase-producing *Klebsiella pneumoniae* isolates of chicken origin from East Java. *Vet. World.* 2019;12(4):578. <https://doi.org/10.14202%2Fvetworld.2019.578-583>

6. Sharma S, Kataria A, Shringi B, et al. Detection of hypermucoviscous *Klebsiella pneumoniae* in camel (*Camelus dromedarius*) during an outbreak of acute respiratory tract infection. *JCPR*. 2013;20(2):139–43.
7. Ibrahim Z. Experimental infection of *Klebsiella pneumoniae* in urinary tract of rats and guinea pigs: Ibrahim ZI and Alwaan MJ. *Iraqi J. Vet. Med.* 2008;32(2):68–79.
8. Pan Y-J, Lin T-L, Chen Y-H, et al. Capsular types of *Klebsiella pneumoniae* revisited by wzc sequencing. *PLoS one*. 2013;8(12):e80670. <https://doi.org/10.1371/journal.pone.0080670>
9. Lee C-R, Lee JH, Park KS, et al. Antimicrobial resistance of hypervirulent *Klebsiella pneumoniae*: epidemiology, hypervirulence-associated determinants, and resistance mechanisms. *Front. cell. infect. microbiol.* 2017;7:483. <https://doi.org/10.3389/fcimb.2017.00483>
10. Lundberg U, Senn BM, Schüller W, et al. Identification and characterization of antigens as vaccine candidates against *Klebsiella pneumoniae*. *Human Vaccines & Immunotherapeutics*. 2013;9(3):497–505. <https://doi.org/10.4161/hv.23225>
11. Al-Samraee IAA. Immune response interaction of *Klebsiella pneumoniae* and *Eimeria tenella*. *Iraqi J. Vet. Med.* 2017;41(1):17–22.
12. Jaafar SW, Abdullah AH. Molecular Detection of Pathogenic in Domestic *Escherichia coli* in Domestic Pigeon (*Columba livia*) in Baghdad, Iraq. *Indian Journal of Ecology*. 2022. 00 Special Issue (00) 000-000
13. Watban H, Al-Maaly N. Bacteriological identification and molecular detection of *Klebsiella pneumoniae* from pneumonic camels in Al-Muthanna province. *Adv Anim Vet Sci*. 2023;11(11):1881–6.
14. Mahdi NR. The Cellular Immunoprotection of BALB/C mice vaccinated with Salt-Extractable *Brucella abortus* S19 antigens and Immunoadjuvant  $\beta$ -glucan challenged with *Brucella abortus* Virulent Strain: Nidhal Raouf Mahdi and Sabrin Ibraheem Mohsin. *Iraqi J. Vet. Med.* 2015;39(2):79–86.
15. Al-Samarrae EA, et al. Humoral immune response of *Salmonella typhimurium* and *Salmonella enteritidis* sonicated antigens in rabbits. *Iraqi J. Vet. Med.* 2012;36(0E):84–8.
16. Humad TJ, Hashim MS, Jafar Karim AK. Immuno-pathological examination of tnf alpha in infected and vaccinated mice with *kelebsiella pneumoniae* in Baghdad, Iraq. *Biochem. Cell.* 2020;20(1).
17. Luna LG. Manual of histologic staining methods of the Armed Forces Institute of Pathology. Manual of histologic staining methods of the Armed Forces Institute of Pathology 1968. p. xii, 258-xii.
18. Al-Juburi LI, Al-Sammarrae IA. The protective role of *Salmonella typhimurium*-whole sonicated killed antigen and *zyzygium aromaticum* extract on the histopathological changes against its infection in rabbits. *Iraqi J. Vet. Med.* 2022;46(2):12–9. <https://doi.org/10.30539/ijvm.v46i2.1399>
19. Hsu H, Nakoneczna I, Guo Y-n. Histopathological evidence for protective immunity induced by sonicated *Salmonella* vaccine. *Can. J. Microbiol.* 1985;31(1):54–61. <https://doi.org/10.1139/m85-012>.
20. Al-Taei K, Al-Dulaimi K. Study the histological changes in intestine of infected rabbits with *entamoeba histolytica* after immunization with *klebsiella pneumoniae* k-antigen. *Adv Anim Vet Sci*. 2020;8(11):1250–5. <https://doi.org/10.17582/journal.aavs%2F2020%2F8.11.1250.1255>
21. Janda JM, Abbott SL. 16S rRNA gene sequencing for bacterial identification in the diagnostic laboratory: pluses, perils, and pitfalls. *J. Clin. Microbiol.* 2007;45(9):2761–4. <https://doi.org/10.1128/jcm.01228-07>
22. Janda JM. The genus *Klebsiella*: an ever-expanding panorama of infections, disease-associated syndromes, and problems for clinical microbiologist. *Clin Microbiol Case Rep*. 2015;1:2.
23. Shon AS, Bajwa RP, Russo TA. Hypervirulent (hypermucoviscous) *Klebsiella pneumoniae*: a new and dangerous breed. *Virulence*. 2013;4(2):107–18. <https://doi.org/10.4161/viru.22718>
24. Yu W-L, Ko W-C, Cheng K-C, et al. Comparison of prevalence of virulence factors for *Klebsiella pneumoniae* liver abscesses between isolates with capsular K1/K2 and non-K1/K2 serotypes. *Diagn Microbiol Infect Dis*. 2008;62(1):1–6. <https://doi.org/10.1016/j.diagmicrobio.2008.04.007>
25. Calderon-Gonzalez R, Lee A, Lopez-Campos G, et al. Modelling the gastrointestinal carriage of *Klebsiella pneumoniae* infections. *Mbio*. 2023;14(1):e03121–22. <https://doi.org/10.1128/mbio.03121-22>

<https://doi.org/10.34883/PI.2025.14.1.057>

Zainab Akram , Eman M. Jarallah  
University of Babylon, College of Science, Babylon, Iraq

# Antibiotic Resistance Profile of *Staphylococcus Aureus* Isolated from Milk and Dairy Products

**Conflict of interest:** nothing to declare.

**Authors' contribution:** Zainab Akram – conceptualization, data curation, investigation, methodology, resources, software, validation, visualization, writing – original draft and writing – review & editing; Eman Jarallah – conceptualization, investigation, methodology, supervision, validation, visualization, writing – original draft and writing – review & editing  
The article is published in author's edition.

Submitted: 20.01.2025

Accepted: 17.03.2025

Contacts: Medicalresearch55@yahoo.com

## Abstract

**Introduction.** Food poisoning bacteria are regarded as one of the most serious health dangers today, as well as an economic issue in which infected material must be eliminated, resulting in significant financial losses for producing firms.

**Purpose.** This research aims to examine the pathogenic strains of *Staphylococcus aureus* that have been obtained from milk and dairy products.

**Materials and methods.** A total of 100 samples were chosen at random from several stores. Additionally, the outcomes of biochemical and microscopy testing were shown. Furthermore, the PCR technique identified *Staphylococcus aureus*, *Staphylococcus epidermidis*, and additional species in the isolates. Sensitivity experiments were performed on each of the represented samples.

**Results.** A sensitivity test was conducted, including the antibiotics Erythromycin, Ciprofloxacin, Trimethoprim, Nitrofurantoin, Clindamycin, Gentamycin, Rifampicin, Tetracycline, and Sulfamethoxazole. Antibiotic resistance among *S. aureus* isolates was found to be variable. The *S. aureus* isolates exhibited the greatest sensitivity to nitrofurantoin (100 percent) and Erythromycin (51.7 percent). The observed pattern unequivocally demonstrated that a significant proportion of *S. aureus* isolates (58.6%) exhibited resistance to Tetracycline, with Trimethoprim (55.1%) and Clindamycin (48.2%). (41.3%) of *S. aureus* isolates had moderate sensitivity to Rifampicin.

**Conclusion.** Staphylococcal foodborne illness is a significant concern in global public health initiatives. *Staphylococcus aureus* could potentially be found in milk and milk products. A significant proportion of bacteria exhibit resistance to the antibiotics frequently employed in the therapy regimens for both human and animal illnesses.

**Keywords:** food poisoning, milk, staphylococcus aureus, antibiotic resistance, enterotoxins

## ■ INTRODUCTION

*S. aureus*, a Gram-positive bacterium, may have caused a large-scale food poisoning incident with its staphylococcal enterotoxins (SEs) [1]. Some of the virulence factors

created by *S. aureus* include "proteases, enterotoxins, hemolysins, leukocidins, exfoliative toxins, and proteins" that modulate the immune system [2].

Strong virulence factors include SEs and a broad family of structurally similar toxins that can multiply T lymphocytes, stimulate the production of cytokines, and eventually induce cell death [3]. Pathogenicity islets, bacteriophages, and plasmids may all convey genes that code for poisons [4]. The toxigenic process in staphylococcal food poisoning is initiated by a family of toxins called SEs, which have mostly been reported in earlier research [5]. These toxins have been linked to a kind of gastroenteritis that causes diarrhea and vomiting [6]. Additionally, rheumatoid arthritis [7], atopic eczema [8], and other conditions are associated with SEs [9]. The majority of SEs are heat-stable, insensitive to digestive enzymes, and capable of causing a range of symptoms, including diarrhea, cramping in the abdomen, nausea, vomiting, and malaise [6]. Remarkably, approximately 95% of food poisoning epidemics resulted from "staphylococcal" bacteria can be attributed to conventional SE forms (A, B, C, D, and E) [10].

The majority of cases of SFP arise from consuming food that has been contaminated at various stages such as collecting, processing, shipping, storage, heating, or handling. Additionally, inadequate refrigeration of food allows for the growth of staphylococcus bacteria and the production of toxins [11]. Enterotoxigenic *S. aureus* can be transmitted by animals that carry or are contaminated with it, such as raw milk, raw milk cheese, and raw and cooked meat products. Despite the fact that human *S. aureus* strains are mostly responsible for SFP, this statement remains accurate. The efficacy of SEs diminishes over time and requires boiling or autoclaving, even when the organism is no longer active and cannot be extracted from food [12, 13].

Milk and milk products are classified as perishable due to their high susceptibility to microbial contamination and the presence of essential proteins and polysaccharides that promote microbial proliferation. The presence of bacteria in milk and milk products poses a significant challenge in the dairy industry. This is especially true in underdeveloped countries where traditional processing methods are used. The primary causes of contamination are linked to inadequate handling practices and insufficient attention to animal health. Milk and milk products contaminated with bacteria may come from primary sources (milk from mastitis-affected heifers, for example) or secondary sources (poor sanitation procedures throughout the milk and milk product supply chains). Milk that has been contaminated with microbes spoils quickly, and the bacteria that were there may infect people or make biochemicals that are toxic and cause milk-borne diseases [14].

The predominant cause of staphylococcal disease outbreaks associated with milk and milk products is *Staphylococcus aureus*. Consequently, milk-based products and consumables derived from milk are often associated with outbreaks of staphylococcal poisoning epidemics [14].

The worldwide community has put a high priority on the bacterium's antibiotic resistance in the treatment of infections resulting from harmful strains of *S. aureus*. Resistance to antibacterial medications has been observed in *S. aureus* ever since the inception of penicillin formulation in 1942, which marked the first antibiotic to be developed. The bacterium's penicillin-resistant strain was subsequently identified in 1959. Since then, much work has gone into creating medicines that can either kill or suppress *S. aureus* that is resistant to penicillin. Methicillin, a synthetic  $\beta$ -lactam antibiotic, was eventually created. Penicillin-resistant *S. aureus* infections were effectively treated

with methicillin because it is resistant to the hydrolysis of the  $\beta$ -lactamase enzyme [15]. Nonetheless, the recent rise of methicillin-resistant *S. aureus* (MRSA) strains has resulted in a paucity of feasible therapeutics for MRSA infections [16].

This research aims to examine the pathogenic strains of *Staphylococcus aureus* that have been obtained from milk and dairy products.

## ■ MATERIALS AND METHODS

### **Collecting the samples**

A total of one hundred samples were gathered randomly from various markets and cooperative milk dairies, cow farms, individual households, milk vendors, and sweet stores in Hilla, Iraq. The samples comprised milk, along with various varieties of cheese and cream. Specimens were gathered from September to November 2023.

### **Preparing the samples**

One gram of any sample was mixed with 9 ml of pure water in a clean environment. This was followed by tenfold dilutions [17].

### **Enumerating the bacteria**

From 100  $\mu$ l, the serial dilution that had been prepared beforehand was cultivated on mannitol salt agar using the pour-plate technique. After that, the plate was incubated for 48 hours at 37°C in an incubator. They were isolated and enumerated to facilitate identification. Following the incubation period, the colonies of bacteria were quantified using the subsequent equation:

CFU per mL: No. of colonies \*Inverted dilution factor/inoculum volume [18].

### **Identifying the *Staphylococcus aureus***

*Staphylococcus aureus* is isolated and identified by growing the germs on MacConkey. To identify the specific staphylococcal bacteria, those that failed to grow on MacConkey agar were then grown on mannitol salt agar, a selective medium. The cultures were then incubated at a temperature of 37 °C [19].

### **Morphological properties**

To make the smear, the isolated culture was placed on a grease-free glass slide and then examined under a microscope. It was subsequently stained using Gram's method. A microscope revealed the pigmented smear. The smear revealed clusters of irregularly shaped, round cells that were Gram-positive, like a bunch of grapes [20].

### **Biochemical analysis**

*S. aureus* was confirmed through biochemical assays employing the Coagulase test, which differentiates Coagulase-positive staphylococci from those that are Coagulase-negative.

### **Antibiotics Susceptibility Testing**

For determining the more susceptible antimicrobial drugs to certain isolates, Disc diffusion was employed. In this investigation, nine antibiotic discs (Erythromycin, Ciprofloxacin, Trimethoprim, Nitrofurantoin, Clindamycin, Gentamycin, Rifampicin, Tetracycline, Sulfamethoxazole) were utilized.

The findings of the current investigation were set in accordance with Clinical and Laboratory Standards Institute standards (CLSI, 2023). The bacterial isolate's colony growth (2–4) was compared to that of the Macfarlaned tube standards after two hours of incubation at 37 °C in a test tube with 5 ml of nourishment broth at a decrease of 0.5 with physiological saline. Using a cotton swab moistened in broth, the bacteria were spread over the Muller Hinton Agar. The tablets were then positioned around the plate in a pattern of four periphery tablets and one central tablet. Incubation of the antibiotics on the plates lasted 18–24 hours at 37 °C. Using standard values and a measuring ruler, damping diameters were calculated.

## ■ RESULTS

One hundred samples of milk and dairy products (canned and non-canned cheese and cream) were obtained in a sterilized and random way from various supermarkets and traditional markets in the city of Babylon, Iraq.

A sensitivity test was conducted, including the antibiotics Erythromycin, Ciprofloxacin, Trimethoprim, Nitrofurantoin, Clindamycin, Gentamycin, Rifampicin, Tetracycline, and Sulfamethoxazole. Antibiotic resistance among *S. aureus* isolates was found to be variable. The *S. aureus* isolates exhibited the greatest sensitivity to nitrofurantoin (100%) and Erythromycin (51.7%). The observed pattern unequivocally demonstrated that a significant proportion of *S. aureus* isolates (58.6%) exhibited resistance to Tetracycline, with Trimethoprim (55.1%) and Clindamycin (48.2%). 41.3% of *S. aureus* isolates had moderate sensitivity to Rifampicin (Table).

### **The number of bacteria that are resistant to different types of antibiotics and the number of bacteria that are sensitive to drugs**

<b>Antibiotic</b>	<b>R</b>	<b>S</b>	<b>I</b>
Erythromycin (10 µg)	41.3%	51.7%	6.8%
Ciprofloxacin (5 µg)	37.9%	44.8%	17.2%
Trimethoprim (10 µg)	55.1%	17.2%	27.5%
Nitrofurantoin (300 µg)	0	100%	0
Clindamycin (2 µg)	48.2%	24.1%	27.5%
Gentamycin (10 µg)	44.8%	51.7%	3.4%
Rifampicin (5 µg)	40.6%	10.3%	41.3%
Tetracycline (10 µg)	58.6%	37.9%	0
Sulfamethoxazole (100 µg)	34.4%	44.8%	20.6%

To differentiate between positive and negative bacteria, we stained all of the samples using Gramme staining, which reveals the cellular structure and morphology. The Gram stain reaction relies on the fact that bacterial cell walls differ in their chemical composition. Gram-positive cells possess a thick peptidoglycan layer that is coated with lipids, whereas gram-negative cells have a comparatively thinner peptidoglycan layer that is enveloped by lipids. Gram-positive bacteria appeared purple because alcohol does not dissolve iodine and crystal violet precipitates in their thicker cell wall. In contrast, Gram-negative bacteria appeared pink and readily released crystal violet from their cells (Fig. 1).

Samples were cultured on Mannitol salt agar by streaking method; many numbers of bacterial colonies were found on the medium (Fig. 2).

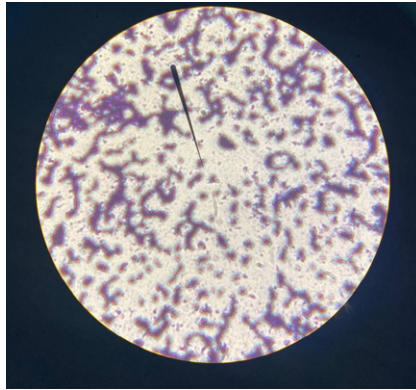


**Fig. 1. Gram stain of bacterial species**



**Fig. 2. Bacterial growth on mannitol salt agar**

To diagnose all kinds of *Staphylococcus* bacteria, we transferred the ineffective samples from MacConkey agar to mannitol salt agar, which allowed us to distinguish *Staphylococcus aureus* from the other *Staphylococcus* species. The medium promotes the growth of organisms that can endure environments high in salt concentrations (sodium chloride). Additionally, the fermentation of mannitol provides diagnostic guidance, as evidenced by the phenol red-yellow change in the pH indicator. The laboratory identified staphylococci as *Staphylococcus aureus* (Fig. 3–5).



**Fig. 3. Bacterial growth on Blood agar**

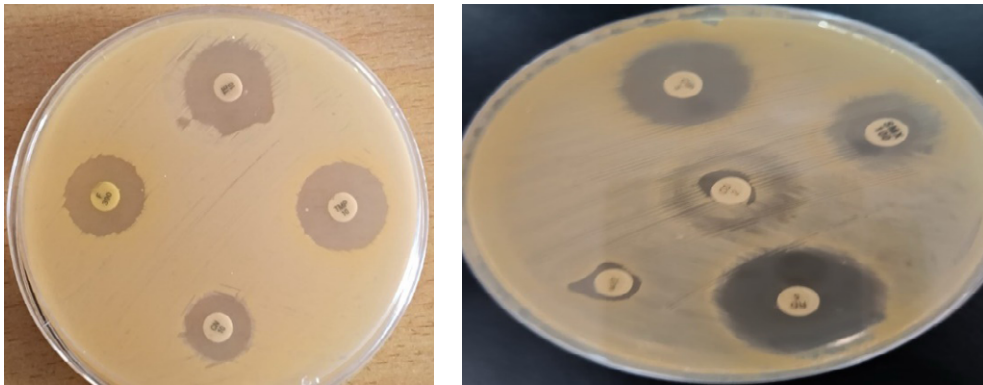


**Fig. 4. Antibiotic susceptibility test bacterial isolates**

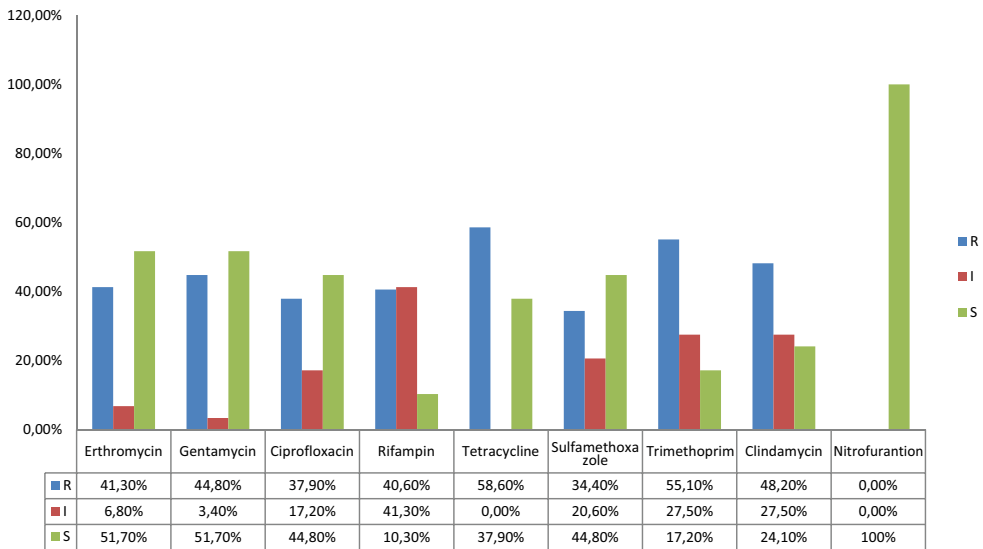


**Fig. 5. Antibiotic susceptibility test of *S. aureus* isolate (n=29) isolated from milk and milk products. S: Sensitive, R: Resistant, I: Intermediate, Erythromycin, Gentamycin, Ciprofloxacin, Rifampicin, Tetracycline, Sulfamethoxazole, Trimethoprim, Clindamycin, Nitrofurantoin**

## DISCUSSION

The isolates exhibited resistance to numerous antibiotics. These findings align with the research conducted by Dai et al. [22] and Jamali et al. [23], which examined the resistance patterns of *S. aureus* strains in raw milk and dairy products. The resistance profiles included tetracycline, penicillin, clindamycin, erythromycin, streptomycin, kanamycin, chloramphenicol, and gentamicin. Antimicrobial resistance poses a significant threat to human health, leading to increased rates of illness and death [24].

The resistance level of *S. aureus* to tetracycline is 58.6%. The findings of Harijani et al. [25] differ from this study, as they reported a success rate of 33%. Tetracycline functions by impeding protein synthesis through the prevention of aminoracilli-tRNA attachment to the ribosome acceptor. This disruption hinders bacterial synthesis, leading to its inability to grow [26].

The majority of illness treatment failures are caused by bacterial resistance to several kinds of antibiotics owing to antibiotic misuse [21]. When someone eats foods that are infected with harmful bacteria that are immune to medicines, they get food poisoning that can be mild to serious and even deadly. After isolation and identification, the isolated bacteria were identified as *Staphylococcus aureus*. According to morphological appearance, microscopic diagnosis, and molecular detection.

The findings of this study were compatible with the results which have been reported by Oliveira et al. [27] who found the resistance was observed for tetracycline (24.2%), and ciprofloxacin (16.1%), and to a lesser extent clindamycin (14.5%), erythromycin (12.9%), trimethoprim (12.9%), gentamicin (9.7%) and trimethoprim – sulfamethoxazole (1.6%).

The resistance to nitrofurantoin (F) was 0%, which means that resistance was not obtained in this study. Antibiotic usage (therapeutic, prophylactic, and growth promotion) in people and animals may have resulted in the selective rise of resistance in bacterial populations, as well as misuse and excessive use leads to increased resistance [28].

## ■ CONCLUSION

Staphylococcal foodborne illness is a significant concern in global public health initiatives. *Staphylococcus aureus* could potentially be found in milk and milk products. A significant proportion of bacteria exhibit resistance to the antibiotics frequently employed in the therapy regimens for both human and animal illnesses.

## ■ REFERENCES

1. Le HHT, Dalsgaard A, Andersen PS, et al. Large-scale *Staphylococcus aureus* foodborne disease poisoning outbreak among primary school children. *Microbiology Research*. 2021;12(1):43–52
2. Oogai Y, Matsuo M, Hashimoto M, et al. Expression of virulence factors by *Staphylococcus aureus* grown in serum. *Applied and environmental microbiology*. 2011;77(22):8097–8105
3. Krakauer T. Staphylococcal superantigens: pyrogenic toxins induce toxic shock. *Toxins*. 2019;11(3):178
4. Dinges MM, Orwin PM, Schlievert PM. Exotoxins of *Staphylococcus aureus*. *Clinical microbiology reviews*. 2000;13(1):16–34
5. Kadariya J, Smith TC, Thapaliya D. *Staphylococcus aureus* and staphylococcal food-borne disease: an ongoing challenge in public health. *Biomed Res Int*. 2014;2014:827965.
6. Argudin MÁ, Mendoza MC, Rodicio MR. Food poisoning and *Staphylococcus aureus* enterotoxins. *Toxins*. 2010;2(7):1751–1773
7. Howell MD, Diveley JP, Lundeen KA, et al. Limited T-cell receptor beta-chain heterogeneity among interleukin 2 receptor-positive synovial T cells suggests a role for superantigen in rheumatoid arthritis. *Proceedings of the National Academy of Sciences*. 1991;88(23):10921–10925
8. Breuer K, Wittmann M, Bösch B, et al. Severe atopic dermatitis is associated with sensitization to staphylococcal enterotoxin B (SEB). *Allergy*. 2000;55(6):551–555
9. Lowy FD. Antimicrobial resistance: the example of *Staphylococcus aureus*. *The Journal of clinical investigation*. 2003;111(9):1265–1273
10. Wang X, Meng J, Zhang J, et al. Characterization of *Staphylococcus aureus* isolated from powdered infant formula milk and infant rice cereal in China. *International journal of food microbiology*. 2012;153(1–2):142–147
11. Hennekinne JA, De Buyser ML, Dragacci S. *Staphylococcus aureus* and its food poisoning toxins: characterization and outbreak investigation. *FEMS microbiology reviews*. 2012;36(4):815–836
12. Zhang J, Wang J, Jin J, et al. Prevalence, antibiotic resistance, and enterotoxin genes of *Staphylococcus aureus* isolated from milk and dairy products worldwide: A systematic review and meta-analysis. *Food Research International*. 2022;162:111969
13. Johler S, Weder D, Bridy C, et al. Outbreak of staphylococcal food poisoning among children and staff at a Swiss boarding school due to soft cheese made from raw milk. *Journal of dairy science*. 2015;98(5):2944–2948
14. Gwandu SH, Nonga HE, Mdegela RH, et al. Assessment of Raw Cow Milk Quality in Smallholder Dairy Farms in Pemba Island Zanzibar, Tanzania. *Vet Med Int*. 2018;2018:1031726.
15. Guo Y, Song G, Sun M, et al. Prevalence and Therapies of Antibiotic-Resistance in *Staphylococcus aureus*. *Front Cell Infect Microbiol*. 2020;10:107.
16. Eshetie S, Tarekegn F, Moges F, et al. Methicillin resistant *Staphylococcus aureus* in Ethiopia: a meta-analysis. *BMC Infect Dis*. 2016;16(1):689.

17. Samaha IA, Ibrahim HAA, Hamada MO. Isolation of Some Enteropathogens from Retailed Poultry Meat in Alexandria Province. *AJVS*. 2012;37(1):17–22.
18. Khalafallah BM, El-Tawab A, Awad A, et al. Phenotypic and genotypic characterization of pseudomonas species isolated from frozen meat. *Benha Vet Med J*. 2020;39(2):47–51.
19. Hafez M, Ibrahim H, Amin R. Assessment of bacterial evaluation of imported frozen meat. *Benha Vet Med J*. 2020;37(2):1–3.
20. Nair PS, Surendran PK. Surendran Biochemical characterization of lactic acid bacteria isolated from fish and prawn. *J Culture Collection*. 2005;4(2004–2005):48–52.
21. Gnanadhas DP, Ben Thomas M, Thomas R, et al. Interaction of silver nanoparticles with serum proteins affects their antimicrobial activity in vivo. *Antimicrobial agents and chemotherapy*. 2013;57(10):4945–4955.
22. Dai J, Wu S, Huang J, et al. Prevalence and Characterization of Staphylococcus aureus Isolated From Pasteurized Milk in China. *Front Microbiol*. 2019;10:641.
23. Jamali H, Paydar M, Radmehr B, Ismail S. Prevalence and antimicrobial resistance of Staphylococcus aureus isolated from raw milk and dairy products. *Food Control*. 2015;54:383–388.
24. Pourbabae M, Hadadi MR, Hooshyar H, et al. Prevalence of Staphylococcus aureus in Raw Hamburgers from Kashan in 2017. *International Archives of Health Sciences*. 2020;7(1):47–50.
25. Harijani N, Wandari A, Effendi MH, Tyasningsih W. Molecular detection of encoding enterotoxin C gene and profile of antibiotic resistant on Staphylococcus aureus isolated from several dairy farms in East Java, Indonesia. *Biochemical and Cellular Archives*. 2020;20(1):3081–3085.
26. Candrasekaran D, Venkatesan P, Tirumurugaan KG, et al. Pattern of antibiotic resistant mastitis in dairy cows. *Vet. World*. 2015;7:389–394.
27. Oliveira R, Pinho E, Almeida G, et al. Prevalence and Diversity of Staphylococcus aureus and Staphylococcal Enterotoxins in Raw Milk From Northern Portugal. *Front Microbiol*. 2022;13:846653.
28. Puah SM, Chua KH, Tan JA. Virulence Factors and Antibiotic Susceptibility of Staphylococcus aureus Isolates in Ready-to-Eat Foods: Detection of S. aureus Contamination and a High Prevalence of Virulence Genes. *Int J Environ Res Public Health*. 2016;13(2):199.